

EFFECTS OF VARIATION IN AUTOCLAVE PRESSURE, CURE TEMPERATURE, AND
VACUUM-APPLICATION TIME ON THE POROSITY AND MECHANICAL PROPERTIES
OF A CARBON/EPOXY COMPOSITE

A Thesis by

Hoda Koushyar

Bachelor of Science, Amirkabir University of Technology, 2007

Submitted to the Department of Mechanical Engineering
and the faculty of the Graduate School of
Wichita State University
in partial fulfillment of
the requirements for the degree of
Master of Science

May 2011

© Copyright 2011 by Hoda Koushyar

All Rights Reserved

EFFECT OF VARIATION IN AUTOCLAVE PRESSURE, CURE TEMPERATURE, AND
VACUUM APPLICATION TIME ON THE POROSITY AND MECHANICAL PROPERTIES
OF A CARBON/EPOXY COMPOSITE

The following faculty members have examined the final copy of this thesis for form and content, and recommend that it be accepted in partial fulfillment of the requirement for the degree of Master of Science with a major in Mechanical Engineering.

Bob Minaie, Committee Chair

Hamid Lankarani, Committee Member

Krishna Krishnan, Committee Member

DEDICATION

To my husband, Behrouz, and my parents
who have made numerous sacrifices during these years

ACKNOWLEDGEMENTS

I would like to express my sincere gratitude to my advisor, Professor Bob Minaie, who provided the opportunity for me to participate in this research. His valuable support, guidance, and encouragement have made this work successful. I would also like to thank Professor Hamid Lankarani and Professor Krishna Krishnan for serving on my thesis committee and also Dr. Melanie Violette for her helpful comments.

I also thank my colleagues, Dr. Seyed Soltani, Shannon Walker, and Tien Vo for their support throughout this study. Special recognition goes to Behrouz Tavakol, Pooneh Roozbehjavan, Dr. Alejandro Rodriguez, Mauricio Guzman, Chee Sern Lim, Nita Yodo, Ashraf Ahmed, Rony Das, and Ronald Joven for their unconditional friendship and cooperation, which made this work more enjoyable.

Finally, I am very much grateful to my husband, my parents, and my brother for their endless help and support.

ABSTRACT

The effect of variation in autoclave pressure, cure temperature, and vacuum-application time on porosity, hot/wet (H/W) and room temperature/dry (RT/D) short beam shear (SBS) strengths, and failure mechanisms of IM7/977-2 unidirectional prepreg was investigated. The stacking sequence for all panels was $[0/90_2/0]_{4s}$. Fourteen cure cycles were designed to study a wide range of cure pressures, cure temperatures, and two different vacuum-application durations, including vacuum vent at recommended pressure and vacuum hold throughout the cure cycle.

It was found that for panels cured at different temperatures and for panels cured at different pressures with a vacuum vent at recommended pressure, SBS strength did not vary significantly over a relatively wide range of cure temperatures and pressures. However, after a certain point, a decreasing trend in the average SBS strength for both H/W and RT/D was observed by reducing the cure temperature as well as the cure pressure.

Panels with the same cure pressure and dissimilar vacuum-application durations showed different SBS strength, with higher properties associated with panels in which the vacuum was vented at the recommended pressure. For panels cured at various cure pressures and the vacuum hold throughout the cure cycles, C-scan results showed a cross-shaped high-porosity in the middle of the panels, which became larger as the cure pressure decreased. This defect is believed to cause higher variability of the SBS strength as the cure pressure is reduced.

SBS strength was found to decrease with increasing void content in the test specimens. Theoretical models were compared to the experimental data of SBS strength vs. void content.

Investigation of the failure mode for each panel revealed a change in both H/W and RT/D failure mechanism by lowering the cure temperature and cure pressure. However, the change was more dominant when the cure temperature was varied.

TABLE OF CONTENTS

Chapter	Page
1. INTRODUCTION	1
1.1 Motivation and Scope	1
1.2 Overview of Thesis	4
2. LITERATURE REVIEW	5
2.1 Effect of Curing Condition on Composite Properties	5
2.1.1 Cure Temperature	5
2.1.2 Cure Pressure	6
2.1.3 Vacuum	11
2.2 Effect of Environmental Condition on Properties of Laminated Composite	11
2.2.1 Environmental Effect on Composites with Void	14
3. TECHNICAL APPROACH	16
3.1 Material	16
3.2 Fabrication and Curing	16
3.3 Thermal Analysis	19
3.3.1 Degree of Cure	19
3.3.2 Glass Transition Temperature	19
3.4 Ultrasonic C-scan and Thickness Variation Measurement	20
3.5 Panels Layout Configuration	20
3.6 Void Content	21
3.7 Short Beam Shear Test	21
3.7.1 Room Temperature/Dry Condition	22
3.7.2 Hot/Wet Condition	23
3.8 Correlation between Void Content, Density, and SBS Strength	23
3.9 Investigation of Failure Mechanisms	24
4. RESULTS AND DISCUSSION	25
4.1 Thermal Analysis	25
4.1.1 Degree of Cure	25
4.1.2 Glass Transition Temperature	26
4.2 Ultrasonic C-Scan	27
4.3 Thickness Variation	28
4.4 Panel Layout Configuration	30
4.5 Void Content	34
4.6 Shot Beam Shear Strength	40
4.6.1 Room Temperature/Dry Condition	41
4.6.2 Hot/Wet Condition	41

TABLE OF CONTENTS (continued)

Chapter	Page
4.6.3 Comparison.....	43
4.7 Correlation between Void Content, Density, and SBS Strength	44
4.7.1 Comparison between Experiment and Theory.....	48
4.8 Failure Mechanism.....	51
4.8.1 Room Temp/Dry Condition	51
4.8.2 Hot/Wet Condition.....	58
5. CONCLUSIONS.....	66
5.1 Conclusions.....	66
5.2 Recommendation for Further Studies	69
REFERENCES	70

LIST OF TABLES

Table	Page
1. SBS strength values for carbon fiber/epoxy composites [23].....	13
2. Recommended cure cycle for 977-2 [41].....	16
3. Designed cure cycles.....	17
4. Statistical results of RT/D and H/W SBS strength of cure cycles 1-14.....	44

LIST OF FIGURES

Figure	Page
1. Micrograph of void region in samples cured at different cure pressure [11]: (a) 0.6 MPa and (b) 0.0 MPa.....	8
2. Percentage of void as function of cure pressure [11].....	8
3. Interlaminar shear strength as function of composite density for AS/PMR-15 [13].....	9
4. Interlaminar shear strength as function of void content for AS/PMR-15 [13].....	10
5. Combined effect of bagging vacuum and autoclave pressure; constant pressure (at 1 bar) indicated by bold lines, and constant vacuum (at 0.3 bar) indicated by dashed lines [6]....	11
6. Interlaminar failure mode observed at: (a) 0° and (b) 0/90° [23].....	13
7. SBS test set up for flat laminates [25]	22
8. DOC during cure for panels 1 to 5 with different cure temperatures	25
9. Final DOC for panels 1 to 5 with different cure temperature	26
10. Glass transition temperature (T_g) for panels 1 to 5 with different cure temperatures	26
11. C-scan results for panels 6 to 14.....	27
12. Average thickness of panels 6 to 14 along with thickness variation shown as error bars.....	28
13. Thickness variation contour plots for panels 6 to 14	29
14. Thickness variation contour plots with designed layout on top, along with C-scan data for panels 6 to 14	31
15. Void content for cure cycles 1 to 14 at center, middle, and corner locations.....	34
16. Void content for cure cycles 6 to 14 at center, middle, and corner locations.....	35
17. Density for cure cycles 6 to 14 at center, middle, and corner locations	35
18. Fiber-volume fraction for cure cycles 6 to 14 at center, middle, and corner locations	36
19. Effect of vacuum-application time on void content for cure pressure of 552 MPa.....	37
20. Effect of vacuum-application time on void content for cure pressure of 276 MPa.....	38
21. Effect of vacuum-application time on void content for cure pressure of 138 MPa.....	38

LIST OF FIGURES (continued)

Figure	Page
22. Void distribution across center of panels 6 to 14.....	40
23. Average RT/D SBS strength for cure cycles 1 to 14	42
24. Average H/W SBS strength for cure cycles 1 to 14.....	42
25. Correlation between RT/D SBS strength and void content	45
26. Correlation between RT/D SBS strength and void content on semi-log scale	45
27. Correlation between H/W SBS strength and void content.....	46
28. Correlation between H/W SBS strength and void content on semi-log scale.....	46
29. Correlation between RT/D SBS strength and composite density	47
30. Correlation between H/W SBS strength and composite density	47
31. Comparison of normalized RT/D SBS strength and theoretical lines	49
32. Comparison of normalized RT/D SBS strength and theoretical lines on a semi-log scale	49
33. Comparison of normalized H/W SBS strength and theoretical lines.....	50
34. Comparison of normalized H/W SBS strength and theoretical lines on a semi-log scale... 50	50
35. Typical acceptable failure modes in SBS testing [25].....	51
36. Typical failed RT/D SBS specimen of panels 1 to 5	52
37. Typical photomicrograph of failed RT/D SBS specimen of cure cycles 1 to 4.....	52
38. Typical photomicrograph of failed RT/D SBS specimen of cure cycle 5	53
39. Panel 6 failed RT/D specimen from center.....	54
40. Panel 7 failed RT/D specimen from center.....	54
41. Panel 8 failed RT/D specimen from center.....	54
42. Panel 9 failed RT/D SBS specimens from: (a) corner, (b) middle, and (c) center	55
43. Panel 10 failed RT/D SBS specimens from: (a) corner, (b) middle, and (c) center	55

LIST OF FIGURES (continued)

Figure	Page
44. Panel 11 failed RT/D specimens from: (a) corner, (b) middle, and (c) center	56
45. Panel 12 failed RT/D SBS specimens from: (a) corner, (b) middle, and (c) center	56
46. Panel 13 failed RT/D SBS specimens from: (a) corner, (b) middle, and (c) center	57
47. Panel 14 failed RT/D SBS specimens from: (a) corner, (b) middle, and (c) center	57
48. Typical failed H/W SBS specimen of panels 1 to 4.....	59
49. Typical failed H/W SBS specimen of panel 5	59
50. Typical photomicrograph of failed H/W SBS specimen of cure cycles 1 to 4.....	60
51. Typical photomicrograph of failed H/W SBS specimen of cure cycle 5.....	60
52. Panel 6 failed H/W SBS specimen from center	61
53. Panel 7 failed H/W SBS specimen from center	61
54. Panel 8 failed H/W SBS specimen from center	61
55. Panel 9 failed H/W SBS specimens from: (a) corner, (b) middle, and (c) center.....	62
56. Panel 10 failed H/W SBS specimens from: (a) corner, (b) middle, and (c) center.....	62
57. Panel 11 failed H/W SBS specimens from: (a) corner, (b) middle, and (c) center.....	63
58. Panel 12 failed H/W SBS specimens from: (a) corner, (b) middle, and (c) center.....	63
59. Panel 13 failed H/W SBS specimens from: (a) corner, (b) middle, and (c) center.....	64
60. Panel 14 failed H/W SBS specimens from: (a) corner, (b) middle, and (c) center.....	64

LIST OF ABBREVIATION/NOMENCLATURE

ASTM	American Society for Testing and Material
CE	Center
CLC	Combined Loading Compression
CMM	Coordinate Measurement Machine
CO	Corner
DOC	Degree of Cure
DSC	Differential Scanning Calorimetry
ED	Edge
H/W	Hot/Wet
ILSS	Interlaminar Shear Strength
MDSC	Modulated Differential Scanning Calorimetry
MI	Middle
MRC	Manufacturer Recommended Cure
RT/D	Room Temperature/Dry
SBS	Short Beam Shear
UD	Unidirectional

LIST OF SYMBOLS

$\alpha(t)$	degree of cure at time t
σ_y	yield stress
σ_{yg}	yield stress at T_g
H_U	ultimate heat of reaction
q	released heat during cure
t	time
T	temperature
T_g	glass transition temperature
V_{fv}	fiber volume fraction
V_v	void content

CHAPTER 1

INTRODUCTION

1.1 Motivation and Scope

Mechanical properties of laminated composite materials depend highly on their curing parameters in the autoclave or oven. Composite material manufacturers specify the proper curing conditions with one or more manufacturer's recommended cure (MRC) cycles. This MRC cycle should be closely followed to cure composite laminates properly and hence attain the best mechanical properties. The curing parameters specified in the MRC cycle for autoclave curing of composite materials are curing time, curing temperature, autoclave pressure, and vacuum pressure. Deviations from the prescribed curing parameters that inevitably happen in production curing may adversely affect the mechanical properties of composite materials. It has always been beneficial to investigate what level of variation in autoclave processing parameters is acceptable without significant change in mechanical properties.

For example, if the curing temperature is not sufficiently high, resin will not cure fully and, therefore, will not support the fibers completely, thus resulting in a reduction of the final mechanical properties of the laminate. Also, insufficient autoclave pressure may lead to poor ply consolidation and higher void contents in the cured part. Trapped volatiles in the resin form voids in laminated composites. Voids tend to develop when the void pressure exceeds the resin pressure before the gel point is reached [1]. Finally, improper application of vacuum pressure can increase porosity of the composite laminate. Voids are one of the most harmful defects in composite materials since they weaken the matrix-dominated mechanical properties, such as shear and compressive strength, by inducing localized stress concentration. In addition, voids can reduce the fatigue life of the composite part. It is possible to improve the quality of cured

laminates by proper selection and control of the curing parameters. However, precise controlling of curing parameters is often costly [2].

Many studies have been conducted to evaluate the relation between curing parameters and composite properties [3-19]. However, except for a few studies on the effect of cure temperature on mechanical properties [7, 8, 10, 12], most have investigated the effect of curing pressure or amount of vacuum on the void content and hence mechanical properties. None of these studies have investigated the effect of vacuum-application duration on different properties. In the first part of this study, the effect of a wide range of cure temperatures on short beam shear (SBS) strength as well as thermal properties was investigated. In the second part of the study, a wide range of cure pressures along with two different vacuum-application durations were utilized to observe their effect on voids and SBS strength. What makes this part of the study unique is the investigation of vacuum-application duration combined with cure-pressure variation, which has never been done before.

Some previous studies have tried to find a relation between mechanical properties and void content [3-5, 9, 11, 13]. However, two micromechanics-based equations were previously developed [20-22] to correlate the void content and fiber volume fraction to SBS strength based on configuration of the voids. In the current study, appropriate curves were fitted to the experimental data and results compared to the lines obtained by the mentioned theoretical formulas.

Some studies have been performed to investigate the effect of environmental conditions on the mechanical properties of composites [15, 16, 23, 24], a few of them on composites containing voids [15, 16]. However, these studies were generally performed on systems with fully cured resin. In the present study, performing hot/wet (H/W) along with room temp/dry

(RT/D) SBS tests provided the unique opportunity to investigate the effect of environmental conditions on the mechanical properties of composites with various degrees of cure (DOC) and void content. It was also possible to compare the sensitivity of interlaminar shear to various amounts of DOC and void content.

Another unique part of this study was to determine the distortion and thickness variation for each panel. Distortion is a one of the major problems in laminated composite, which may have some effect on the final properties. It is beneficial to investigate the effect of different cure parameters on the distortion as well as thickness of the laminates. A coordinate measurement machine (CMM) was used to obtain the distortion of the laminates along with the thickness variation.

One mechanical tests that has been widely used in previous studies is the short beam shear (SBS) test (ASTM D 2344 [25]). This method has become popular due to its simplicity. Also, performing this method at cryogenic or elevated temperature is relatively easy [26]. This technique was chosen for the current study because of its simplicity, ease of testing in different conditions, and verified sensitivity to defects in the laminates. The specimen used in this test is relatively small, typically 4 cm long by 1.2 cm wide, depending on thickness, which makes it possible to cut a large number of test specimens out of a moderately sized panel.

The SBS test is not commonly used for design purposes due to the complexity of failure modes [25]. Further study on the SBS failure mechanism would be useful in order to be able to fully benefit from the test results. Investigation of failure mechanisms can also reveal more information about the true influence of curing parameters and defects on the mechanical properties. The last part of the current study involved the investigation of the failure mechanism of the SBS sample from all the panels with various curing parameters. The work in this section

provided the opportunity to comprehensively study the effect of curing parameters along with environmental conditions on the failure mechanism.

1.2 Overview of Thesis

This study was performed to comprehensively investigate the effect of curing conditions on the final properties of the 977-2 laminated composite. The effects of variation in curing parameters, including cure temperature, cure pressure, and vacuum-application time on the DOC, glass transition temperature (T_g), void, and thickness variation, was studied. Also, the role of each defect in the variation of SBS strength and SBS failure mechanism was inspected.

The experiments were performed in two categories. In the first category, the effect of isothermal cure temperature on DOC, T_g , SBS strength (RT/D and H/W), and consequent failure mechanism was investigated. In the second category, the effect of pressure and vacuum-application duration on void content, void distribution, SBS strength (RT/D and H/W) and consequent failure mechanism was investigated.

Chapter 2 of this thesis provides a brief background on the effect of different curing parameters on the properties of composite parts. Chapter 3 covers the details of methodology and the experimental works that was done in this project. Chapter 4 provides the results of the experimental works and also the correlations among curing parameters, defects, and mechanical properties. This chapter also discusses the failure modes observed for different curing procedures. Finally, the conclusions are presented in Chapter 5.

CHAPTER 2

LITERATURE REVIEW

2.1 Effect of Curing Condition on Composite Properties

The effect of variations of curing parameters on the final mechanical properties of composite materials has been studied extensively. In most of these studies, various defects are induced in the laminates by varying one or two curing parameters. Then, the measured mechanical properties are correlated to the variations of the curing parameters as well as the observed defects [3-19].

2.1.1 Cure Temperature

One of the main curing parameters in autoclave processing of prepreg is the curing temperature. Reducing the cure temperature from the recommended temperature affects the final matrix properties including DOC, T_g , storage modulus and some viscoelastic properties such as gel time and vitrification time [8].

Lee and Springer obtained the correlation between isothermal cure temperature, thus DOC, and mechanical properties for Fiberite T300/976 laminates [10]. Gernaat reported the effect of isothermal curing temperature variation on short beam shear (SBS) and combined loading compression (CLC) strength of the Cycom 5215 plain weave prepreg [7]. Kashani observed that the selected properties of the MTM 45-1 prepreg including DOC, T_g , storage modulus, gel time, and vitrification time were changed by varying the isothermal curing temperature [8]. Alavi investigated the rheological, thermal, and mechanical properties of 977-2/UD cured with different one-stage and two-stage cure cycles and reported no significant change in the final viscoelastic and mechanical properties over a wide range of dwell temperature in the case of one stage cure cycles [12].

As mentioned previously, reducing the cure temperature decreases the T_g value. The yield stress of thermosetting resins at temperatures below T_g , can be related to the T_g using the following equation [27]:

$$\sigma_y = \sigma_{yg} + b(T_g - T) \quad (1)$$

where σ_y is the yield stress at T , σ_{yg} is the yield stress at T_g , T is the temperature, T_g is the glass transition temperature, and b is a positive constant. So, in elevated temperature, samples with lower T_g values show less strength.

2.1.2 Cure Pressure

Many studies addressed cure pressure as one of the parameters that can be used in optimization of cure cycles [3-5, 9]. In most of these studies cure pressure was used as a functional tool to create different levels of voids in the laminates. Having different void volume fractions, it was tried to find a relation between void and mechanical properties and in some cases between pressure and mechanical properties [3-5, 9, 11]. All of the previous studies confirmed that decreasing the pressure increases the porosity which in turn reduces the mechanical properties, especially matrix dominated properties such as SBS Strength. Due to significant effect of voids on composite properties, voids will be discussed comprehensively in the next section.

One of the major defects in laminated composites is the presence of voids and their possible effect on the mechanical properties. Due to their importance, a considerable number of studies have been performed on the effect of voids on the mechanical properties of laminated composites [9, 14, 17-19, 24, 28]. Voids can be created as the result of different parameters, such as entrapped air during resin impregnation or layup, and volatiles arising from the resin system that do not have a chance to escape during cure [9]. Voids continuously grow once the void

pressure exceeds the resin pressure before the gel point is reached [1]. Porosity created during fabrication presents itself in the form of isolated or connected elongated voids at the fiber/matrix or ply interface [29]. Proper selection of curing parameters, mainly autoclave pressure and vacuum, can help squeeze out the entrapped air and volatiles. However, the precise controlling of curing parameters results in higher costs [2, 30]. Studying the effects void content on mechanical properties can provide allowable ranges for curing-process parameters which in turn can reduce manufacturing costs.

Knowing the microstructure of defects along with the volume fraction can help in determining a more realistic relation between the defect and mechanical properties. Voids can be divided into two main categories based on their shape. At a lower void content, e.g., less than 1.5 %, voids are usually small and their shape is mainly spherical. However, at higher void contents, voids are much larger and tend to be interlaminar in nature and also have cylindrical and flattened shapes [18, 31].

Huang and Talreja [32] tried to find a quantitative relation between characteristics of voids and composite properties. They considered void volume fraction, distribution, shape, and size as the characteristics and tried to relate them to effective elastic constants of unidirectional (UD) fiber-reinforced laminates. They also performed finite element analysis along with empirical models to study the influence of void distribution and geometry on elastic properties. Based on their results, the effect of voids on decreasing the out-of-plane properties is much greater than the effect on in-plane properties.

Cure pressure can affect the level of voids in the laminate as well as their morphology. A photomicrograph of a void area obtained by Guo et al. [11] can be seen in Figure 1. Figure 1(a) shows the cross section of a laminate cured at higher pressure with low porosity, and Figure 1(b)

shows the samples cured at lower pressures with higher void content. It can be seen that at high porosity levels, voids which were created at the plies interface were larger and more elongated than the voids in low-porosity samples.

In some studies [3, 4, 9, 11], the relation between void content and cure pressure was captured using an exponential curve fitting. Although the values reported were not very similar, the trends observed in these studies were comparable. Figure 2 shows the trend obtained in one of these studies [11].

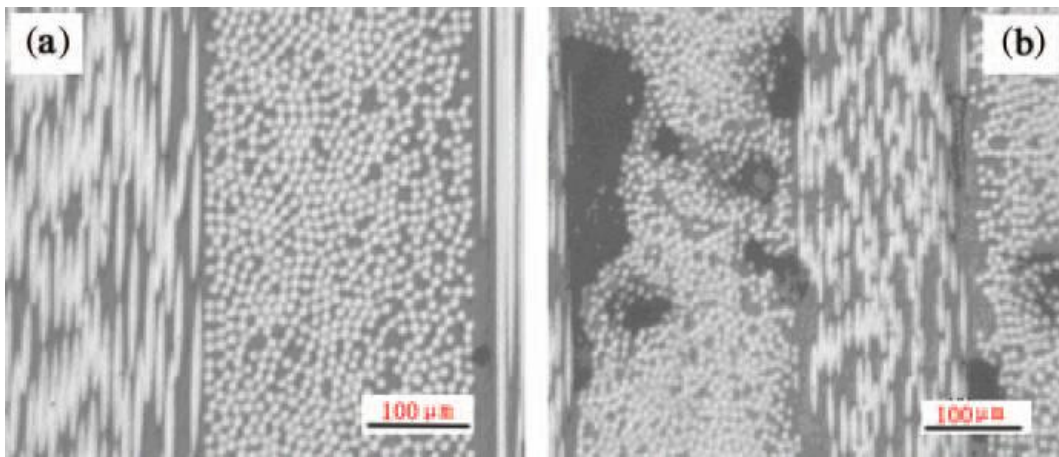


Figure 1. Micrograph of void region in samples cured at different cure pressure [11]: (a) 0.6 MPa and (b) 0.0 MPa.

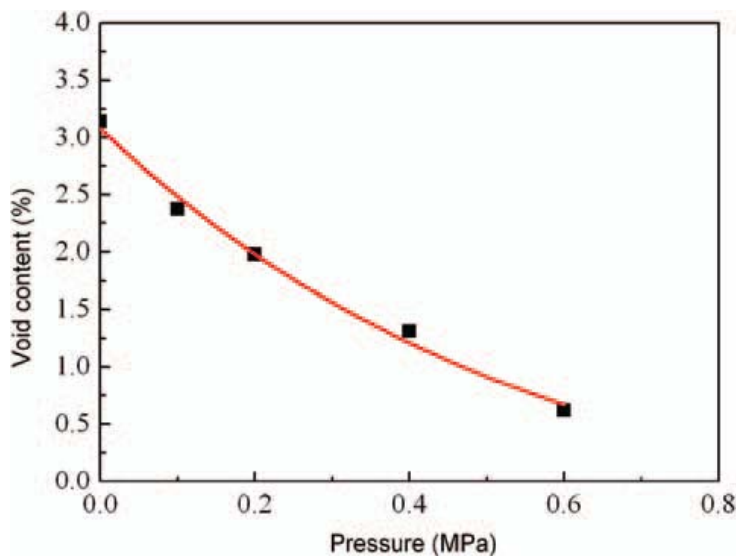


Figure 2. Percentage of void as function of cure pressure [11].

Some empirical correlations between void content and interlaminar shear strength were reported [9, 13]. However, two theoretical equations were developed [20-22] to correlate void content and fiber volume fraction to the interlaminar shear strength based on the configuration of the voids.

For cylindrical voids the equation (2) can be defined as

$$ILSS_r = 1 - [4V_v/3.14(1 - V_{fv})]^{1/2} \quad (2)$$

For spherical voids the equation (3) can be defined as:

$$ILSS_r = 1 - 0.785[6V_v/3.14(1 - V_{fv})]^{2/3} \quad (3)$$

where V_v is void content, V_{fv} is fiber volume fraction, and $ILSS_r$ is the ratio of interlaminar shear strength of the laminates with voids to the interlaminar shear strength of void-free laminates.

Bowles and Frimpong investigated the effect of voids on the interlaminar shear strength of a graphite-fiber-reinforced composite [13]. As can be seen in Figure 3, they found an empirical power equation that could capture the correlation between interlaminar shear strength and composite density.

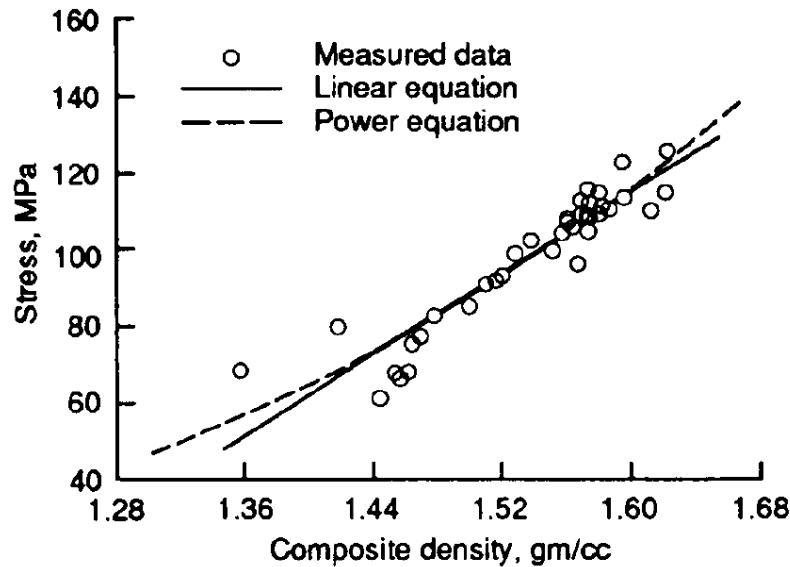


Figure 3. Interlaminar shear strength as function of composite density for AS/PMR-15 [13].

They also obtained a correlation between void content and percent of ILSS retention. The results can be seen in Figure 4. They compared their experimental data to the results obtained by theoretical formulas—equation (2) and equation (3) for cylindrical and spherical voids, respectively— as well as the results taken from ICAN software. The comparison can also be seen in Figure 4, which shows that assumption of spherical voids could capture the experimental data fairly well. However, the formula for cylindrical voids and also ICAN software underestimated the strength as the void content increased.

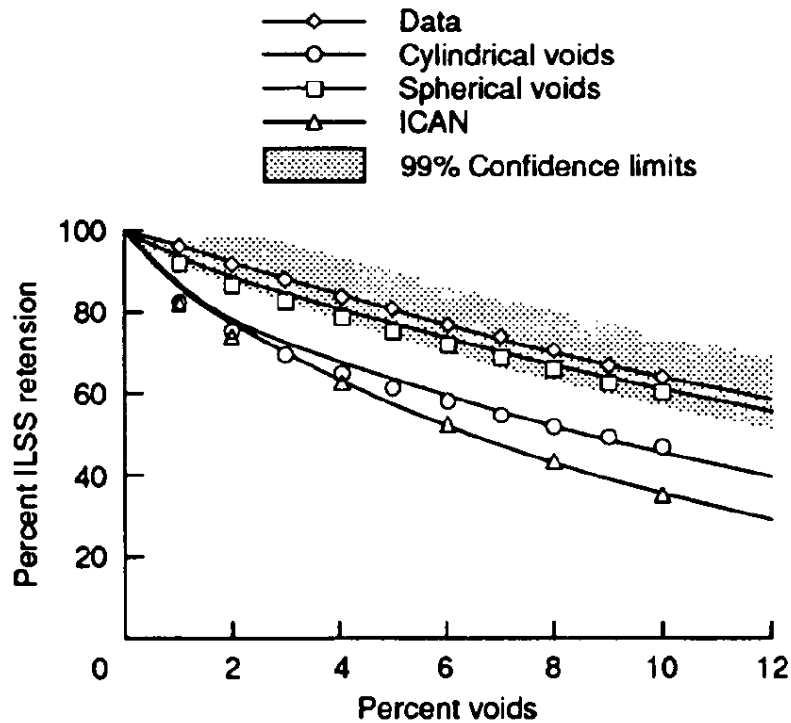


Figure 4. Interlaminar shear strength as function of void content for AS/PMR-15 [13].

Most previous studies focused on low to intermediate levels of laminate porosity. However, about 50 percent reduction in interlaminar shear strength was reported when the porosity level reached 25% for a glass-fiber-reinforced polymer [19].

2.1.3 Vacuum

The effect of vacuum on the mechanical properties of laminated composites has not been studied as extensively as the effect of pressure. In one study by Boey and Lye, the effect of vacuum and pressure on void content and consequently on flexural strength and modulus of an epoxy glass fiber composite was investigated [6]. It was concluded that increasing the bagging vacuum, especially at the initial stages, reduces the void content and consequently increases the flexural strength and modulus. Their results are shown in Figure 5. However, this study focused only on the amount of vacuum applied, and no further investigation was performed on the duration of applying the vacuum.

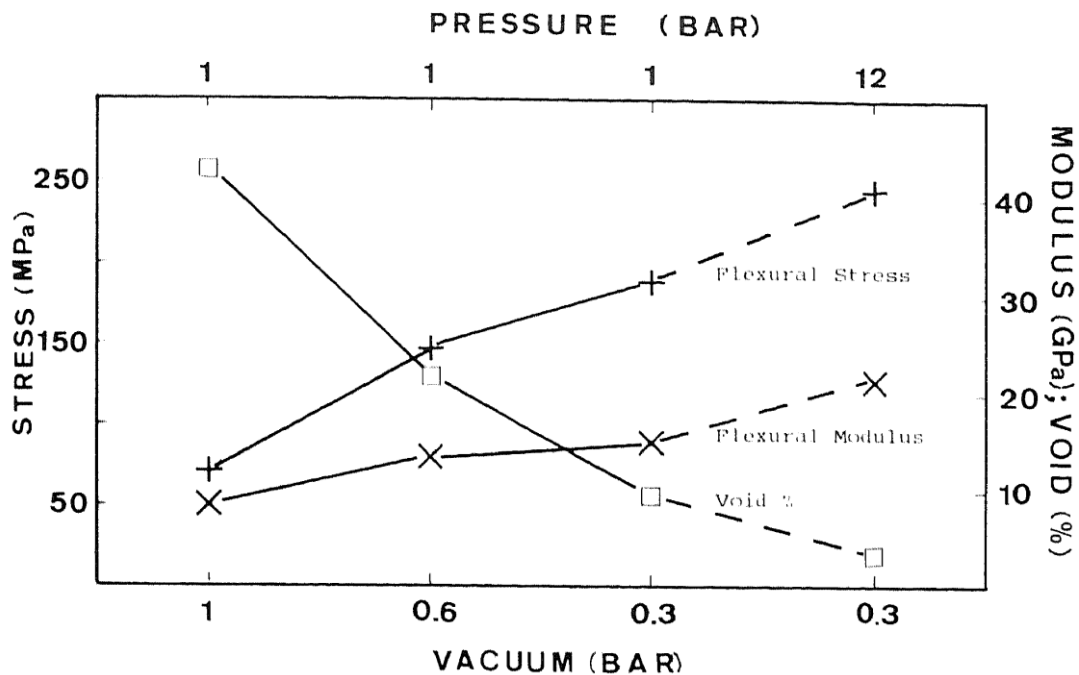


Figure 5. Combined effect of bagging vacuum and autoclave pressure; constant pressure (at 1 bar) indicated by bold lines, and constant vacuum (at 0.3 bar) indicated by dashed lines [6].

2.2 Effect of Environmental Condition on Properties of Laminated Composite

Polymeric composites are subjected to different environmental conditions in service. The main environmental parameters that may affect the composite's performance are temperature,

moisture, contact with chemicals, and radiation [15]. The presence of these factors, especially moisture and temperature, may influence composite properties, including thermal, physical, and mechanical properties [33, 34]. The effect of these environmental factors on composite behavior must be studied, in order for the design to use properties appropriate to the conditions that will be seen in service. Moisture is an important environmental factor to be studied since humidity exists in the atmosphere at different levels [16, 35]. An increase in moisture usually decreases mechanical properties, such as interlaminar shear strength, compressive strength, tensile strength, fracture strain, and stiffness [36].

Temperature combined with humidity can affect the composite's mechanical properties drastically. Matrix plasticization, either reversible or irreversible, can occur as the results of water absorption. And plasticization combined with temperature change can cause considerable variation in matrix toughness, which consequently affects the laminate properties. Additionally, both temperature and humidity can create dimensional variation, which can induce stresses in the laminates and therefore degrade the fiber-matrix interface [37]. Another influence of water on the laminate is a reduction in cross-link density [36]. Most of these effects can be eliminated after drying, but when system that contains water is subjected to load, whether external or internal, it undergoes some internal damage, which can weaken the system permanently [38].

Botelho et al. studied the hygrothermal effect on the shear properties of a carbon fiber/epoxy composite and concluded that hygrothermal conditioning reduces the SBS strength about 18% to 21%, depending on stacking sequence [23]. The results can be seen in Table 1. They also observed a similar failure mode for H/W and RT/D samples. In the case of $[0^{\circ}]_s$ stacking sequence, interlaminar shear between layers in horizontal direction was the dominant failure mode. On the other hand, in the case of $[0/90^{\circ}]_s$ stacking sequence, the laminates showed

interlaminar cracks in both the horizontal and vertical directions. The cross sections can be seen in Figure 6.

TABLE 1

SBS STRENGTH VALUES FOR CARBON FIBER/EPOXY COMPOSITES [23]

τ (MPa)	Before hygrothermal conditioning	After hygrothermal conditioning
$[0/0]_s$	84.5 ± 3.3	60.8 ± 2.0
$[0/90]_s$	66.4 ± 2.1	49.6 ± 1.9

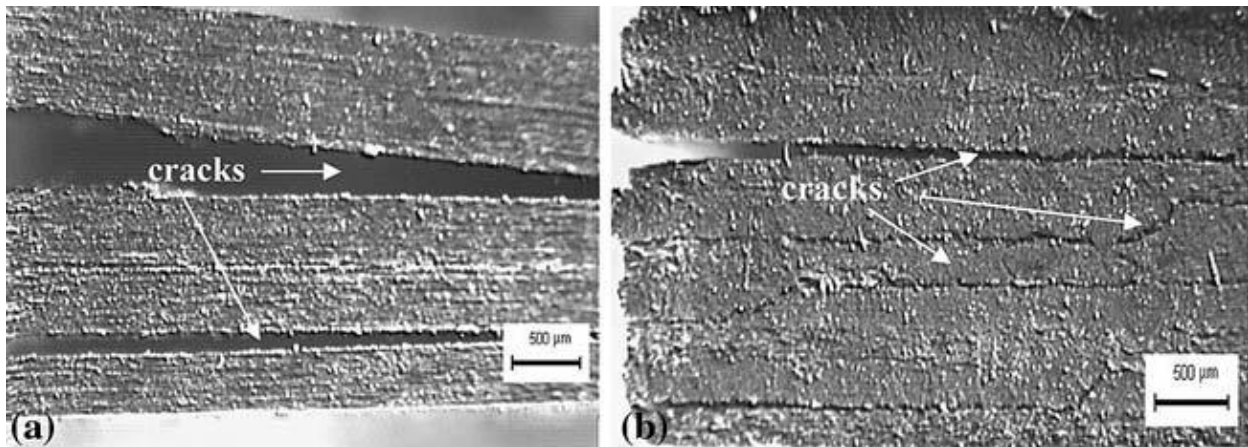


Figure 6. Interlaminar failure mode observed at: (a) 0° and (b) $0/90^\circ$ [23].

A major review paper investigated different studies on the effect of environmental condition on fiber-reinforced composites (FRPs) [39]. The authors concluded that interlaminar shear strength can be a good representative of the degradation in a fiber-matrix interface.

Imaz et al. analyzed humidity absorption kinetics under various hygrothermal conditions [24]. They found a Fickian variation for the absorbed moisture versus time. They also found that some mechanical properties like compressive and flexural strength decreases in the presence of moisture.

2.2.1 Environmental Effect on Composites with Void

Voids are created when entrapped airs and volatiles are unable to escape from the laminates during the cure process. The presence of voids in the composite mainly affects the matrix-dominated properties, such as interlaminar shear and flexural strength. Environmental conditions also affect matrix-dominated properties, and can amplify the effect of voids. On the other hand, voids provide passages for moisture absorption, which increases the effect of moisture on the laminates. Voids also facilitate the passage of air, which may oxidize fibers or cause fiber-matrix degradation [28, 40].

Many studies have been performed to investigate the effect of either voids or environmental condition on the properties of composites, but a few literature sources can be found to study the combined effects of these two. De Almeida and De Mas Santacreu investigated the effect of four different environmental conditions (room temp/dry, room temp/wet, elevated temp/wet, and low temp/wet) on the interlaminar shear strength of carbon/epoxy laminates with three levels of void content [16]. They also performed a limited number of tests by applying thermal shock cycles. A critical void content was found for different conditions, which demonstrated the level of void below which the strength of laminate was not affected to a large extent. They concluded that when thermal shock is not applied, moisture decreases the critical void content but increases the laminate toughness. On the other hand, temperature increases the critical void level but reduces the laminate toughness.

Costa et al. investigated the strength of a hygrothermally conditioned polymer composite with voids [15]. They studied the effect of environmental condition on the interlaminar shear and compressive strength of laminates with different types of reinforcement and resin systems with different void levels. The authors concluded that, in the presence of voids, the effect of

environmental condition on interlaminar shear strength is negligible in the case of carbon-epoxy tape but significant in the case of carbon- epoxy fabric laminates. They also determined that the toughness of both carbon-epoxy tape and carbon-epoxy fabric is not significantly affected by environmental condition.

CHAPTER 3

TECHNICAL APPROACH

3.1 Material

The material used in this study was IM7/977-2 unidirectional which is a commercial prepreg manufactured by Cytec. Cycom 977-2 UD is a toughened epoxy resin reinforced by unidirectional (UD) carbon fiber, which is designed for autoclave or press molding curing. This material provides good impact resistance along with high strength and low weight; therefore, its main usage is in the primary and secondary structures of aircraft, cryogenic tanks, ballistics, etc. [41]. The Cytec-recommended cure cycle for this prepreg is shown in Table 2 [41].

TABLE 2

RECOMMENDED CURE CYCLE FOR 977-2 UD [41]

Ramp Up (°C/min)	Dwell Temperature (°C)	Dwell Time (min)	Ramp Down (°C/min)	Cure Pressure (kPa)	Vacuum
2.8	177	180	2.8	586	Applied at beginning of cure cycle and removed when pressure reaches 69 kPa

3.2 Fabrication and Curing

The stacking sequence $[0/90_2/0]_{4s}$ was used to fabricate 14 balanced and symmetric laminates. A total of 32 unidirectional tapes were used to make each panel. Panels 1 to 5 were fabricated using 430×430 mm plies, and panels 6 to 14 were fabricated using 305×305 mm plies. All laminates were laid up by hand. Debulking was performed for each set of four laid-up plies for five minutes, and final debulking was done for 30 minutes. The panels were cured in an autoclave using the cure cycles 1 to 14 shown in Table 3. Non-perforated Tedlar was used to

avoid pulling too much resin out of the panels. The cure cycles were chosen to cover a wide range of cure temperature, cure pressure, and duration of applying vacuum.

TABLE 3
 DESIGNED CURE CYCLES

Cure Cycle (Panel) Number	Ramp Up (°C/min)	Dwell Temperature (°C)	Dwell Time (min)	Ramp Down (°C/min)	Cure Pressure (kPa)	Vacuum
1	2.8	182	180	2.8	586	vent at 69 kPa
2**	2.8	177	180	2.8	586	vent at 69 kPa
3	2.8	171	180	2.8	586	vent at 69 kPa
4	2.8	160	180	2.8	586	vent at 69 kPa
5	2.8	149	180	2.8	586	vent at 69 kPa
6	2.8	177	180	2.8	552	vent at 69 kPa
7	2.8	177	180	2.8	276	vent at 69 kPa
8	2.8	177	180	2.8	138	vent at 69 kPa
9	2.8	177	180	2.8	690	throughout
10	2.8	177	180	2.8	552	throughout
11	2.8	177	180	2.8	414	throughout
12	2.8	177	180	2.8	276	throughout
13	2.8	177	180	2.8	138	throughout
14	2.8	177	180	2.8	0	throughout

** Manufacturer’s recommended cure cycle.

The first five cure cycles were used to study the effect of isothermal cure temperature, ranging from 182° C to 149° C, on the panel’s final properties including σ_{TS} , SBS strength, and SBS failure mechanism in both H/W and RT/D conditions. As mentioned earlier, the effect of cure temperature on the mechanical properties has not been studied previously to a large extent.

Reducing the cure temperature decreases the DOC of the resin, which eventually affects the matrix-dominated mechanical properties.

As mentioned previously many studies have been performed to investigate the effect of environmental condition on the mechanical properties of composites. However, nearly all of these were performed on the systems with fully cured resin. Performing H/W testing along with RT/D testing on the first five cure cycles provided a unique opportunity to investigate the effect of environmental condition on the mechanical properties of composite with various degrees of cure.

Cure cycles 6 to 8 were utilized to investigate the effect of autoclave pressure, ranging from 552 kPa to 138 kPa, on the void content, SBS strength (H/W and RT/D), and the SBS failure mechanism. As mentioned earlier, cure pressure has direct effect on the void content; therefore, correlations among cure pressure, void content, and SBS strength can be determined. In these cure cycles, vacuum was vented at 69 KPa, which was the recommended time for vacuum ventilation.

Finally, cure cycles 9 to 14 were utilized to study the combined effect of autoclave pressure and maintaining the vacuum throughout the cure cycle on laminate properties. In cure cycles 9 to 14 the vacuum was maintained throughout the cure cycle, while the pressure changed from 690 KPa to 0 KPa. As mentioned before, the manufacturer recommends venting out the vacuum when the pressure reaches 69 kPa. The deviation from this recommended procedure on the final properties including SBS strength, SBS failure mechanism (H/W and RT/D), and glass transition temperature were investigated using cure cycles 9 to 14.

The effect of vacuum magnitude on the void content and eventually on the mechanical properties has been studied previously [6]. However, the effect of the vacuum-application

duration in the cure cycle has not been studied. To investigate this effect, the results of panels 10, 12, and 13 were compared to the results from panels 6, 7, and 8 respectively, since the only difference between these two sets of panels was the vacuum-application duration.

3.3 Thermal Analysis

Performing thermal analyses is always beneficial to investigate the cure state of the resin system. In this study, two parameters, DOC and T_g , were determined for panels 1 to 5 to determine the resin's state of cure. The DOC and T_g were not measured for panels 6 to 14, since they all had the same cure temperature, and pressure and vacuum are expected to have minimal effect on DOC and T_g .

3.3.1 Degree of Cure

The DOC was obtained using TA Instruments Q2000 differential scanning calorimetry (DSC) for panels 1 to 5. Samples of approximately 10 to 15 mg were cut from three layers of uncured prepreg and encapsulated in Tzero aluminum pans. DSC runs were performed to simulate cure cycles 1 to 5. The DOC was calculated as:

$$\alpha(t) = \frac{\int_0^t q dt}{H_U} \quad (4)$$

where $\alpha(t)$ is the degree of cure at time t , q is the released heat during cure from time 0 to t , and H_U is the ultimate heat of reaction. DSC was used to obtain q and H_U .

3.3.2 Glass Transition Temperature

The T_g of the laminates cured at different curing temperatures was obtained using TA Instruments Q2000 modulated differential scanning calorimetry (MDSC) according to ASTM E 2602-09 [42]. Samples of approximately 5 to 15 mg were cut from each cured panel and encapsulated in Tzero aluminum hermetic pans. A ramp rate of 1.5°C/min was utilized, and the

samples were heated from 45° C up to 290° C. The modulation amplitude was $\pm 1^\circ$ C, and the modulation period was 60 seconds.

3.4 Ultrasonic C-scan and Thickness Variation Measurement

C-scan is one of the non-destructive test (NDT) methods that can be used as an inspection technique for laminated composites. In this method, a short pulse of ultrasonic energy is transmitted through the specimen, and the attenuation of pulse can be used to characterize defects, including voids. In addition to voids, other defects, including delamination, fiber volume fraction, condition of the fiber-matrix interface, and other unwanted inclusions, can affect the results of C-scan [29]. In the current study, all panels were inspected with a through-thickness ultrasonic C-scan to obtain the porosity distribution across panels. Panels 6 to 14 were inspected using a coordinate measurement machine (CMM), because of the apparent distortion and thickness variation after the curing process, especially in the case of panels 9 to 14. In order to obtain the thickness variation of these panels, a seven-axis ROMER arm was utilized. Laminates cured at different isothermal temperatures (panels 1 to 5) were not scanned, since no significant distortion and thickness variation was observed.

3.5 Panels Layout Configuration

According to the C-scan and thickness-variation measurements, panels 1 to 5 had uniform thickness and porosity distribution. One layout was designed for all of these panels, and the location of SBS specimens and acid digestion coupons were evenly distributed across them. However, this assignment method could not be used for panels 6 to 14 since panels 6 and 7 did not have uniform thickness, and panels 8 to 14 had considerable thickness variations and non-uniform porosity distribution.

The SBS and void content test coupons for these panels were obtained from different porosity levels. At least two SBS specimens were assigned to each different porosity level, in order to perform consistent H/W and RT/D SBS testing. The size of each SBS specimen (width and length) was determined based on the thickness-variation results.

3.6 Void Content

Based on the layout configuration, void-content specimens were cut and their densities measured. The method used here for measuring the densities of the majority of the samples was water immersion. However, for specimens with visible surface voids, this method could not be utilized, so the size and mass of the samples were used to calculate the density.

There are different methods to investigate the void content in laminated composites. The method of characterizing voids plays an important role in obtaining realistic results. The acid digestion method, which can be performed according to ASTM 3171-99 [43], is one acceptable test method for obtaining the void contents of samples. In the current study, this method was performed to obtain the void-content and fiber-volume fraction of all samples.

3.7 Short Beam Shear Test

SBS tests were performed according to ASTM D2344 [25]. This test method is one of the popular methods used for quality control, primarily because of its simplicity. Also, performing this test at cryogenic or elevated temperature is relatively easy [26]. This method was chosen since it is very sensitive to matrix properties and void content. A schematic picture of the SBS test method for flat laminates can be seen in Figure 7 [25]. The results of this method give the apparent interlaminar shear strength of the composite, which is a matrix-dominated property that is affected to a large extent by the void level in the laminate and also the environmental condition.

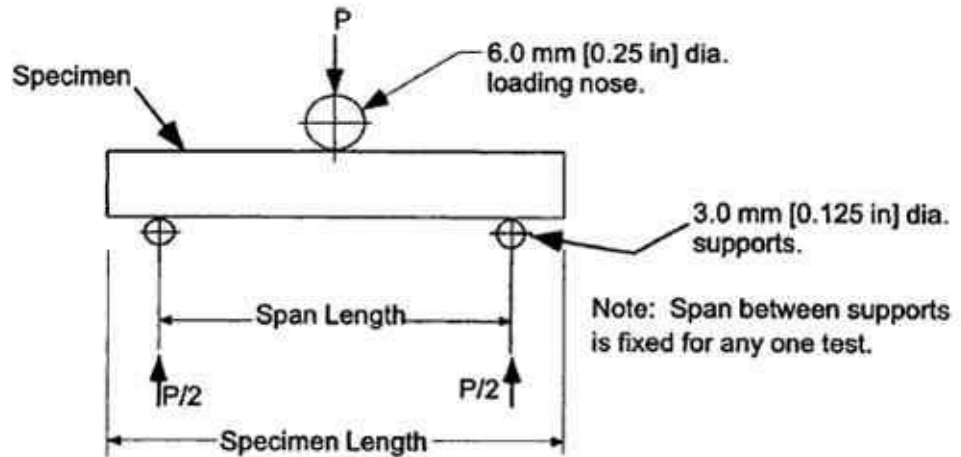


Figure 7. SBS test set up for flat laminates [25].

As mentioned previously, the location of SBS test coupons was assigned randomly for panels 1 through 5. However, the SBS test coupons for panels 6 to 14 were obtained from different spots with different porosity levels.

To perform RT/D and H/W testing, half of the coupons cut from the panels were conditioned and the other half remained unconditioned. According to ASTM D2344 [25], for the specimen with a different thickness from the typical value in the standard, width and length dimensions were determined by the thickness multiplied by 2 and the thickness multiplied by 6, respectively. For example, for panel 6 in the present study, typical specimen dimensions were length 2.5 cm, width 0.8 cm, and thickness 0.42 cm.

3.7.1 Room Temperature/Dry Condition

Tests were performed at room temperature on unconditioned coupons. The average value and standard deviation of SBS strength were reported for each panel. In addition, for panels 6 through 14, the value of SBS strength for each test specimen was reported and correlated with the specimen's porosity level.

3.7.2 Hot/Wet Condition

Test coupons were conditioned at 71° C with 85% relative humidity for 30 days according to ASTM D5229/D5229M-92(2004) [44]. Testing was performed at 82° C. The average value and standard deviation of SBS strength were reported for each panel. In addition, for panels 6 to 14, the value of SBS strength for each test coupon was reported and correlated with the specimen's porosity level.

3.8 Correlation between Void Content, Density, and SBS Strength

To correlate the SBS strength to the void content, the average void content, density, and fiber-volume fraction (obtained by acid digestion method) of the coupons near each SBS sample was utilized.

An exponential model was fitted to the experimental data relating SBS strength to the void content and density.

As mentioned in the literature review, most previous studies have focused on finding the empirical relation between SBS strength and void content. However, two theoretical equations were previously developed [20-22] to correlate void content and fiber-volume fraction to the interlaminar shear strength based on configuration of the voids.

For cylindrical voids, equation (2) can be defined as:

$$ILSS_r = 1 - [4V_v/3.14(1 - V_{fv})]^{1/2} \quad (2)$$

For spherical voids, equation (3) can be defined as:

$$ILSS_r = 1 - 0.785[6V_v/3.14(1 - V_{fv})]^{2/3} \quad (3)$$

where V_v is void content, V_{fv} is fiber-volume fraction, and $ILSS_r$ is the ratio of the interlaminar shear strength of laminates with voids to the interlaminar shear strength of void-free laminates.

Experimental data and the exponential model fitted to them were compared to the theoretical prediction obtained using equations (2) and equation (3).

3.9 Investigation of Failure Mechanisms

The short beam shear method is not commonly used for design purposes because of the complexity of failure modes. Further study on the failure mechanism occurring in the SBS test would be helpful in order to fully benefit from the results.

In most studies, only the values of interlaminar strength have been reported, and the failure mechanism has not been investigated. In this study, the cross sections of failed SBS specimens (H/W and RT/D) were observed using a Zeiss optical microscope to investigate any variation in failure mode.

CHAPTER 4

RESULTS AND DISCUSSION

4.1 Thermal Analysis

4.1.1 Degree of Cure

Degree of cure was obtained for cure cycles 1 to 5, due to the known effect of cure temperature on the degree of cure. The results can be seen in Figure 8. The maximum DOCs for these cure cycles are shown in Figure 9. As can be seen, there is a decreasing trend in the DOC value by reducing the isothermal cure temperature. This drop is most significant for panel 5, which had the lowest curing temperature.

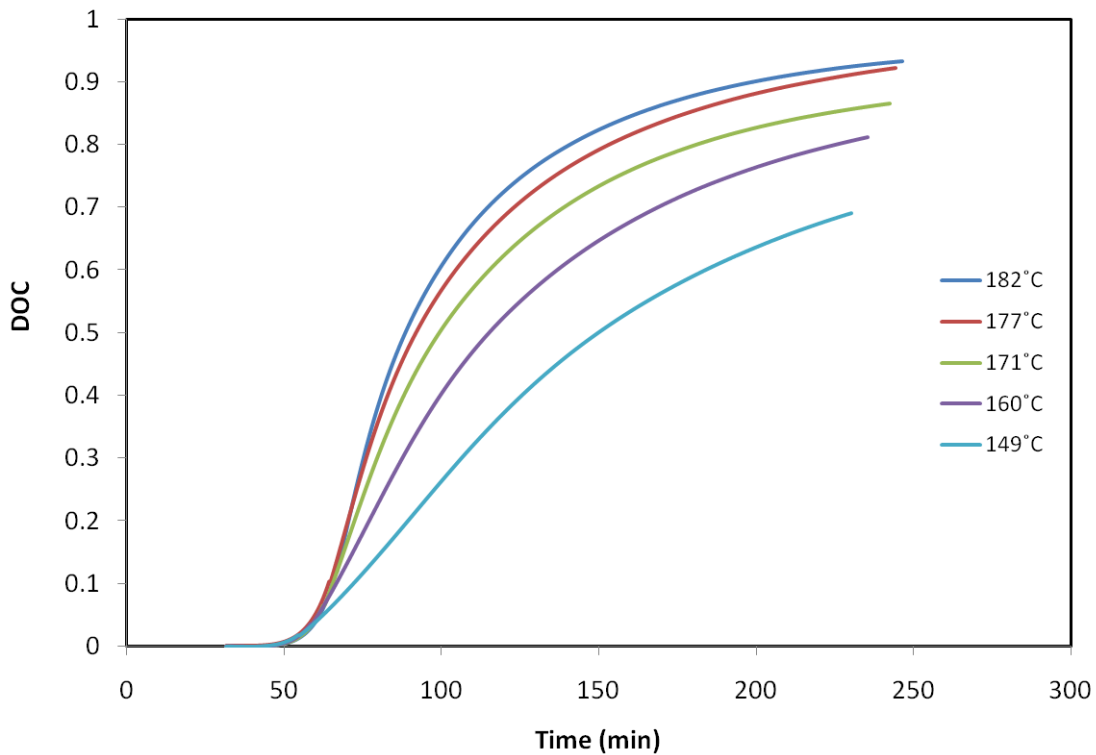


Figure 8. DOC during cure for panels 1 to 5 with different cure temperatures.

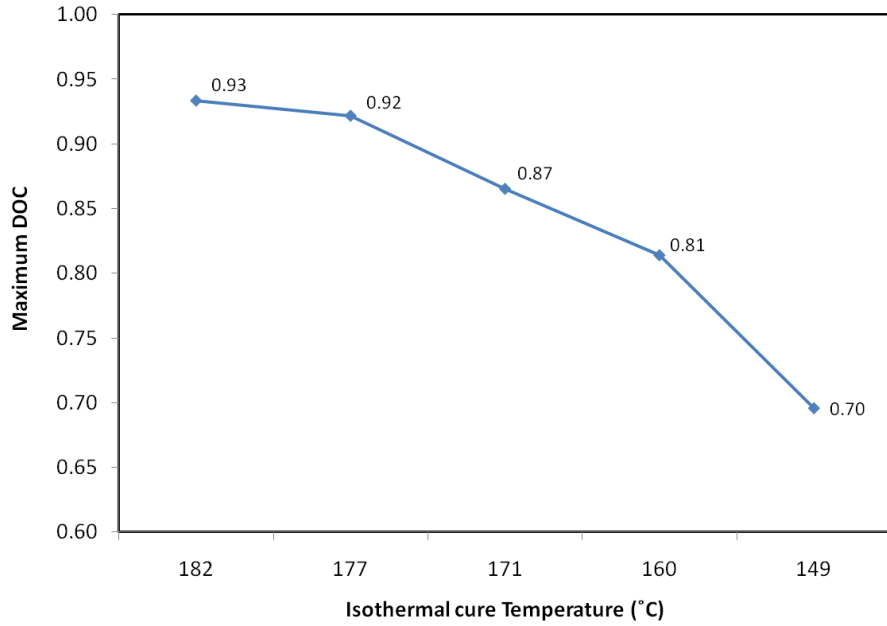


Figure 9. Final DOC for panels 1 to 5 with different cure temperature.

4.1.2 Glass Transition Temperature

Similar to the final DOC, the glass transition temperature (T_g) value shows a decreasing trend with reduced cure temperature, with the lowest value associated with panel 5, which had the lowest curing temperature. Results can be seen in Figure 10.

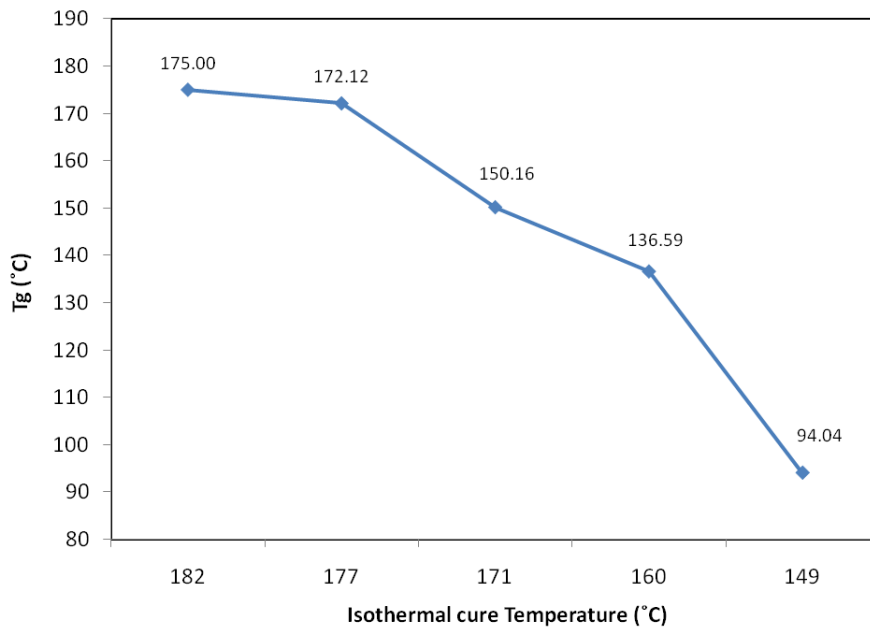


Figure 10. Glass transition temperature (T_g) for panels 1 to 5 with different cure temperatures.

4.2 Ultrasonic C-Scan

C-scan results for panels 6 to 14 can be seen in Figure 11. C-scans of panels 1 to 5 are similar to those for panels 6 and 7, and are not shown here. No defects were detected in C-scan results for panels 1 to 7. A large nebulous defect was detected in the middle of panel 8. For panels 9 to 13, which were under vacuum throughout the cure, a cross-shaped defect was observed at the center of the panels. For panel 10, which was cured according to MRC cycle, except for holding vacuum throughout, the defects were distributed more evenly. It is interesting to note that the dimensions of the observed cross-shaped defect increased with decreasing cure pressure. Panel 14, which was cured with no pressure, had very little ultrasonic signal transmitted, indicating widespread defects throughout the panel.

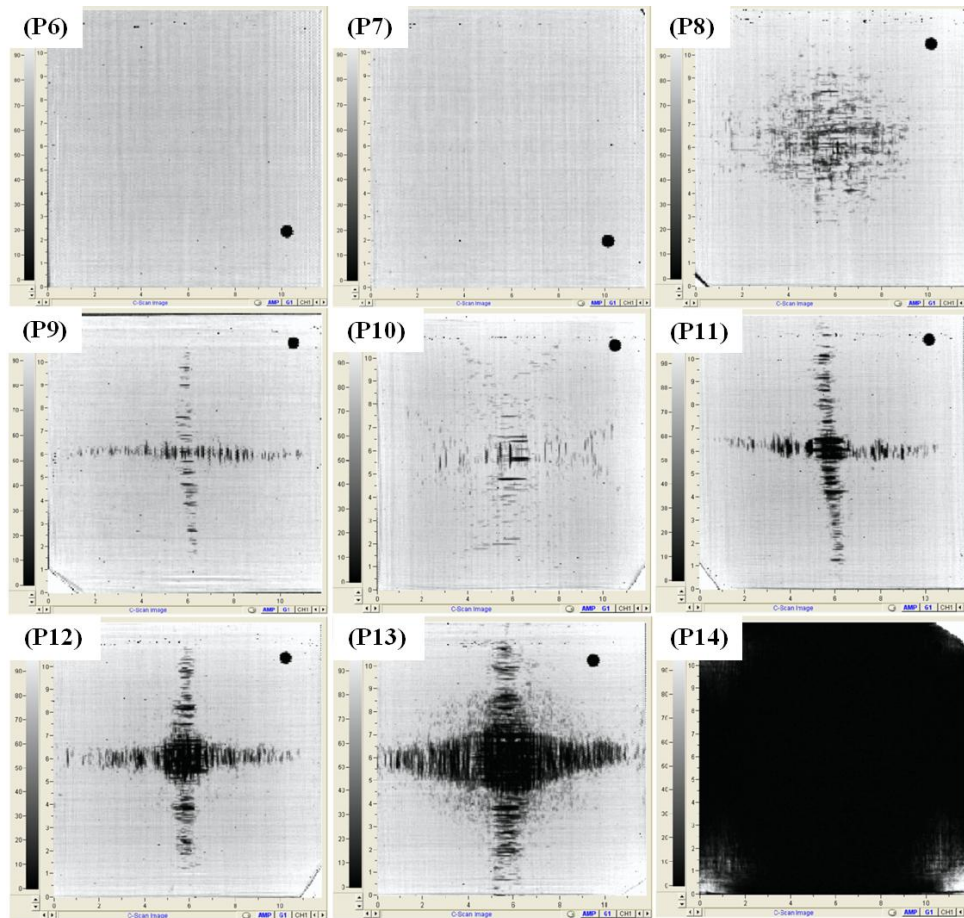


Figure 11. C-scan results for panels 6 to 14.

4.3 Thickness Variation

It was observed that panels 1 to 5, unlike the rest of the panels, did not have significant thickness variations. Apparent distortion and thickness variation could be observed with the naked eye in panels 6 to 14, which was expected, due to reduced pressure and/or inappropriate application of vacuum. Therefore, panels 6 to 14 were inspected using a coordinate measurement machine.

Figure 12 shows the average thickness and thickness variation for panels 6 to 14. As it shown, the thickness variation of panels 6 to 8 was less than that of panels 9 to 14, primarily due to the difference in vacuum application. While the vacuum was vented once the cure pressure reached 69 kPa for panels 6 to 8, it was maintained throughout the cure cycle for panels 9 to 14. Moreover, the thickness variation increased as the cure pressure was reduced for panels 9 to 14. Thickness measurements and C-scan results suggest that pressure is required to obtain a uniform panel that is free of defects.

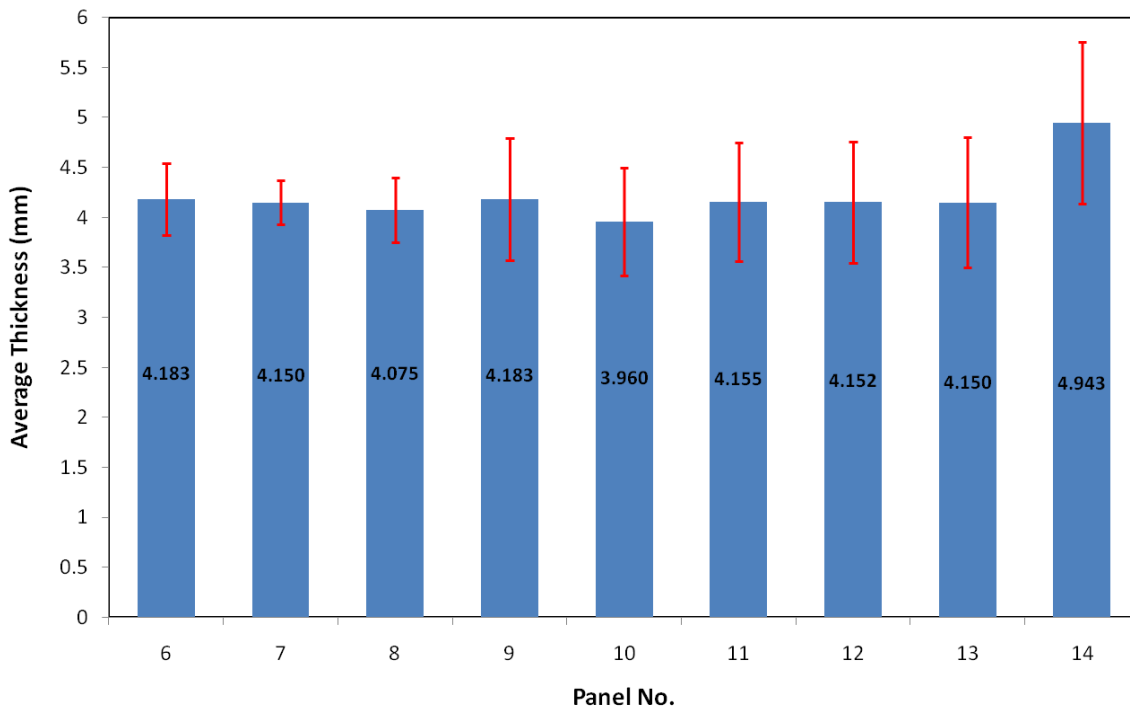


Figure 12. Average thickness of panels 6 to 14 along with thickness variation shown as error bars.

Figure 13 shows the contour plots of thickness variation for panels 6 to 14. The maximum thickness for all panels was detected in the center, and thickness decreased gradually toward the edges in a circular pattern. For panels 6 to 13, the variation range on the plot is from 1.5 mm to 5 mm, and for panel 14, which is the one that had no pressure but vacuum hold throughout the cure cycle, the range is from 1.5mm to 6 mm. The wider range of variation for this panel shows the effect of autoclave pressure on thickness.

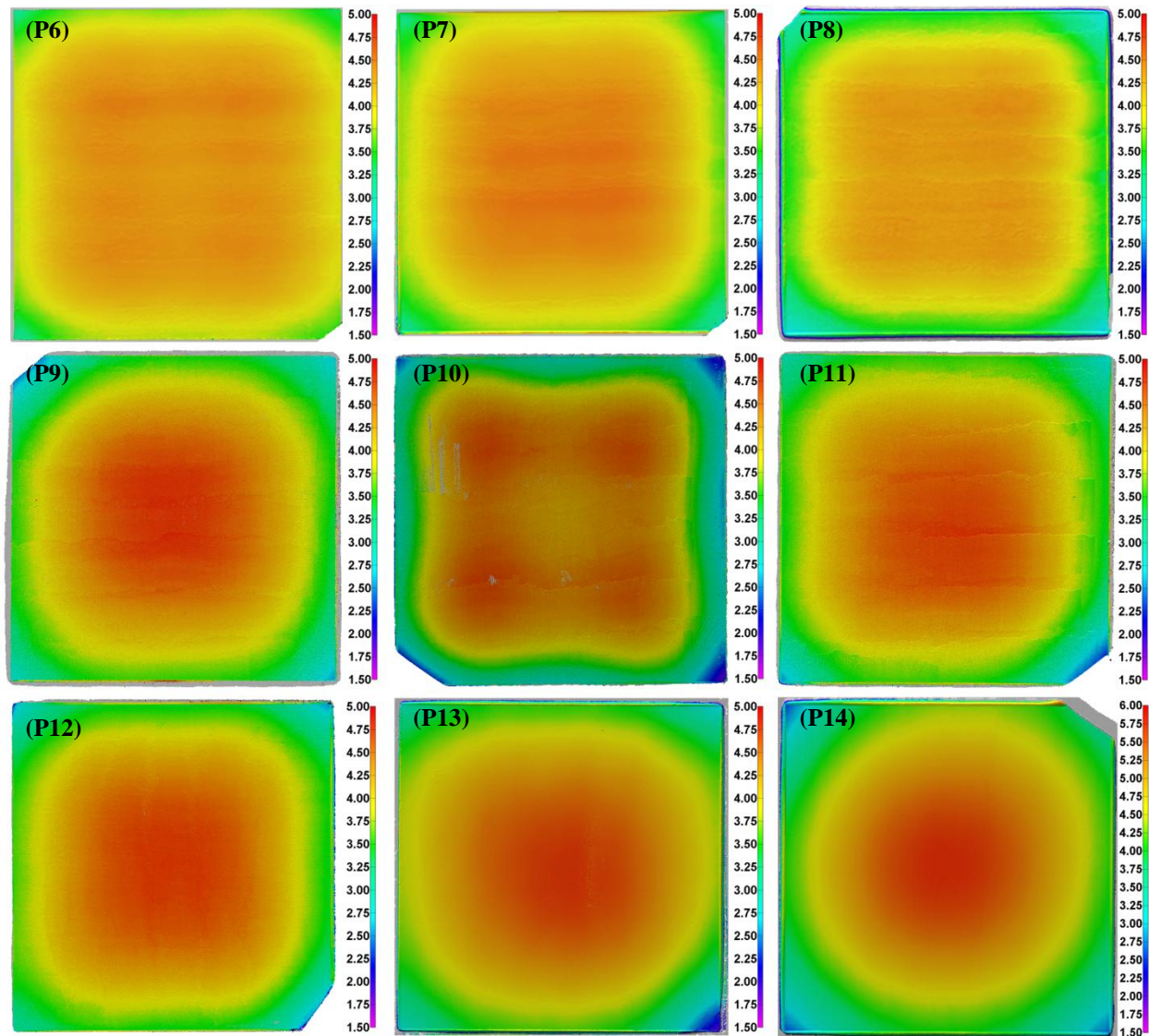


Figure 13. Thickness variation contour plots for panels 6 to 14.

4.4 Panel Layout Configuration

Due to the uniformity observed in panels 1 to 5, one layout was designed for all panels, and the location of SBS specimens and acid digestion coupons were evenly distributed across the panels. Different parameters, including thickness and C-scan data, were considered in choosing the proper layout for panels 6 to 14, in order to thoroughly investigate their properties and make meaningful correlations. The layout for panels 6 to 14 can be seen in Figure 14, superimposed on top of the thickness variation contours, along with the C-scans. Due to the thickness variations for panels 6 to 14, the thickness contours obtained with a CMM were utilized to calculate the dimensions of the SBS specimen (width and length), in order to maintain the ratios required by ASTM D2344.

The layouts used for panels 6 to 14 were very similar to each other except for some changes in the size of SBS coupons due to variation in thickness. Moreover, for panels that did not have cross-shaped defects, the location of SBS samples in the center and also void content samples at the edges were more evenly distributed. As can be seen in Figure 14, the SBS and acid digestion test coupons for panels with cross-shaped defects were obtained from different porosity levels including the cross-shaped defects.

Acid digestion samples were marked as center (CE), middle (MI), corner (CO), and edge (ED); and SBS specimens (RT/D) were marked with numbers in order to be able to assign proper porosity and density to each SBS specimen. As an example in Figure 14, the average values obtained for samples CE and MI were assigned to specimen number one. Following the same pattern, the average of MI and ED was assigned to sample 2, MI was assigned to sample 3, ED was assigned to sample 4, and CO was assigned to samples 5, 6, and 7.

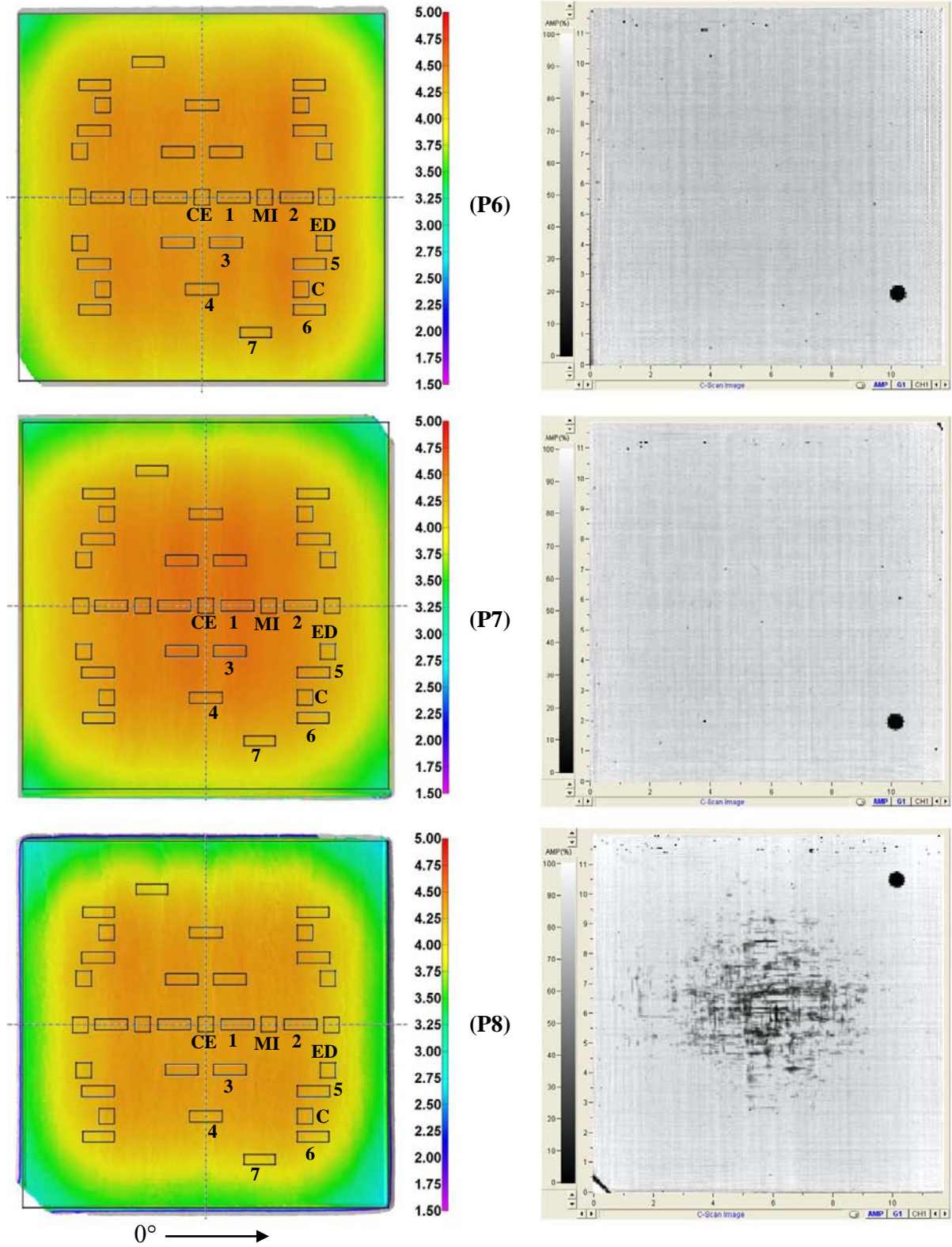
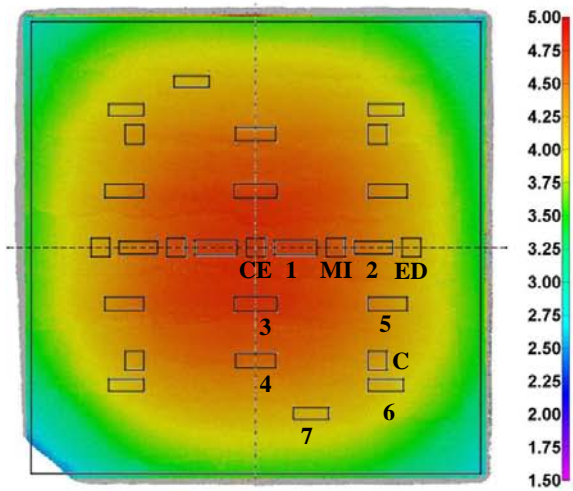
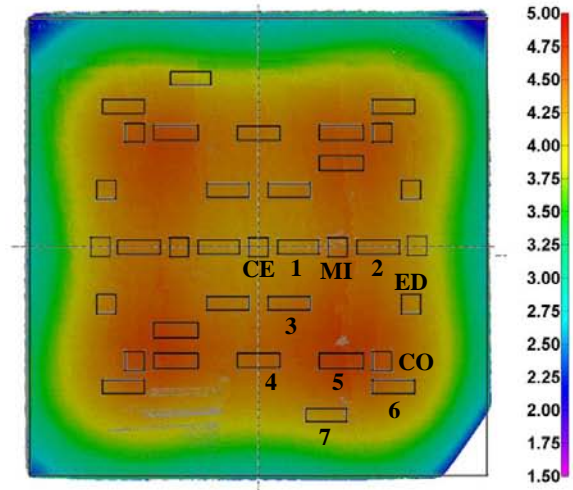
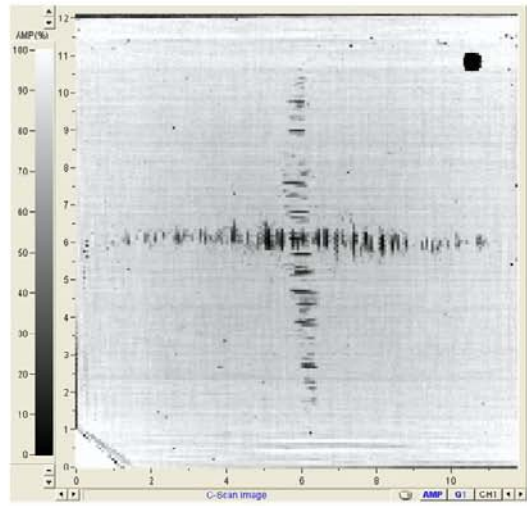


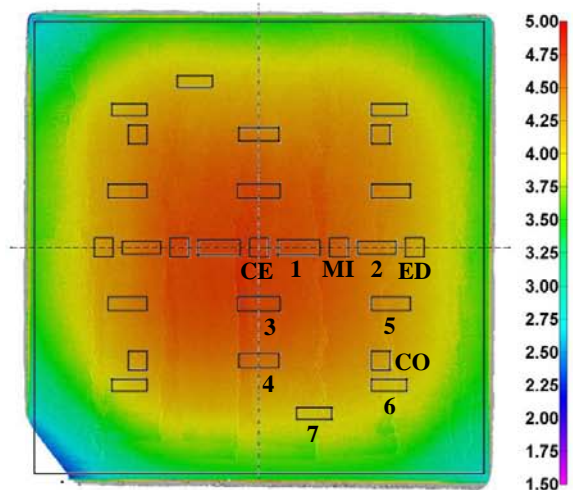
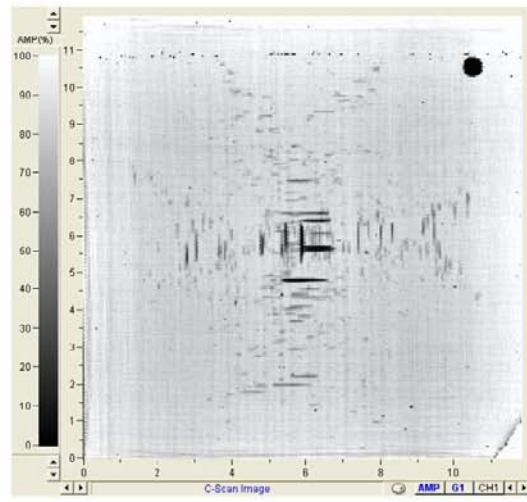
Figure 14. Thickness variation contour plots with designed layout on top, along with C-scan data for panels 6 to 14.



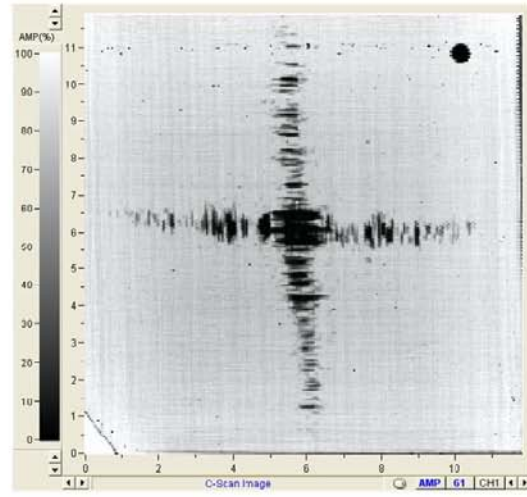
(P12)



(P10)



(P11)



0° →

Figure 14 (continued)

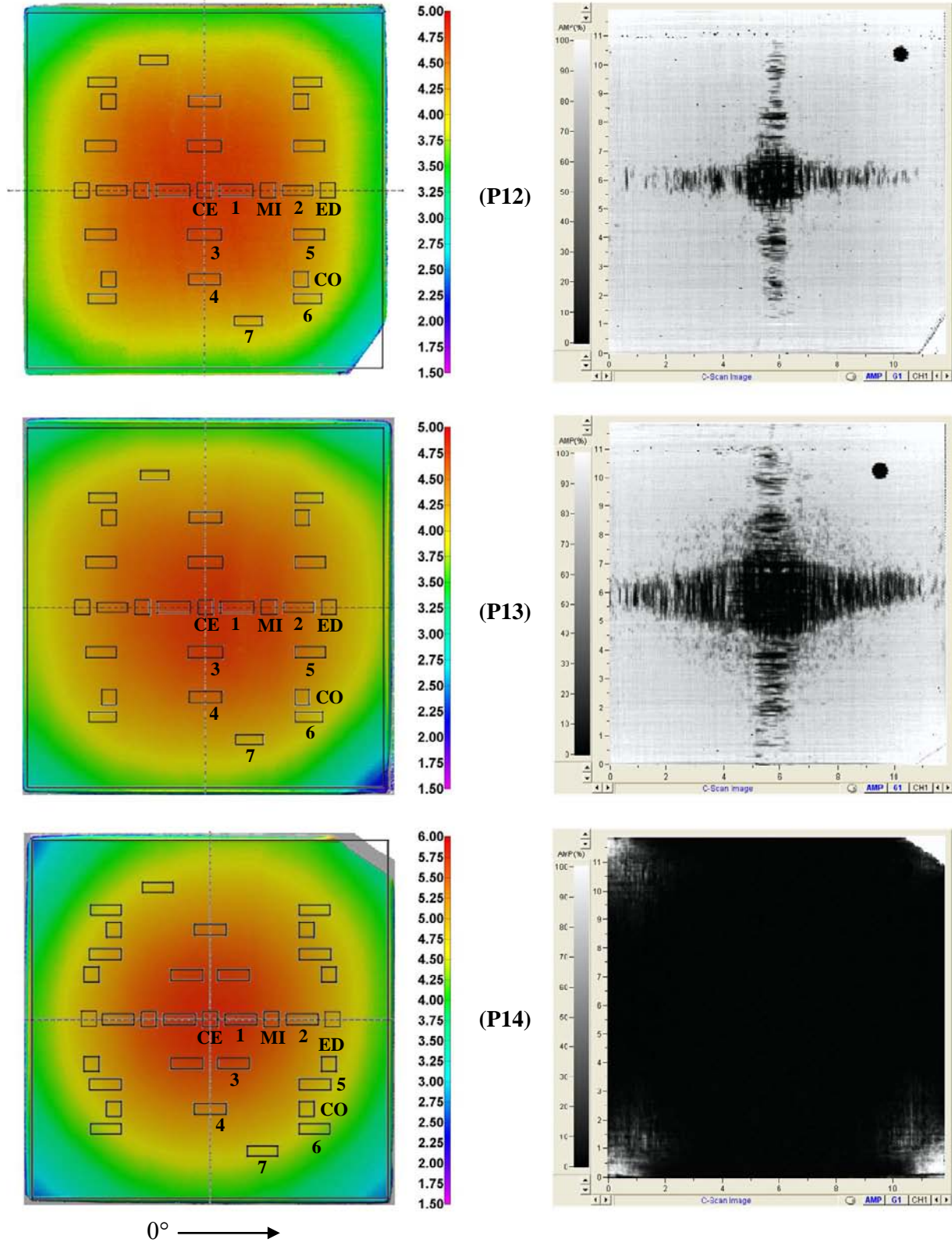


Figure 14 (continued)

The same procedure was performed to assign porosity levels to H/W samples. These samples were taken from the upper left side of the panels to be consistent with RT/D specimens. These assignments were used to determine the relation between SBS strength and some properties including void content, density, and fiber-volume fraction.

4.5 Void Content

The average void content for all panels can be seen in Figure 15 which shows the void content for center, middle, and corner locations. As expected, no significant void volume content was observed for panels 1 to 5.

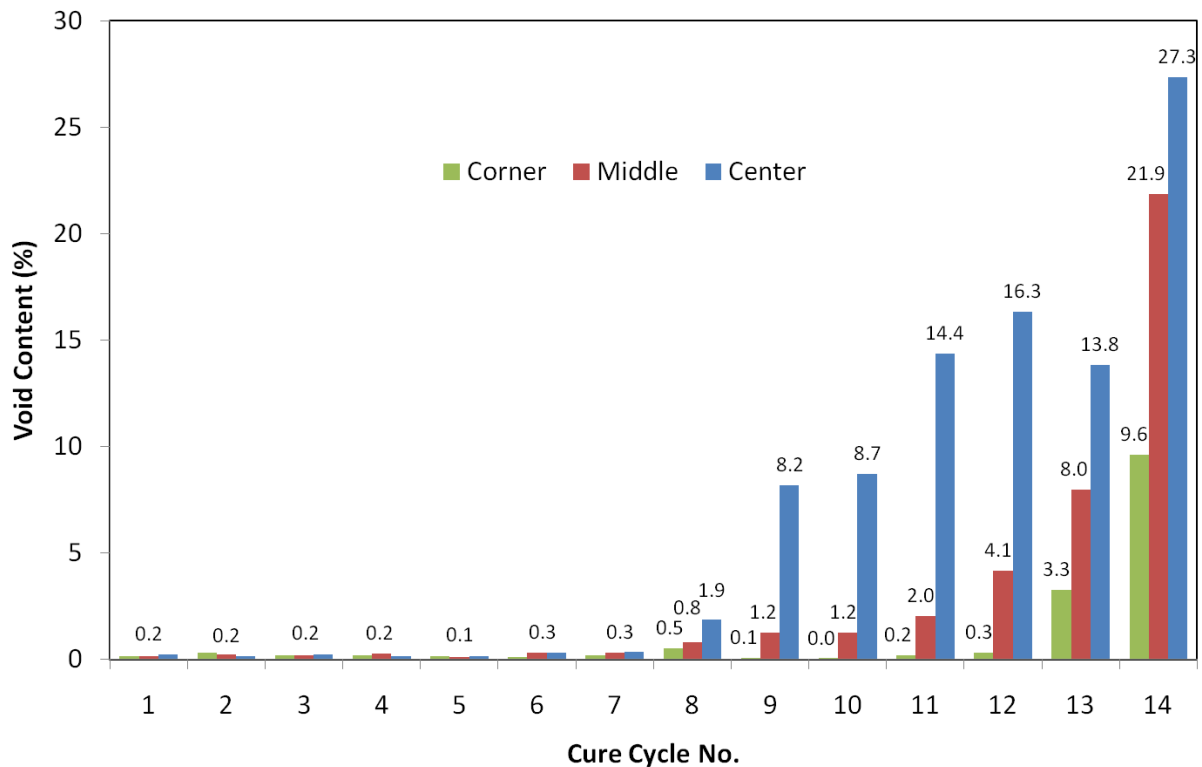


Figure 15. Void content for cure cycles 1 to 14 at center, middle, and corner locations.

Figure 16 illustrates void volume content vs. cure pressure for panels 6 to 14. As can be seen, void volume content increased significantly when vacuum was kept throughout the cure cycle. This increase was more dominant for samples taken from the center of panels. The average density of cured prepreg vs. cure pressure for panels 6 to 14 can be seen in Figure 17.

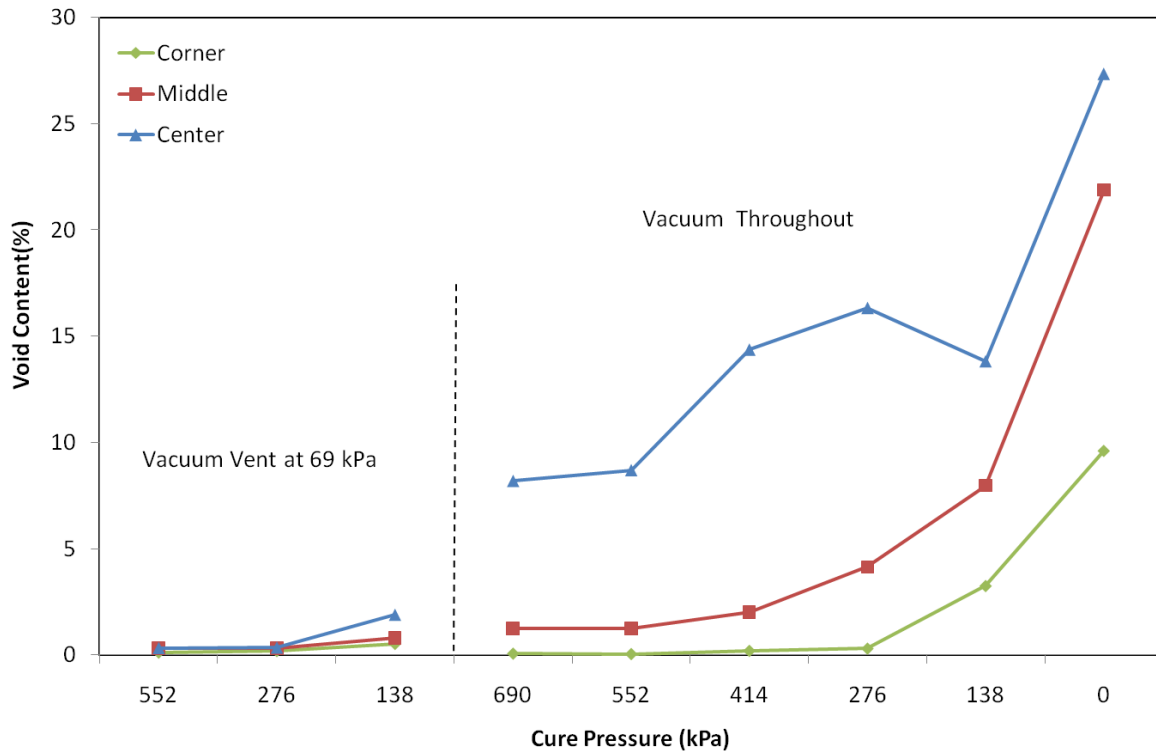


Figure 16. Void content for cure cycles 6 to 14 at center, middle, and corner locations.

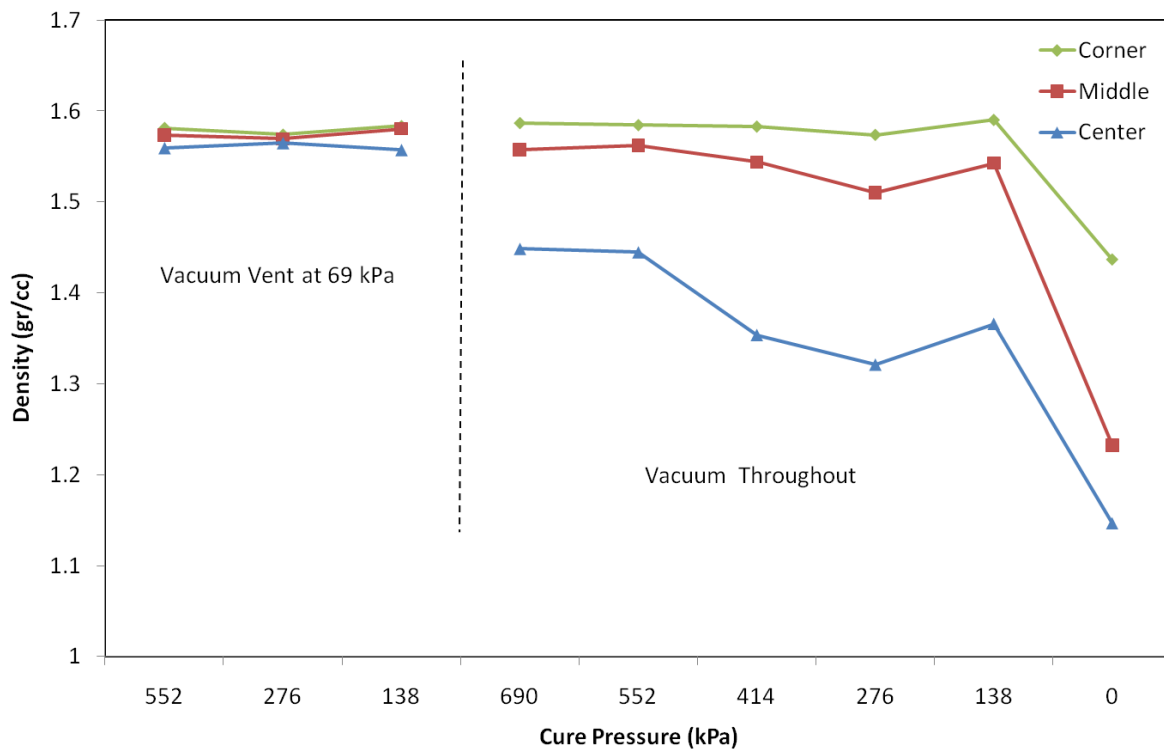


Figure 17. Density for cure cycles 6 to 14 at center, middle, and corner locations.

As Figure 17 shows, the density of the cured prepreg dropped as the cure pressure decreased. This drop in density was more pronounced for panels 9 to 14 for which vacuum was maintained throughout the cure cycle. Similar to the results for void content, the most significant variation was observed for the center coupons.

Figure 18 shows the average fiber-volume fraction vs. cure pressure for panels 6 to 14. It can be seen that panels 9 to 14, where vacuum was held during the cure cycle, had more variation in the fiber-volume fraction.

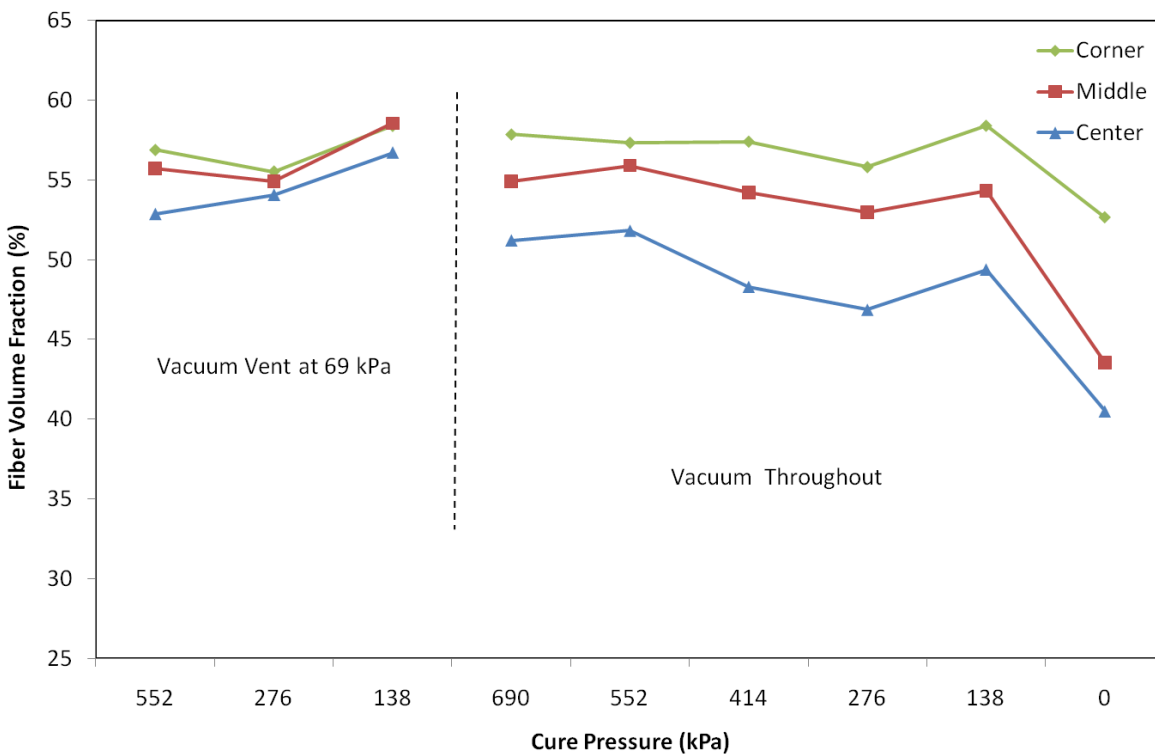


Figure 18. Fiber-volume fraction for cure cycles 6 to 14 at center, middle, and corner locations.

There is a good consistency in the trend of void content, density, and fiber-volume fraction as the pressure decreased. Based on the results of C-scan in Figure 11 and also void content results in Figure 16, it can be concluded that since panels 9 and 10 had a narrow cross-shaped defect in the middle, void content of the CE sample was higher than the MI and CO samples. Panels 11 and 12 had broader cross-shaped defects and dark splotches in the middle,

which created much higher voids in the CE than in the MI and CO. The void content of the CE sample for panel 13 did not follow the exact trend of panels 9 to 12, but it is worth noting that void levels of MI and CO specimens were much higher than those of panels 9 to 12. One of the reasons might be the much wider cross-shaped defect in this panel, which caused not much higher void content in the center, relative to panels 11 and 12, than at the corner and middle. Finally, panel 14 had one large splotch; therefore, CE, MI, and CO all showed high void levels.

To further investigate the effect of vacuuming on the quality of the cured laminate, the average void volume content of panels 6, 7, and 8 was compared with that of panels 10, 12, and 13, respectively. As it can be seen in Figure 19, Figure 20, and Figure 21, maintaining vacuum throughout the cure cycle increased the average void volume content and induced a non-uniform porosity distribution in the panels. As could be observed from the results, holding the vacuum throughout the cure cycle is not beneficial and can cause severe porosity in the laminate.

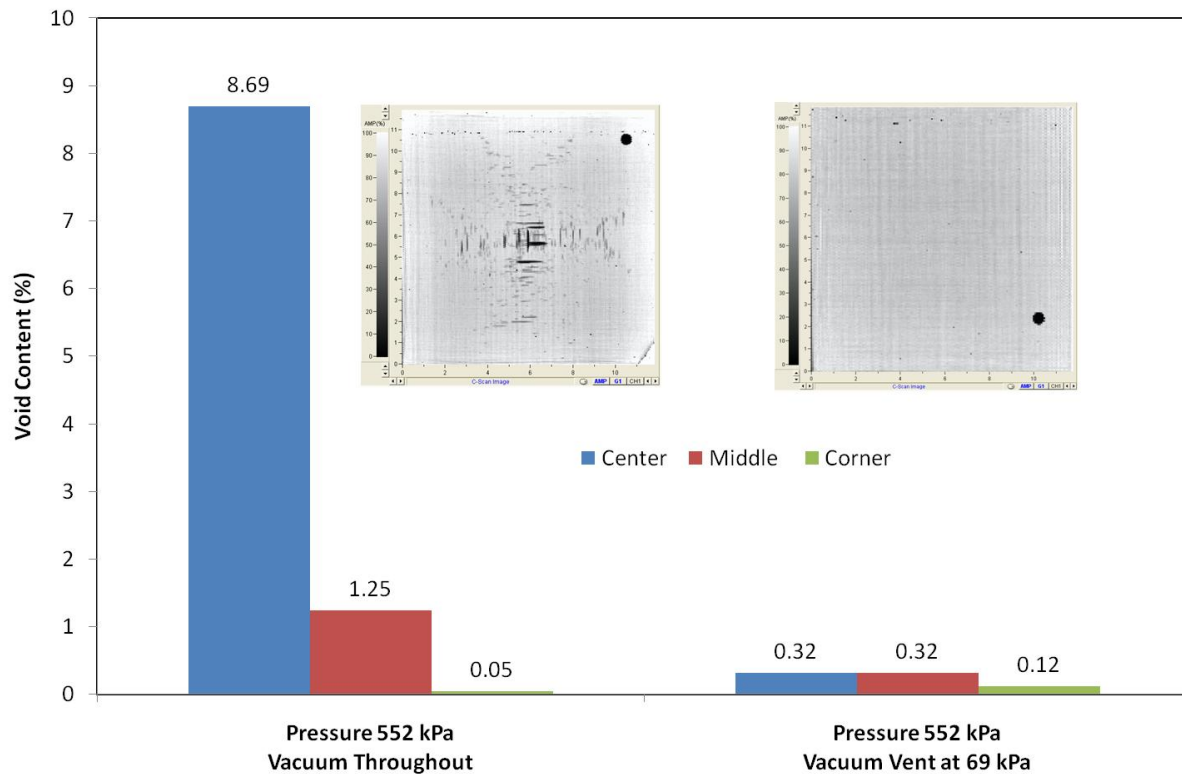


Figure 19. Effect of vacuum-application time on void content for cure pressure of 552 MPa.

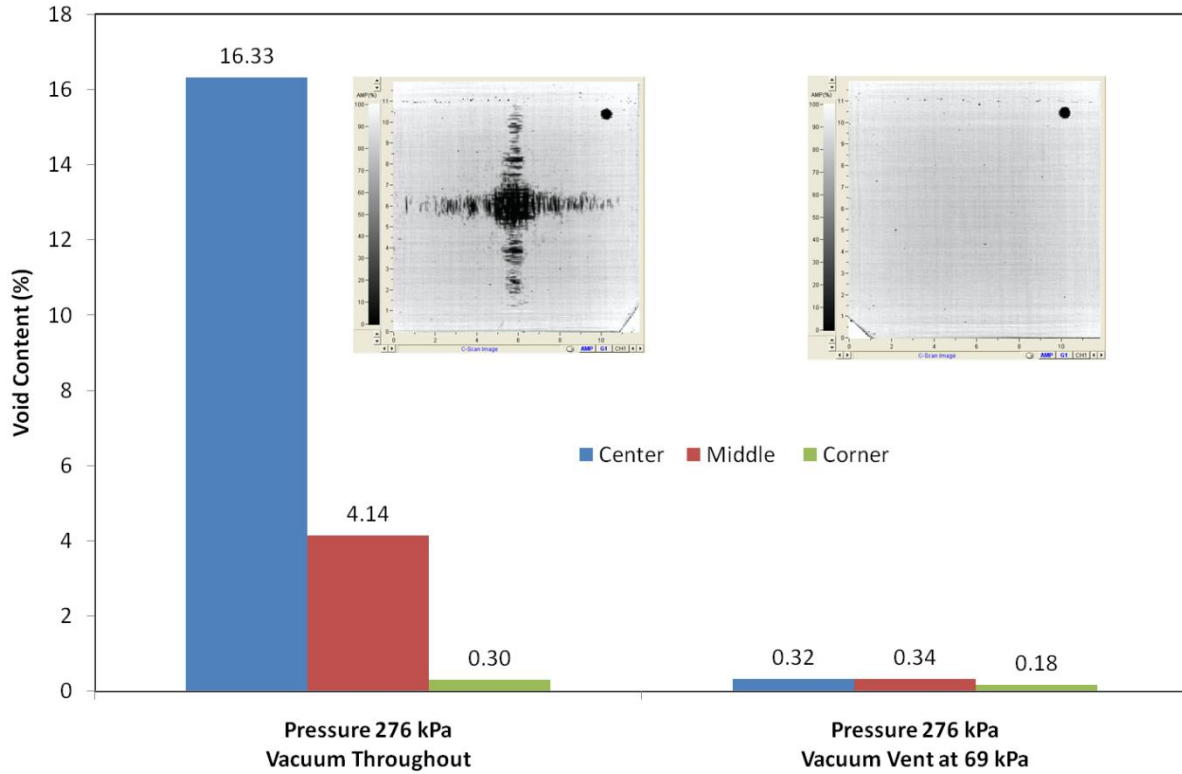


Figure 20. Effect of vacuum-application time on void content for cure pressure of 276 MPa.

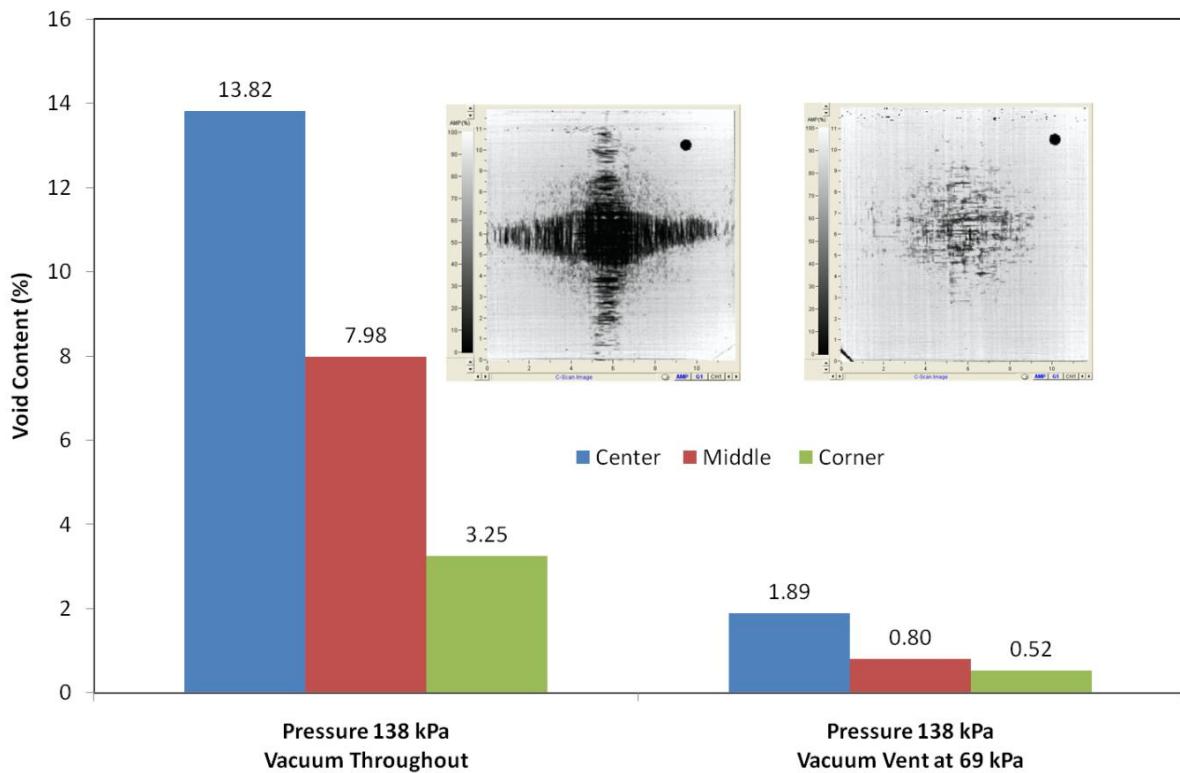


Figure 21. Effect of vacuum-application time on void content for cure pressure of 138 MPa.

Generally, one of the reasons for venting vacuum at certain pressures is to avoid void formation due to excessive resin bleed, especially for a resin system that has a tendency to drop to low viscosity during cure. If the vacuum is held when the resin viscosity is low, then the resin flows to the breather, up to the point that the resin is under vacuum and the bag pressure is fully supported by the fibers. At this stage, the resin has enough volatiles that it may boil and push more resin out of the fibers, which results in the creation of voids. It can also be said that the resin pressure is of great importance, especially before gelation. At this stage, voids may form and grow if the pressure of volatile vapor in a curing laminate goes above the pressure on the liquid resin [1]. It is the pressure on the resin that keeps volatiles dissolved in the solution. In other words, volatiles have a chance to come out of the solution and form voids if the resin pressure becomes less than the volatile vapor pressure. Venting the vacuum ensures that the resin pressure never drops below a certain value.

Figure 22 shows the void distribution across the center of panels 6 to 14. The pictures were taken using a microscope x-y stage. The length of each sample was about 25 cm. As can be seen, no significant voids were observed across panels 6 and 7 (cured at 552 kPa and 276 kPa with vacuum ventilation at 69 kPa). Some scattered voids, mainly in the center, were observed in panel 8, which was cured under 138 kPa pressure with vacuum ventilation at 69 kPa. A pattern can be observed for panels 9 to 14. As mentioned previously, autoclave pressure was the variable in these panels, and vacuum was held during cure cycle.

It can also be seen that the void distribution increased from panel 9 to 14. Panel 9 had just a few visible voids across the cross section, but panel 14 had voids over the entire specimen. Also, debonding could be observed in panel 13 and 14. Another interesting aspect was the distribution of voids in the center. For most of the panels, voids were more dominant in the

center. Also the shape of the voids changed from the middle to the corner. Voids were more cylindrical in shape in the center and more spherical at the corners.

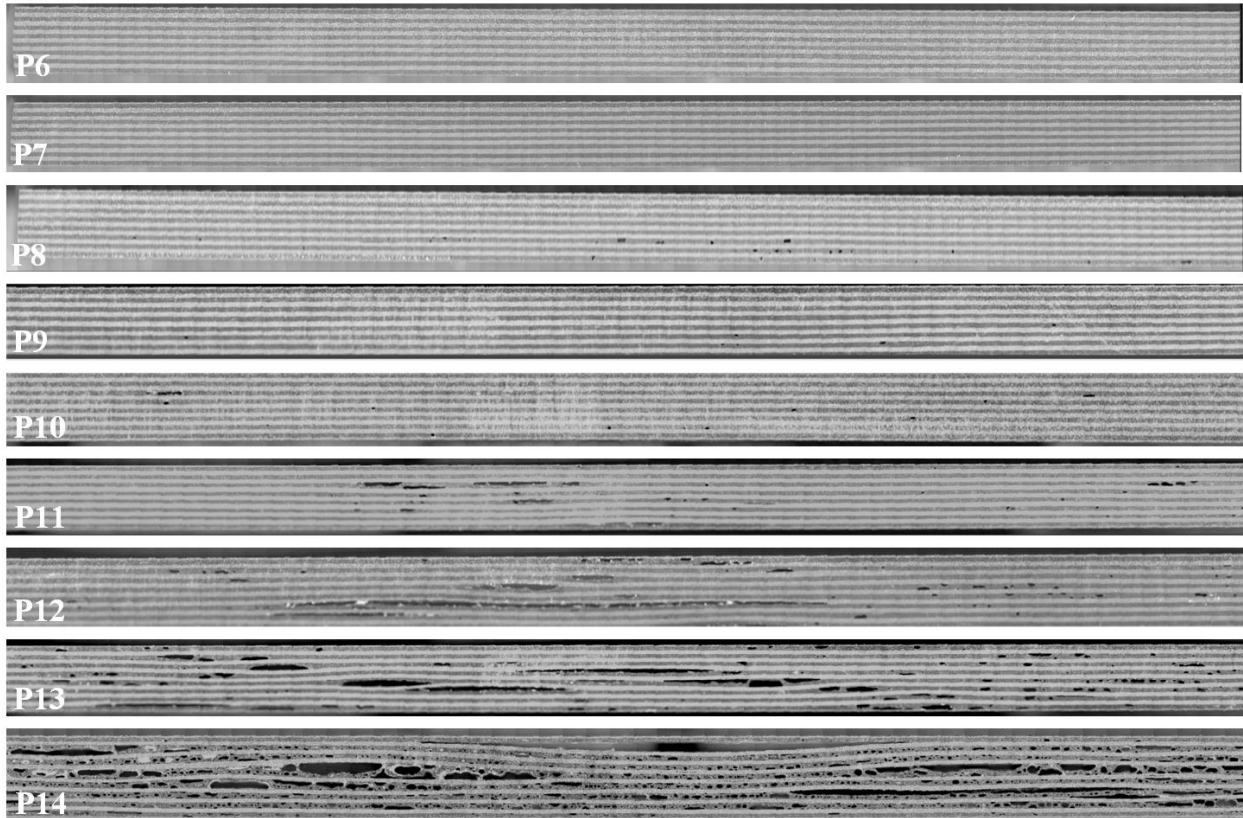


Figure 22. Void distribution across center of panels 6 to 14.

Comparing sections of panels 8 and 13, the effect of vacuum on the void distribution and shape can be observed. It is clear that the panel that had vacuum through the cure cycle showed a very high amount of void relative to panel for which vacuum was held up to 69 kPa.

4.6 Shot Beam Shear Strength

Room temp/dry as well as hot/wet testing was performed for all panels. Panels 9 to 14 had non-uniform porosity distribution. As such, in addition to the average SBS strength of each panel, the SBS strength of each individual coupon was reported for these panels.

4.6.1 Room Temperature/Dry Condition

Figure 23 shows the average RT/D SBS strength for panels 1 to 14. As can be seen, no significant variation in the average SBS strength was observed for panels 1 to 4. However, statistical analysis showed that the average RT/D SBS strength of panel 5 was significantly less than that of the preceding panels. According to the experimental data, the average SBS strength of panel 5 was 10% less than that of panel 4.

A decreasing trend in interlaminar shear strength was observed by reducing the cure pressure. This trend was more pronounced for cure cycles 10 to 14, which had vacuum applied throughout. As can be seen in Figure 23, the standard deviation of SBS strength increased with decreasing cure pressure. The SBS strength variation for panels 9 to 14 was caused by non-uniform porosity distribution in these panels.

It is interesting to notice that for the panels that were not cured properly, for example panel 13 (138 kPa cure pressure), the SBS strength was as high as 88 MPa in low-void areas and as low as 48.2 MPa in high-void locations (near the center). In general, the specimens with lower porosity had higher SBS strength, as will be seen later on in Figure 26.

4.6.2 Hot/Wet Condition

The average H/W SBS strength for panels 1 to 14 is shown in Figure 24. For each panel, the average H/W SBS strength was lower than the corresponding average RT/D SBS strength. A decreasing trend can be observed for panels 1 to 5. Similar to the RT/D condition, the drop was more significant for panel 5.

For panels 6 to 14, the observed trend of H/W SBS strength for all panels was similar to that of RT/D SBS strength. Similar to the RT/D case, deviation in the H/W SBS strength for panels cured with low pressures can be observed.

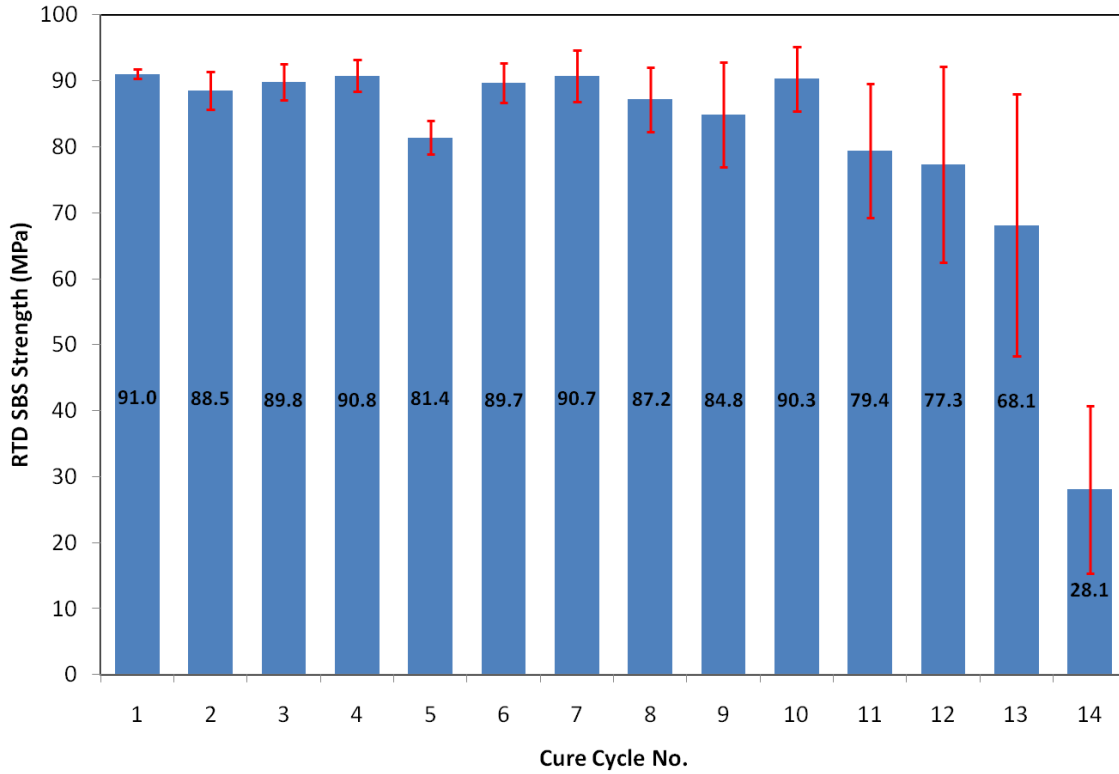


Figure 23. Average RT/D SBS strength for cure cycles 1 to 14.

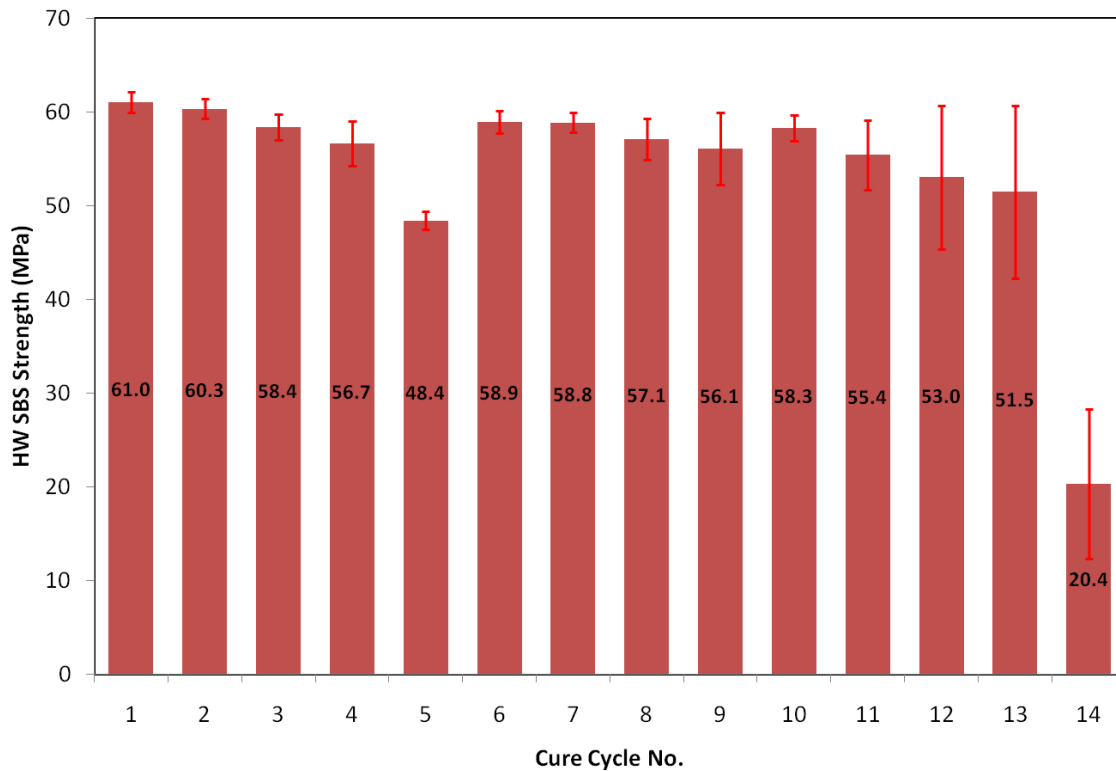


Figure 24. Average H/W SBS strength for cure cycles 1 to 14.

There are several reasons for the reduction observed in the H/W SBS strength of epoxy laminate. First of all, water absorption can cause matrix plasticization which can reduce the glass transition temperature. Also humidity and temperature can affect matrix properties, which decrease the laminate strength. In addition, these two factors can induce stresses that may cause fiber-matrix degradation.

4.6.3 Comparison

Table 4 contains the average values of RT/D and H/W SBS strengths along with standard deviations and coefficients of variation for panels 1 to 14. The percentage reduction of H/W SBS strength as compared to RT/D SBS strength for each panel is also included in the table and indicates the extent of the effect of the H/W environment.

For panels 1 to 5, the percentage of reduction increased by reducing the cure temperature, and consequently decreasing the degree of cure. However, for panels 6 to 14, the reduction percentage decreased by reducing the cure pressure. Overall, it appears that the H/W SBS strength is more sensitive to the cure temperature variation than to the cure pressure variation and ultimately variation in void content. One of the reasons might be the lower T_g value as the cure temperature decreases.

As mentioned in the literature review, the yield stress of thermosetting resins at temperatures below T_g is related to T_g values [27]. Based on equation (1), samples with lower T_g values show less strength in elevated temperatures. The decreasing trend of H/W SBS strength for panels 1 to 5 is consistent with this theory [27]. The observation is especially dominant for the H/W SBS strength of panel 5, which was cured the least and had the lowest amount of T_g .

TABLE 4

STATISTICAL RESULTS OF RT/D AND H/W SBS STRENGTH OF CURE CYCLES 1 TO 14

Cure Cycle No.	Room Temperature/Dry			Hot/Wet			Reduction (%)
	Strength (MPa)	STDEV (MPa)	COV (%)	Strength (MPa)	STDEV (MPa)	COV (%)	
1	91.01	0.72	0.79	61.03	1.10	1.80	32.93
2	88.54	2.88	3.25	60.32	1.07	1.77	31.88
3	89.85	2.70	3.00	58.37	1.35	2.31	35.03
4	90.78	2.39	2.63	56.67	2.38	4.21	37.57
5	81.38	2.55	3.14	48.41	0.97	2.01	40.51
6	90.72	3.89	4.28	58.83	1.05	1.79	35.15
7	89.71	3.05	3.40	58.92	1.18	2.00	34.32
8	87.16	4.90	5.62	57.06	2.19	3.83	34.54
9	84.84	7.93	9.35	56.09	3.88	6.91	33.89
10	90.32	4.89	5.42	58.28	1.41	2.41	35.47
11	79.42	10.20	12.84	55.40	3.73	6.74	30.24
12	77.29	14.85	19.22	53.03	7.63	14.39	31.39
13	68.12	19.89	29.20	51.46	9.18	17.84	24.46
14	28.07	12.72	45.31	20.35	7.98	39.20	27.49

4.7 Correlation between Void Content, Density, and SBS Strength

The correlation between void volume content and RT/D SBS strength can be seen in Figure 25. Figure 26 shows the correlation on a semi-logarithmic scale. It can be seen that the RT/D SBS strength decreased exponentially by increasing the void content. As such, an exponential equation was fitted to the experimental data and is shown on the graph. Figure 27 illustrates the correlation between void volume content and H/W SBS strength. The relation can be seen in Figure 28 on a semi-logarithmic scale. The trend of H/W SBS strength versus void

content was very similar to the trend observed in RT/D case. It can be seen in Figure 27 that H/W SBS strength decreased exponentially by increasing the void content. Therefore, an exponential equation was fitted to the experimental data and is shown on the graph.

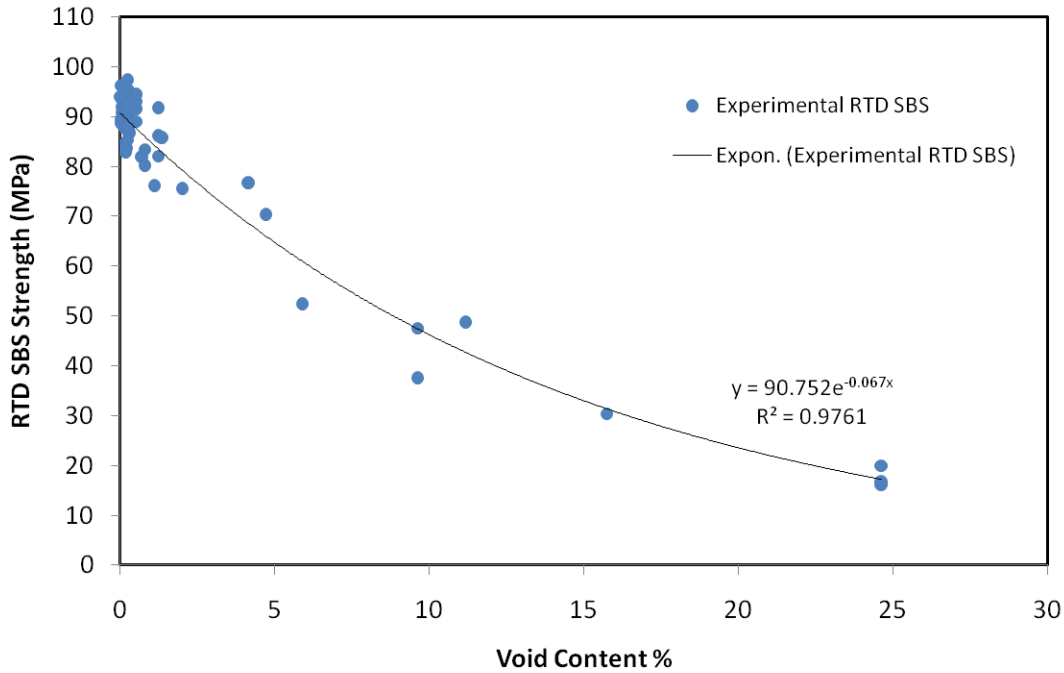


Figure 25. Correlation between RT/D SBS strength and void content.

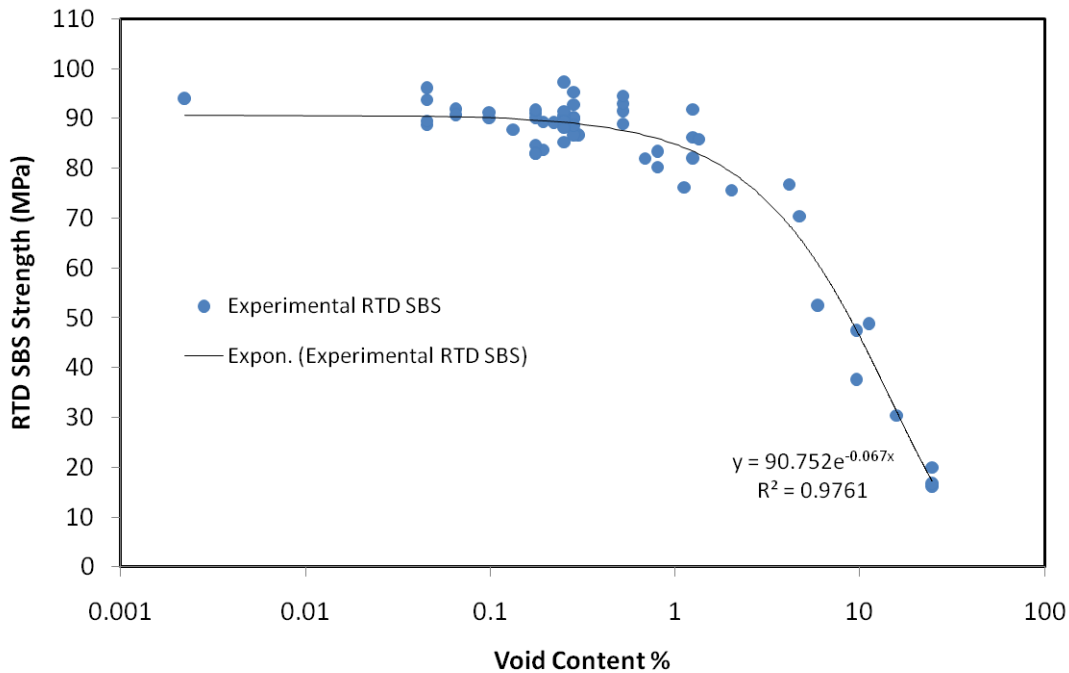


Figure 26. Correlation between RT/D SBS strength and void content on semi-log scale.

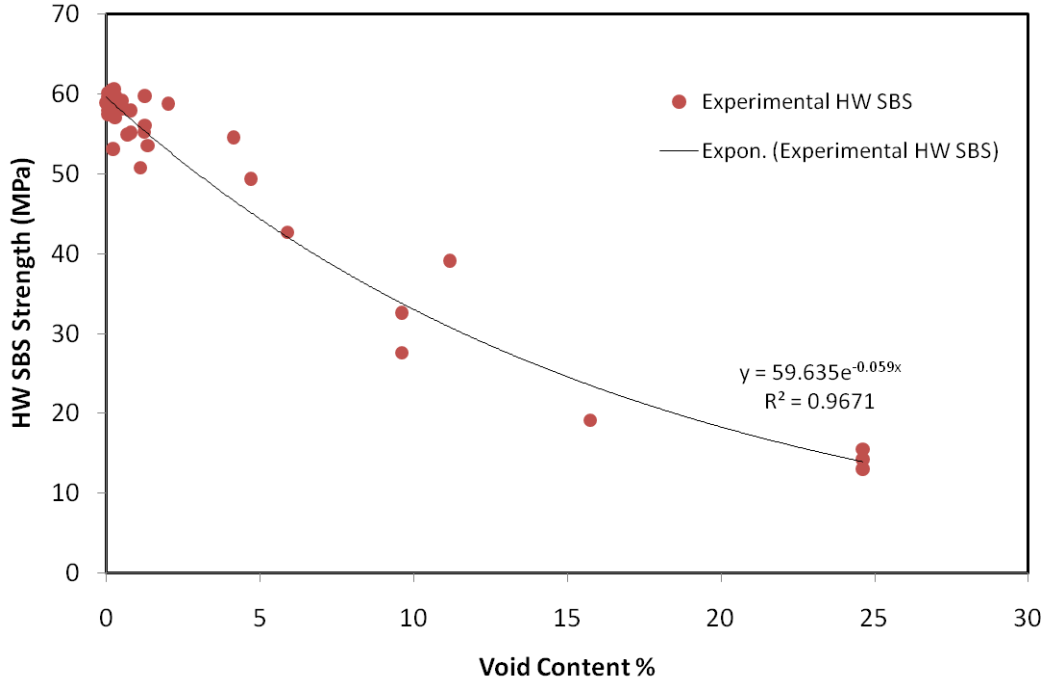


Figure 27. Correlation between H/W SBS strength and void content.

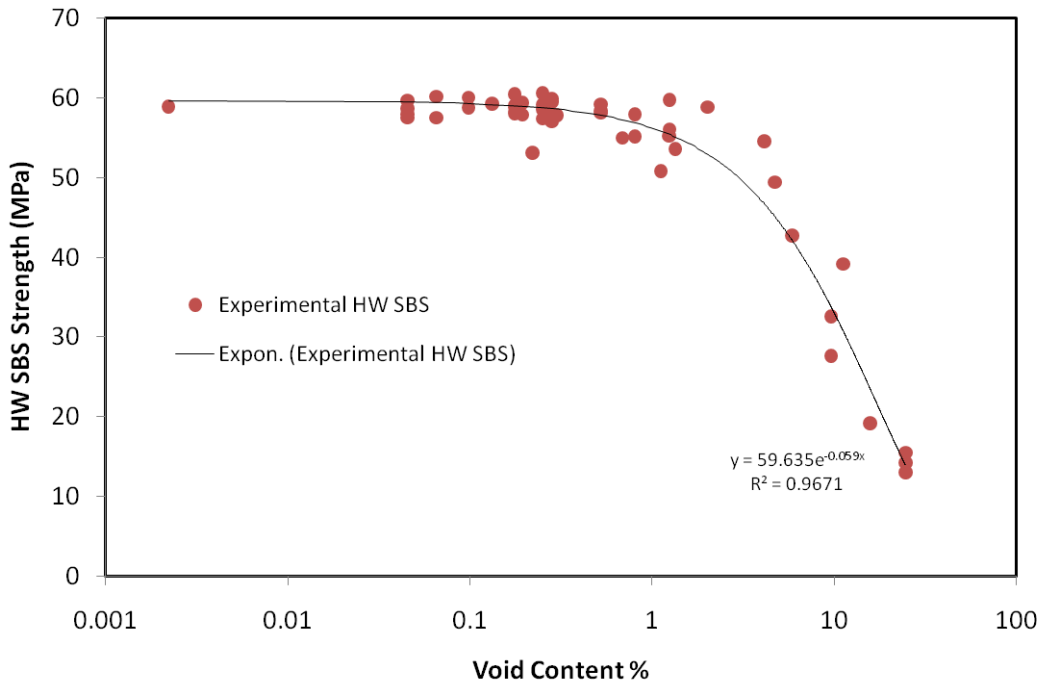


Figure 28. Correlation between H/W SBS strength and void content on semi-log scale.

The correlation between cured laminate density and RT/D SBS strength is shown in Figure 29, and Figure 30 illustrates the correlation between cured laminate density and H/W SBS strength. Results show that RT/D and H/W SBS strengths increased exponentially as the density

of the cured laminate increased. As such, an exponential equation was fitted to the experimental data. However, the fit was better in the RT/D correlation case.

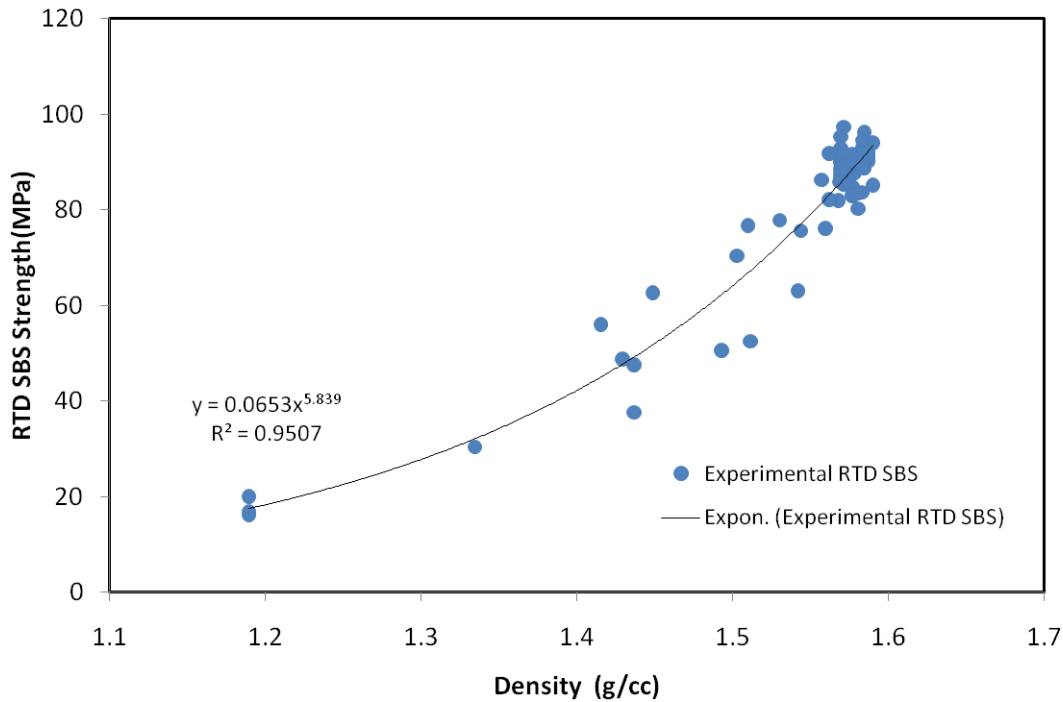


Figure 29. Correlation between RT/D SBS strength and composite density.

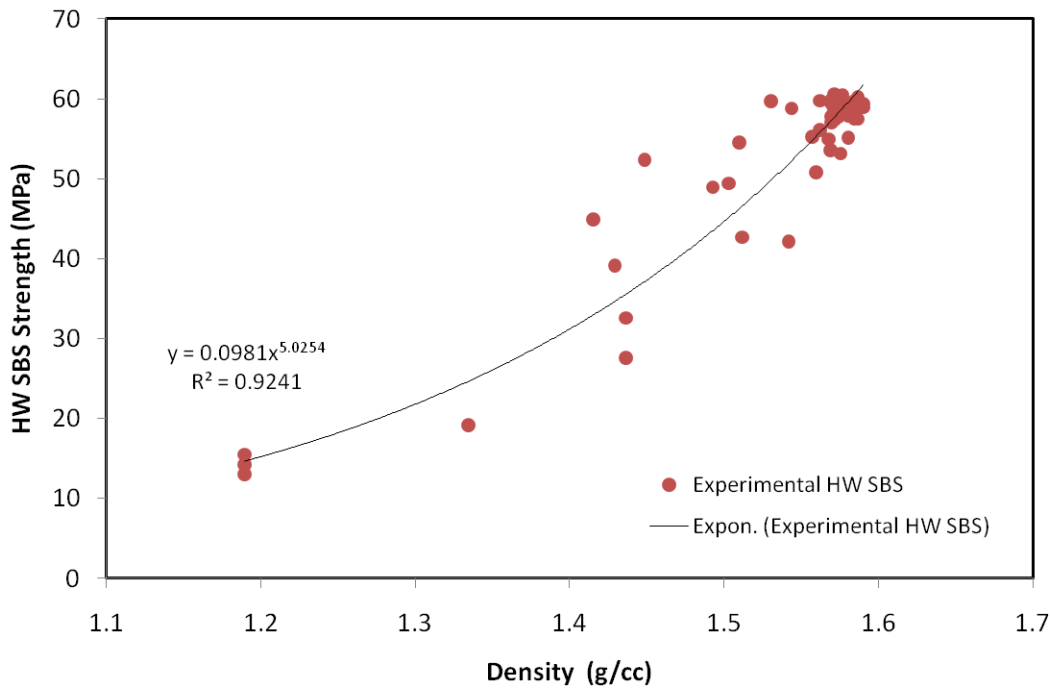


Figure 30. Correlation between H/W SBS strength and composite density.

4.7.1 Comparison between Experiment and Theory

Figure 31 shows the experimental RT/D SBS strength data along with two theoretical curves obtained with equations (2) and equation (3). The data have been normalized, dividing by the average SBS strength of the void-free specimens. The results on a semi-logarithmic scale can be seen in Figure 32.

Figure 33 shows the normalized experimental H/W SBS strength data along with two theoretical curves obtained with equations (2) and (3). The results can be seen on a semi-logarithmic scale in Figure 34. As the figures show, the trend of H/W SBS strength is similar to that of RT/D SBS strength. Similar to the RT/D SBS case, debonding may have caused a deviation from the theoretical line.

Overall, equation (2), which is for cylindrical voids, is closer to the experimental data than equation (3), which was developed for spherical voids. The results are consistent with the voids observed in the failed specimens, which appeared to be elongated and aligned in the fiber directions.

Moreover, as the figures also show, for void volume contents less than 1%, the experimental data agreed well with the theoretical models. However, as the void volume content increased, the models gradually deviated from the experimental data. One of the main reasons for this deviation might be the presence of delaminations in the laminates, which were considered as voids in measurements but more severely affect SBS strength.

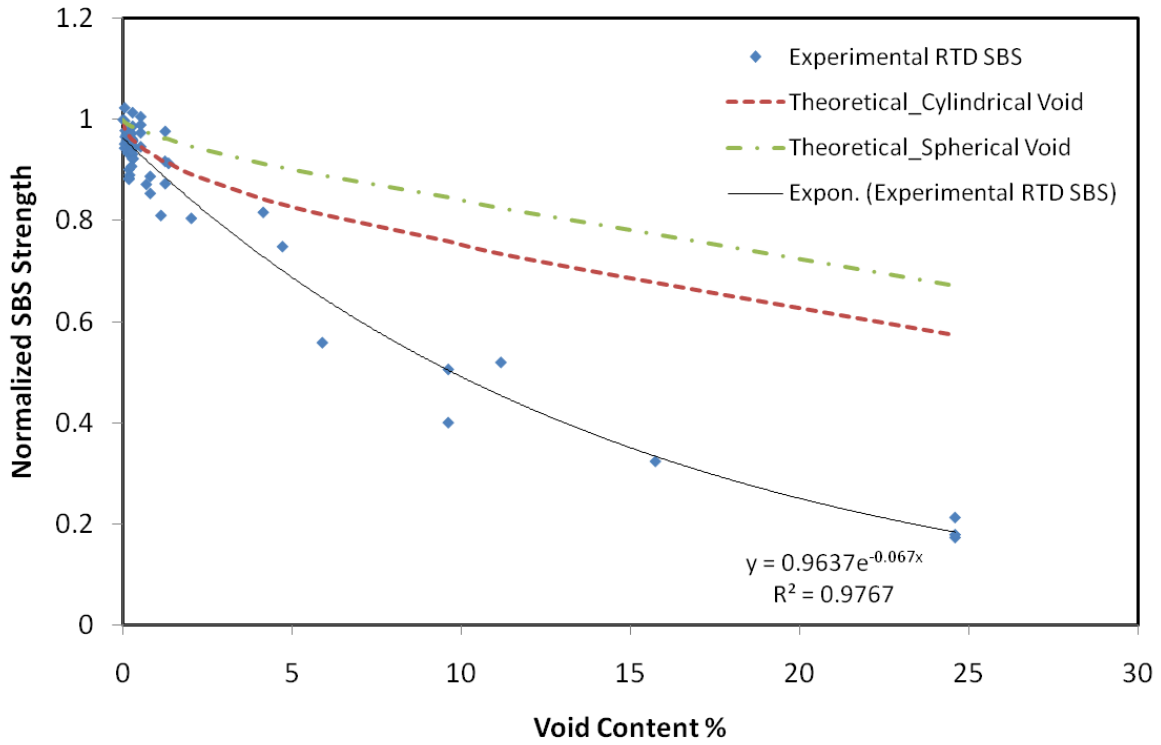


Figure 31. Comparison of normalized RT/D SBS strength and theoretical lines.

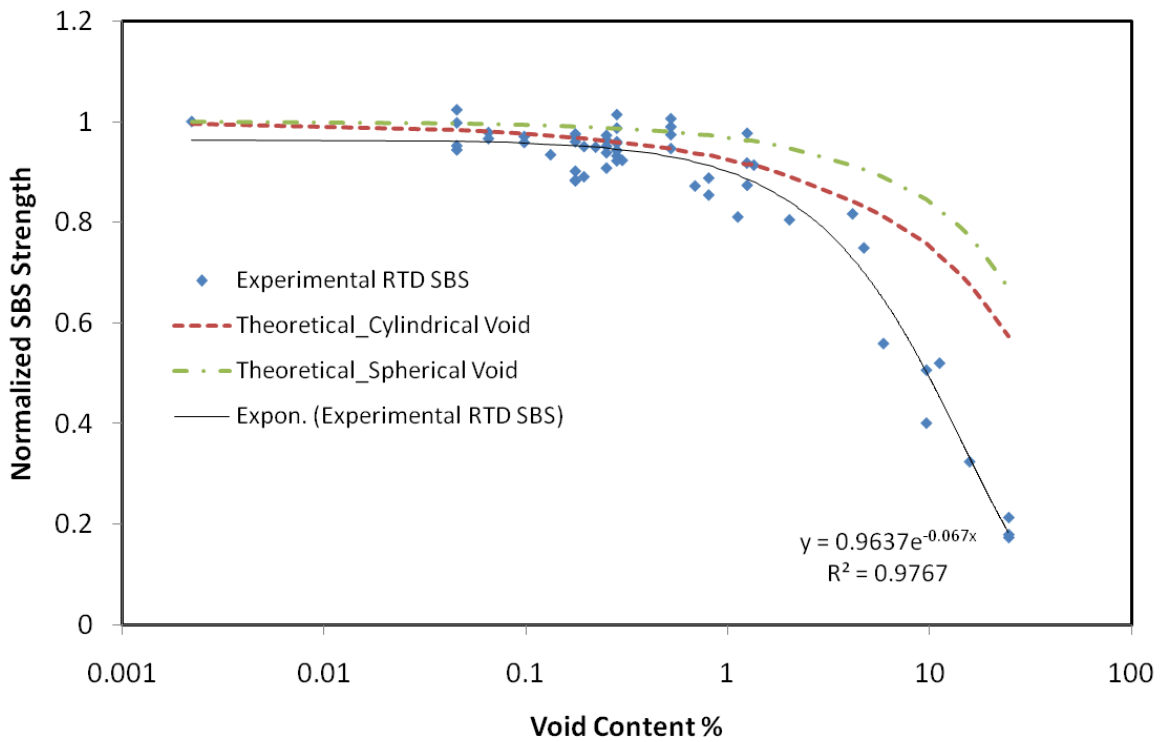


Figure 32. Comparison of normalized RT/D SBS strength and theoretical lines on a semi-log scale.

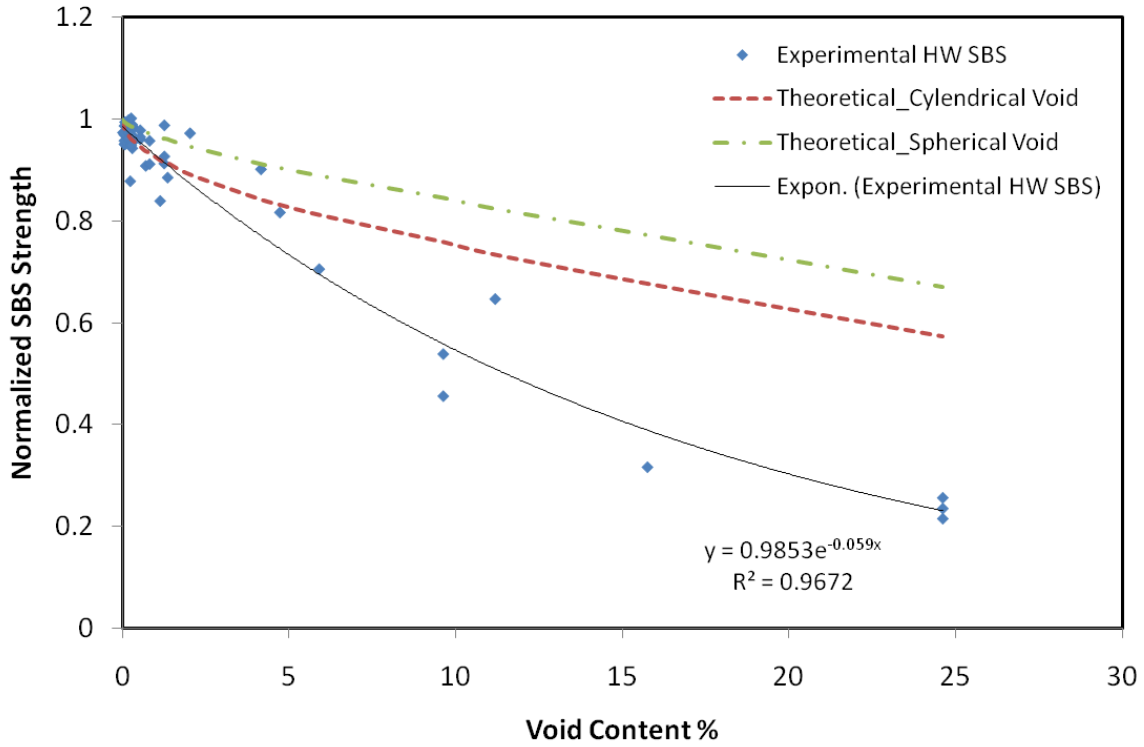


Figure 33. Comparison of normalized H/W SBS strength and theoretical lines.

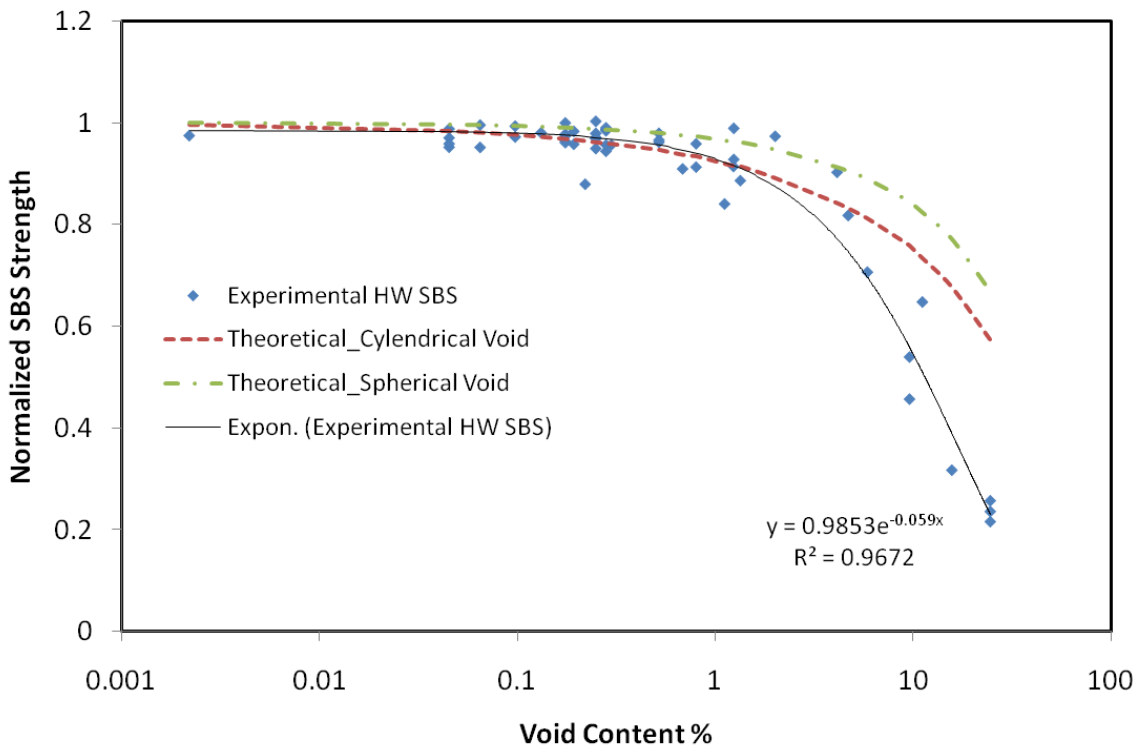


Figure 34. Comparison of normalized H/W SBS strength and theoretical lines on a semi-log scale.

4.8 Failure Mechanism

One of the main components of this study was to investigate the SBS failure mechanism for all different cure cycles. Images in the following sections were taken using a motorized x-y stage under an optical microscope. The acceptable failure modes for SBS testing are shown in Figure 35 [25]. The failure mechanisms for RT/D and H/W tests are discussed in the following sections.

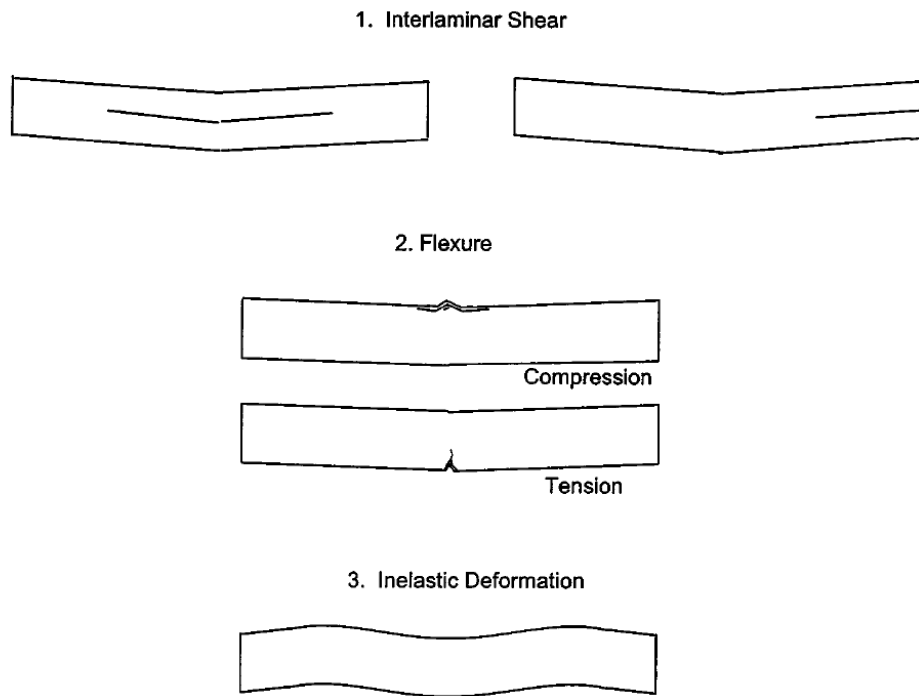


Figure 35. Typical acceptable failure modes in SBS testing [25].

4.8.1 Room Temp/Dry Condition

The cross section of a typical failed SBS specimen for panels 1 to 5 is shown in Figure 36. The lighter bands are 0° plies, with fibers running from left to right in the photo. The darker bands are 90° plies, with fibers perpendicular to the page. For these specimens, failure started under the loading nose and propagated toward the edges. It was found that the SBS failure mode for all panels except panel 5 was compression-interlaminar shear. The failure mode for panel 5

was interlaminar shear. The failure modes for all panels were acceptable according to ASTM D2344 [25]. To further investigate the failure mode for different panels, SBS specimens were observed under an optical microscope.

Figure 37 shows a typical photomicrograph of the failed SBS specimen at the middle and under the loading region for the sample from panels 1 to 4. The failure mode was mostly similar for samples of panels 1 to 4.



Figure 36. Typical failed RT/D SBS specimen of panels 1 to 5.

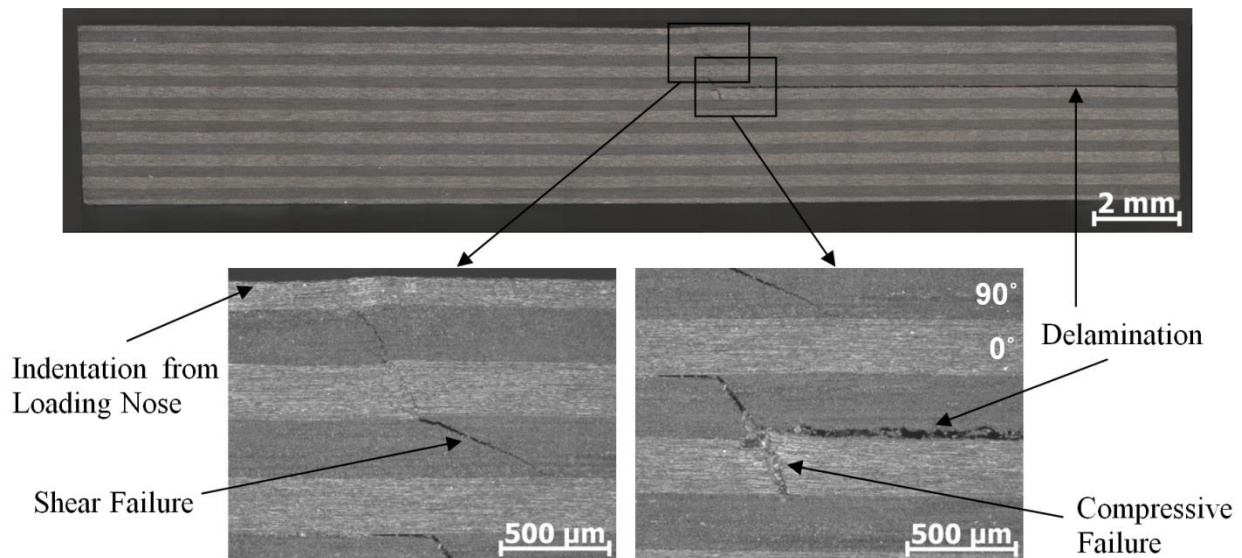


Figure 37. Typical photomicrograph of failed RT/D SBS specimen of cure cycles 1 to 4.

Figure 37 shows the cross section of a failed SBS specimen under the loading nose region. As can be seen, compression of 0° plies occurred under the loading nose in the form of fiber kinking (microbuckling), and a crack started beneath that. The resulting crack propagated into different layers of the specimen causing delamination. However, the cracks did not

propagate up to the very end of the section in the transverse direction. It should be mentioned that in those areas far from the loading nose, cracks propagated through the 90° plies rather than the 0° plies.

The mechanism of crack initiation and progression observed for panels 1 to 4 was not exactly observed for panel 5. The photomicrograph of the failed SBS specimen at the middle and under the loading region for the sample from panel 5 can be seen in Figure 38. The samples failed due to interlaminar shear at multiple locations. For most of these specimens, 0° ply fiber kinking could not be observed around the loading nose. Moreover, failure propagated in 90° plies rather than 0° plies all across the sample.

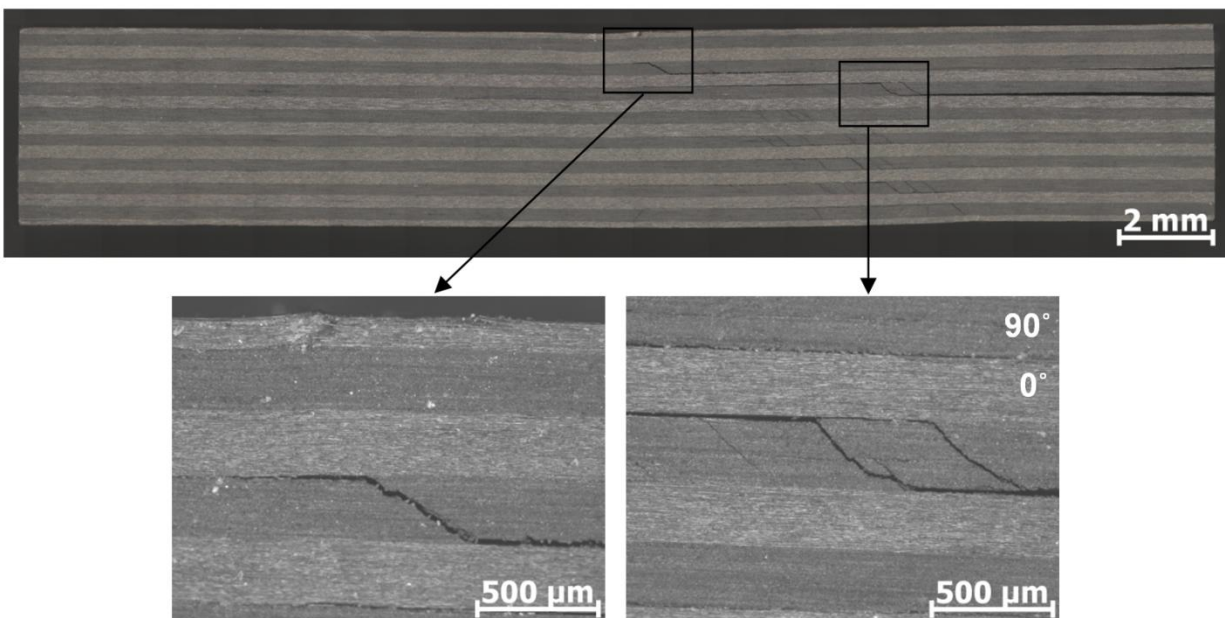


Figure 38. Typical photomicrograph of failed RT/D SBS specimen of cure cycle 5.

The difference between panel 5 and panels 1 to 4 can be explained by the lower cure temperature for panel 5 and its resulting low DOC. The poorly cured matrix could not support the fibers properly so no fractures transverse to the fibers occurred. One other problem might be a weak bond between different layers in the laminate. The bond between the 0° and 90° plies in the panel with less-cured resin may not be as strong as the others with higher curing temperature.

This weak bond along with the lack of transverse fiber fracture can justify the drop in SBS strength.

Figure 39 to Figure 41 show the failed SBS specimens from the center of panels 6 to 8 and Figure 42 to Figure 47 show the failed SBS specimens from center, middle, and corner locations (samples 1, 2, and 6) for panels 9 to 14. As can be seen in Figure 39 to Figure 47, the failure mode for most samples was compression-interlaminar shear. Major interlaminar failure for most of the samples occurred at the edge. Cracks propagated in 90° plies through the thickness.

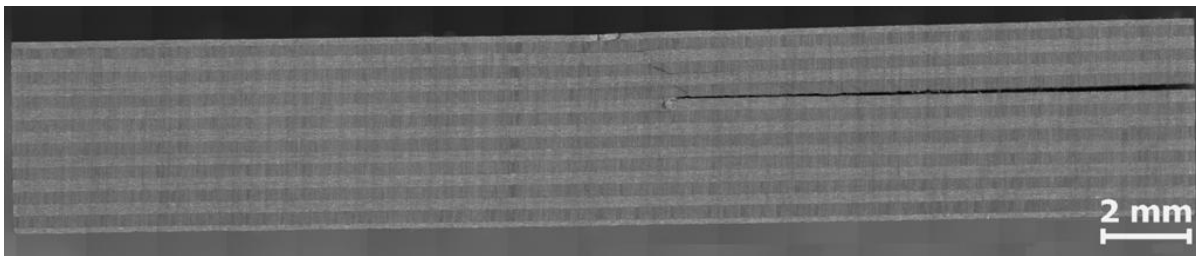


Figure 39. Panel 6 failed RT/D specimen from center.

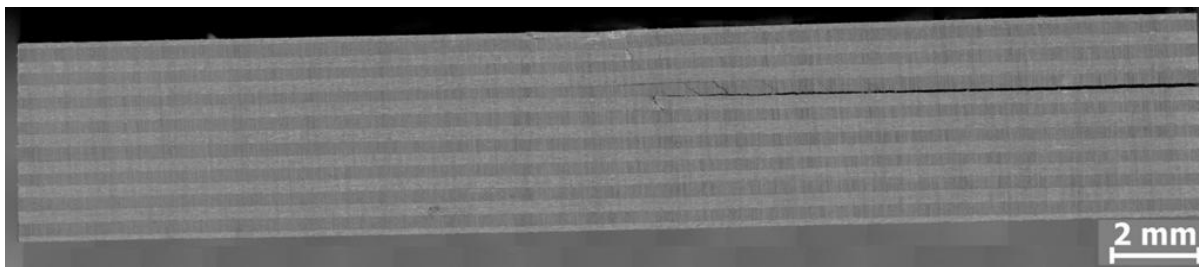


Figure 40. Panel 7 failed RT/D specimen from center.

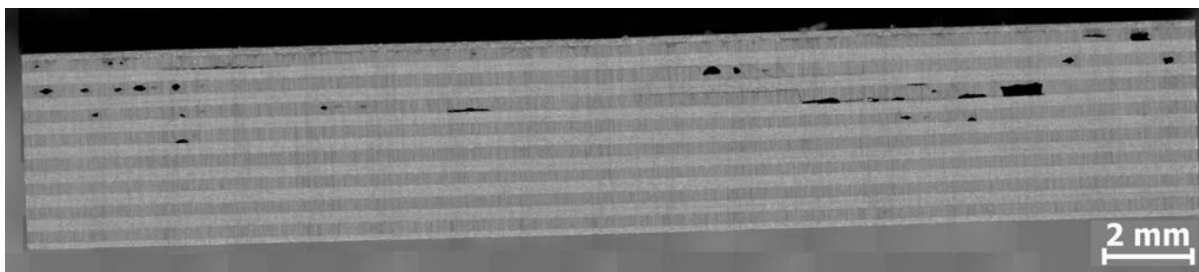


Figure 41. Panel 8 failed RT/D specimen from center.

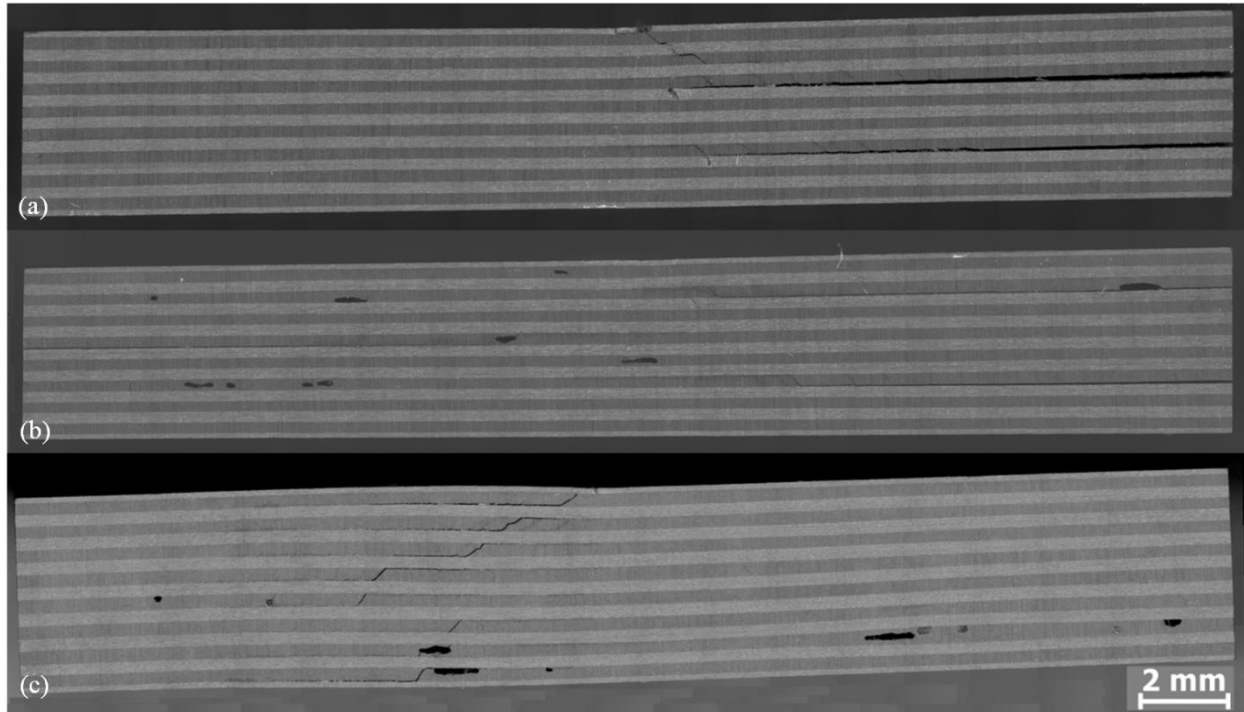


Figure 42. Panel 9 failed RT/D SBS specimens from: (a) corner, (b) middle, and (c) center.

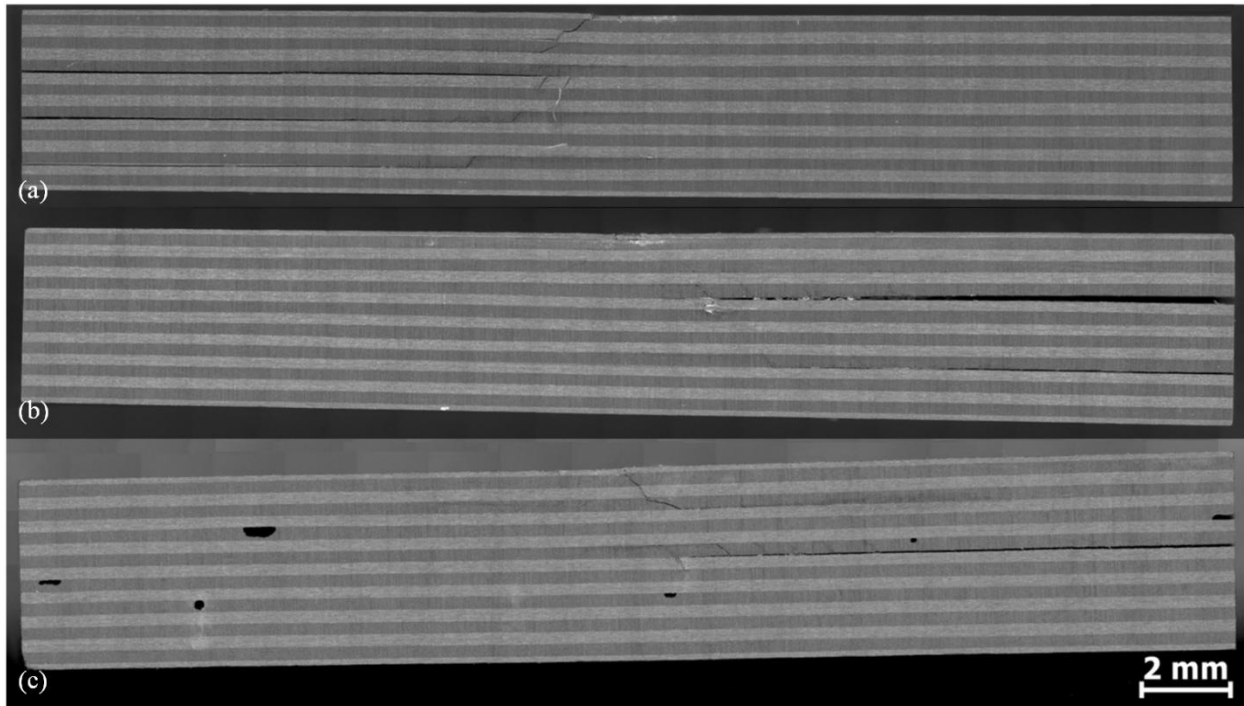


Figure 43. Panel 10 failed RT/D SBS specimens from: (a) corner, (b) middle, and (c) center.

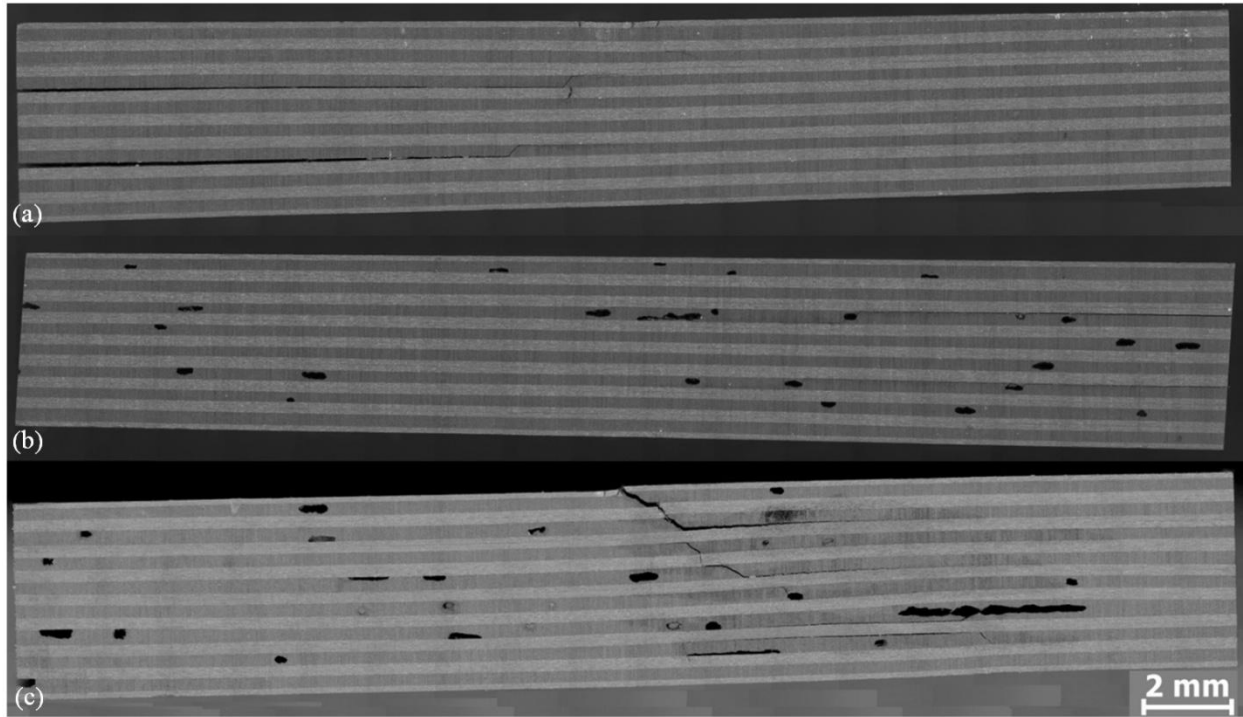


Figure 44. Panel 11 failed RT/D specimens from: (a) corner, (b) middle, and (c) center.

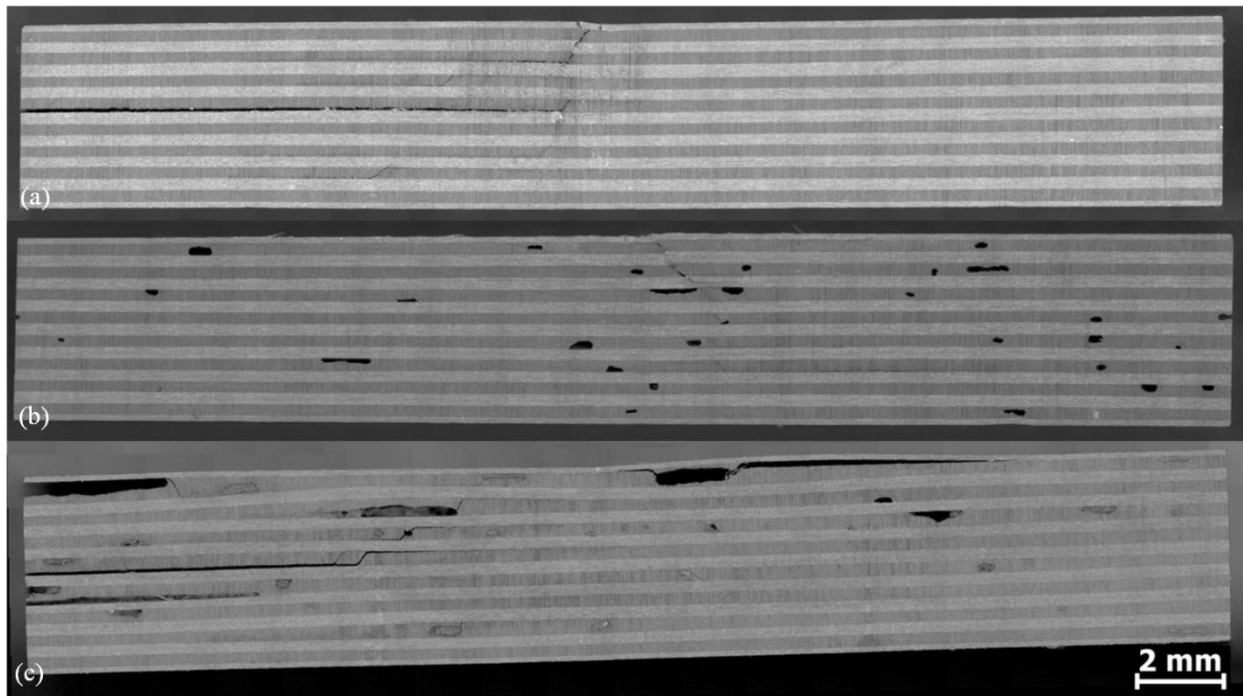


Figure 45. Panel 12 failed RT/D SBS specimens from: (a) corner, (b) middle, and (c) center.

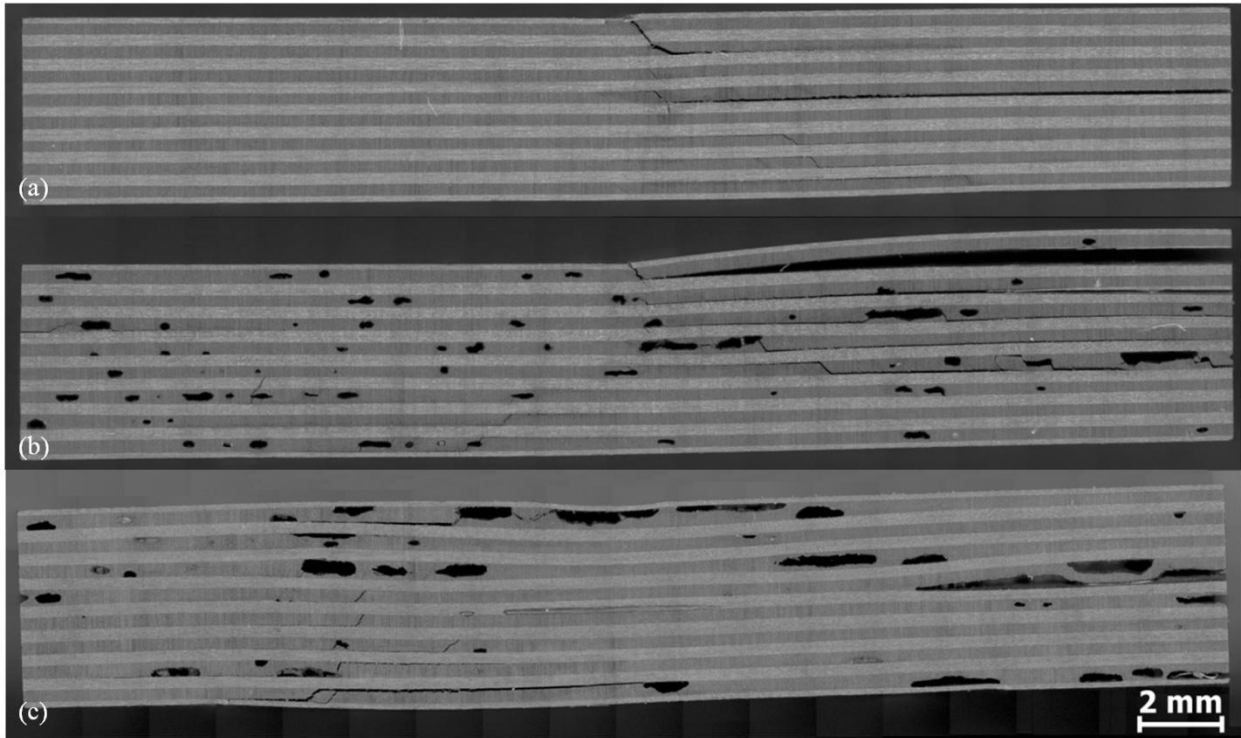


Figure 46. Panel 13 failed RT/D SBS specimens from: (a) corner, (b) middle, and (c) center.

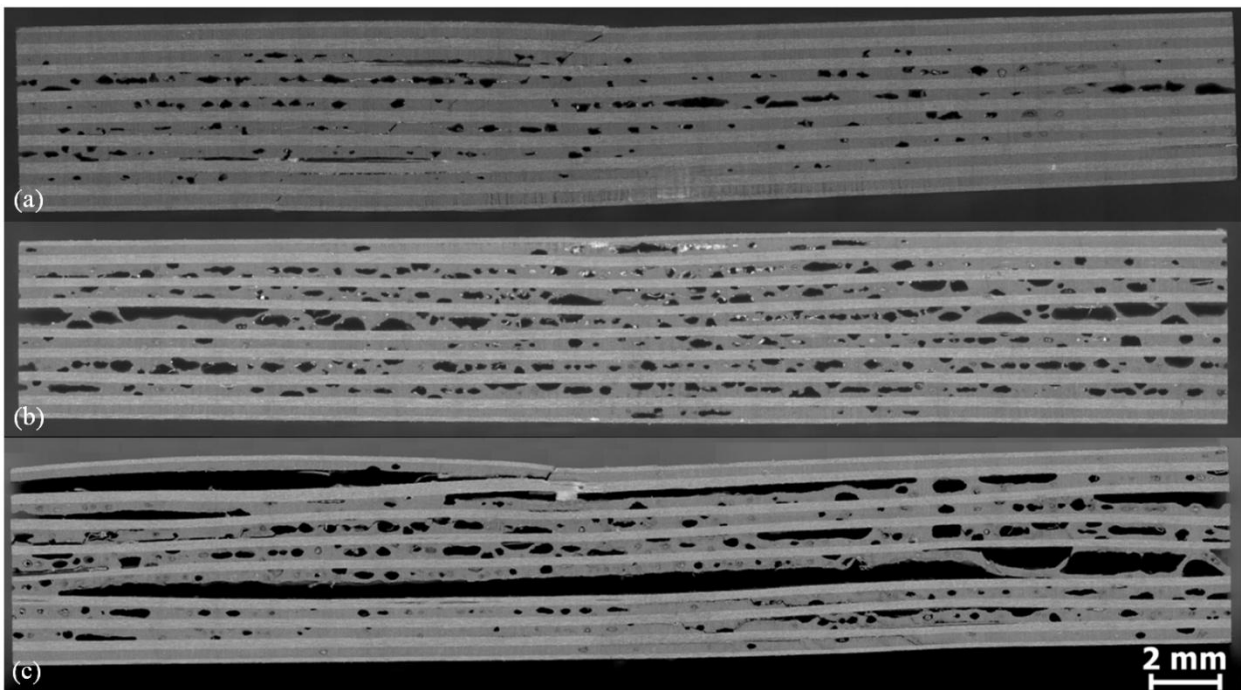


Figure 47. Panel 14 failed RT/D SBS specimens from: (a) corner, (b) middle, and (c) center.

It can be seen in Figure 44 to Figure 47 that voids played an important role in propagation of cracks as they assisted the spread of voids. Also, the increase in void content reduced the ply interface area. These events can justify the decrease in the interlaminar shear strength of the samples as the void content increases. Comparison of samples (a), (b), and (c), especially for panels 12 to 14, revealed the variation in the magnitude of void level as well as configuration of the voids by moving from the corner to the center of the panels. Void content was the highest for the center samples, and voids transformed from spherical to cylindrical shapes from the corner to the center. It is worth noting that the voids are visible in the 90° plies (dark bands), which suggests that they form parallel to the fibers. This is consistent with the earlier observation that the data were closer to the equation for cylindrical voids.

The amount of voids for panel 14 was very high. Beside voids, debondings were also prevalent especially for the sample from the center.

4.8.2 Hot/Wet Condition

Cross sections of failed H/W SBS specimens for cure cycles 2 and 5 are shown in Figure 48 and Figure 49. The dominant H/W SBS failure mode for cure cycles 1 to 5 was inelastic deformation. However, for those specimens cured at lower cure temperatures, the inelastic deformation was more pronounced. For these specimens, a slight flexure (compression) could also be observed along with inelastic deformation. For the H/W specimens, unlike the RT/D specimens, no failure was observed at the edges. To further investigate the failure mode for different panels, SBS specimens were observed under the optical microscope. It was found that failure started under the loading nose and propagated into edges of the middle section. The failure modes for all of the specimens were acceptable according to ASTM D2344 [25].



Figure 48. Typical failed H/W SBS specimen of panels 1 to 4.

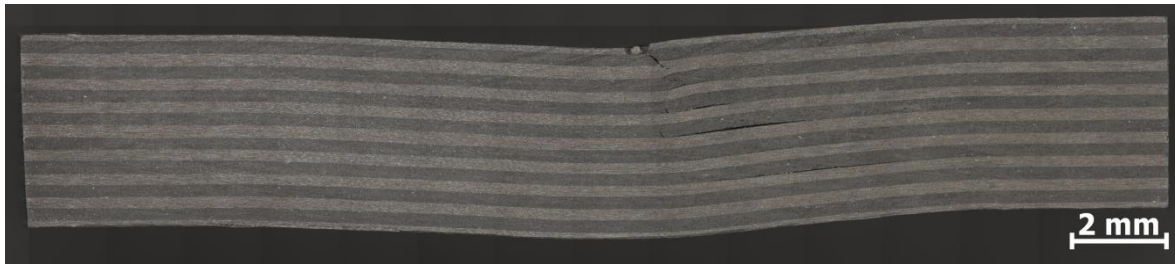


Figure 49. Typical failed H/W SBS specimen of panel 5.

Figure 50 shows the photomicrograph of a typical failed SBS specimen under the loading region for panels 1 to 3. It should be noted that in most of the specimens cured by cure cycles 1 to 3, the fiber kinking in 0° plies did not occur. The cracks propagated by 90° plies down to the bottom of the specimen showed itself as delamination between layers at several locations.

Figure 51 shows the photomicrograph of a typical failed SBS specimen under loading region for panels 4 and 5. It should be noted that the separation of layers and inelastic deformation was most dominant in panel 5 specimens. The number of delamination locations was also higher for cure cycle 5 SBS specimens. It seems that humidity and temperature reduced the resin mechanical properties even more for cure cycle 5 specimens, which in turn created weaker bonds between layers.

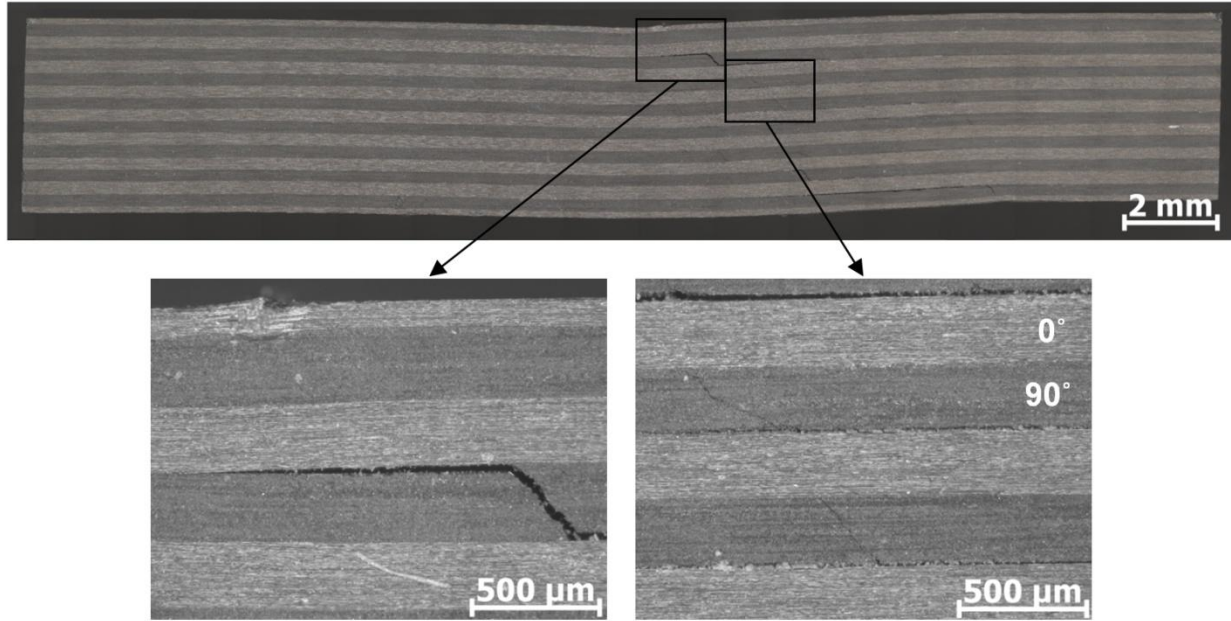


Figure 50. Typical photomicrograph of failed H/W SBS specimen of cure cycles 1 to 4.

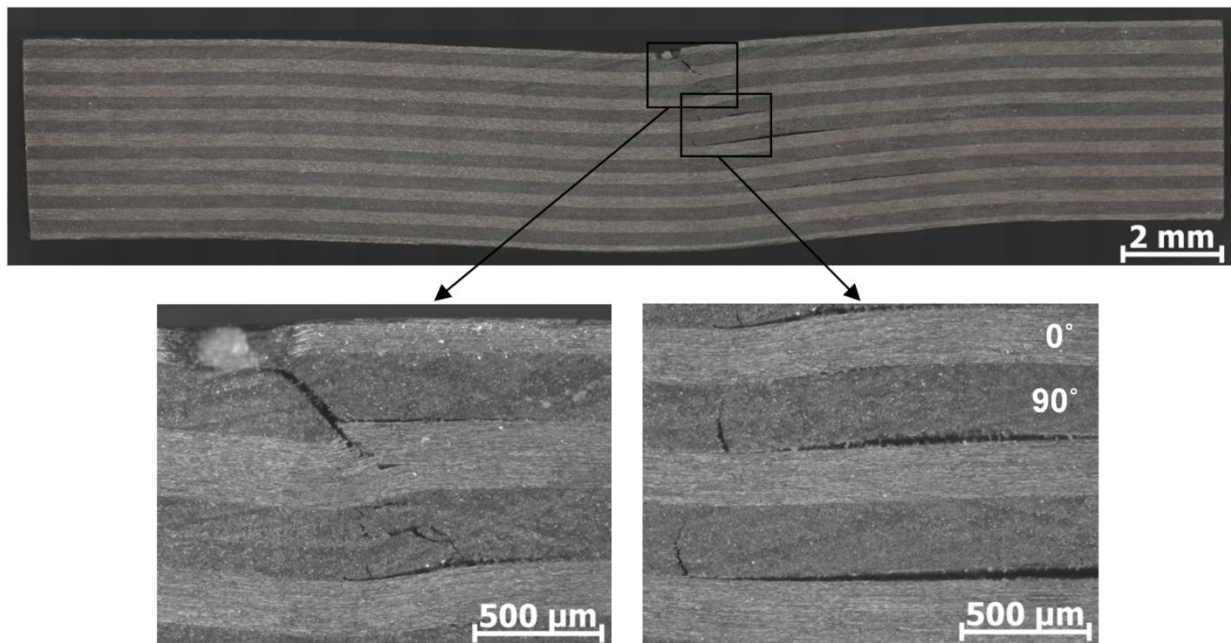


Figure 51. Typical photomicrograph of failed H/W SBS specimen of cure cycle 5.

Figure 52 to Figure 54 show the failed SBS specimens from the center of panels 6 to 8 and Figure 55 to Figure 60 show the failed SBS specimens from center, middle, and corner locations (samples 1, 2, and 6) for panels 9 to 14. As can be seen, the failure mode for panels 6 to

8 was compression-interlaminar shear in all locations. However, a slight inelastic deformation could be seen in most of the failed specimens. Cracks propagated across the thickness through the 90° plies. Unlike the RT/D samples, interlaminar failure happened in the middle section and not at the edges. For panel 8, the voids were not widespread, and it seems that they barely affected the short beam shear failure of the specimens. As shown in Figure 55 to Figure 60, the failure mode for panels 9 to 14 was compression-interlaminar shear. However, similar to panels 6 to 8, inelastic deformation could be observed for most of the specimens. The largest inelastic deformation was observed for panel 14, which was cured with no pressure and had the highest void content based on both acid digestion and C-scan data.

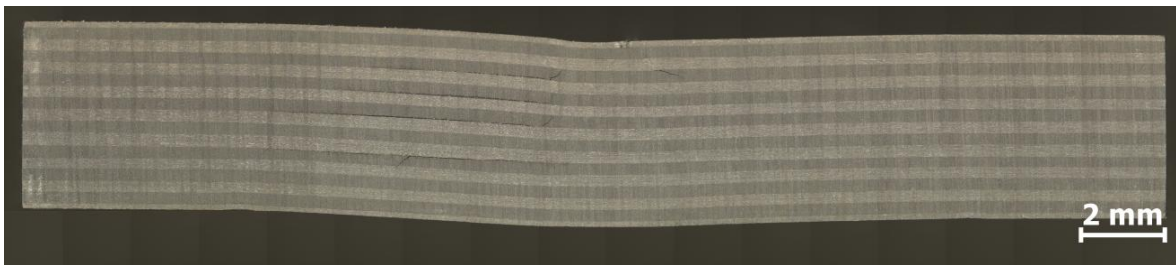


Figure 52. Panel 6 failed H/W SBS specimen from center.



Figure 53. Panel 7 failed H/W SBS specimen from center.



Figure 54. Panel 8 failed H/W SBS specimen from center.

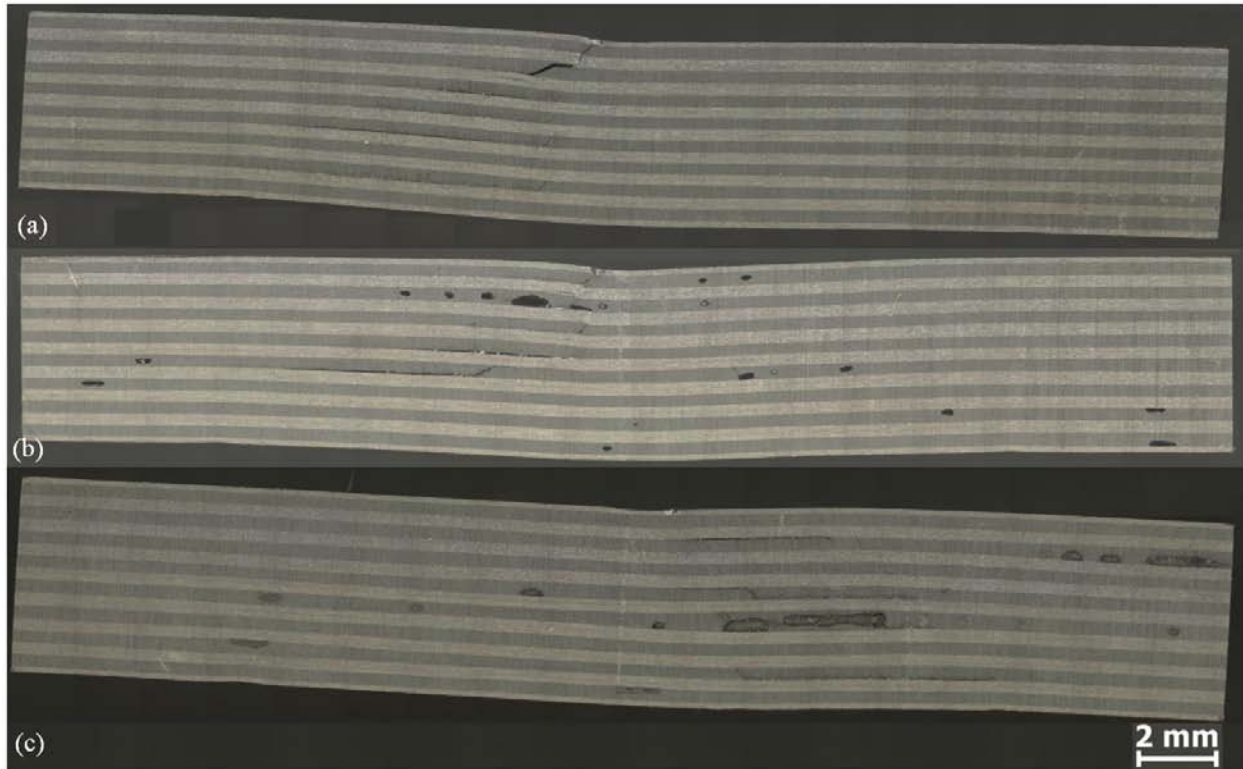


Figure 55. Panel 9 failed H/W SBS specimens from: (a) corner, (b) middle, and (c) center.

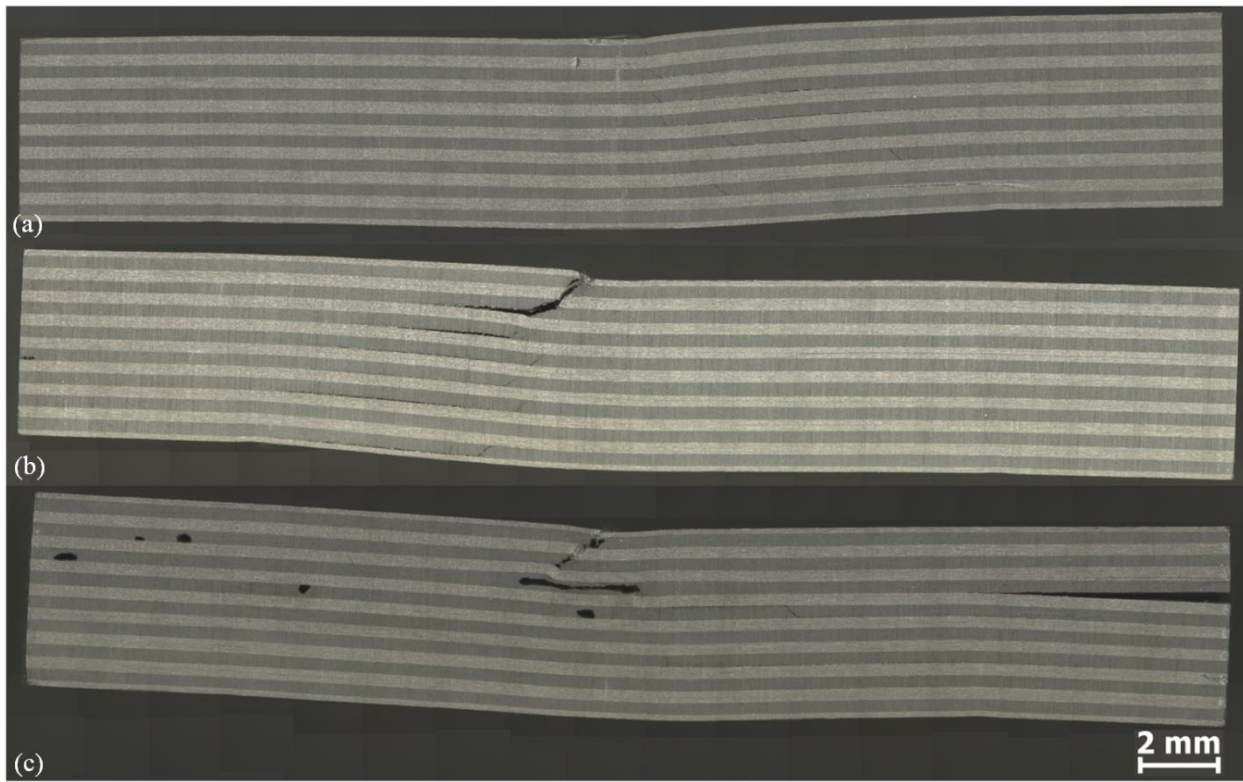


Figure 56. Panel 10 failed H/W SBS specimens from: (a) corner, (b) middle, and (c) center.

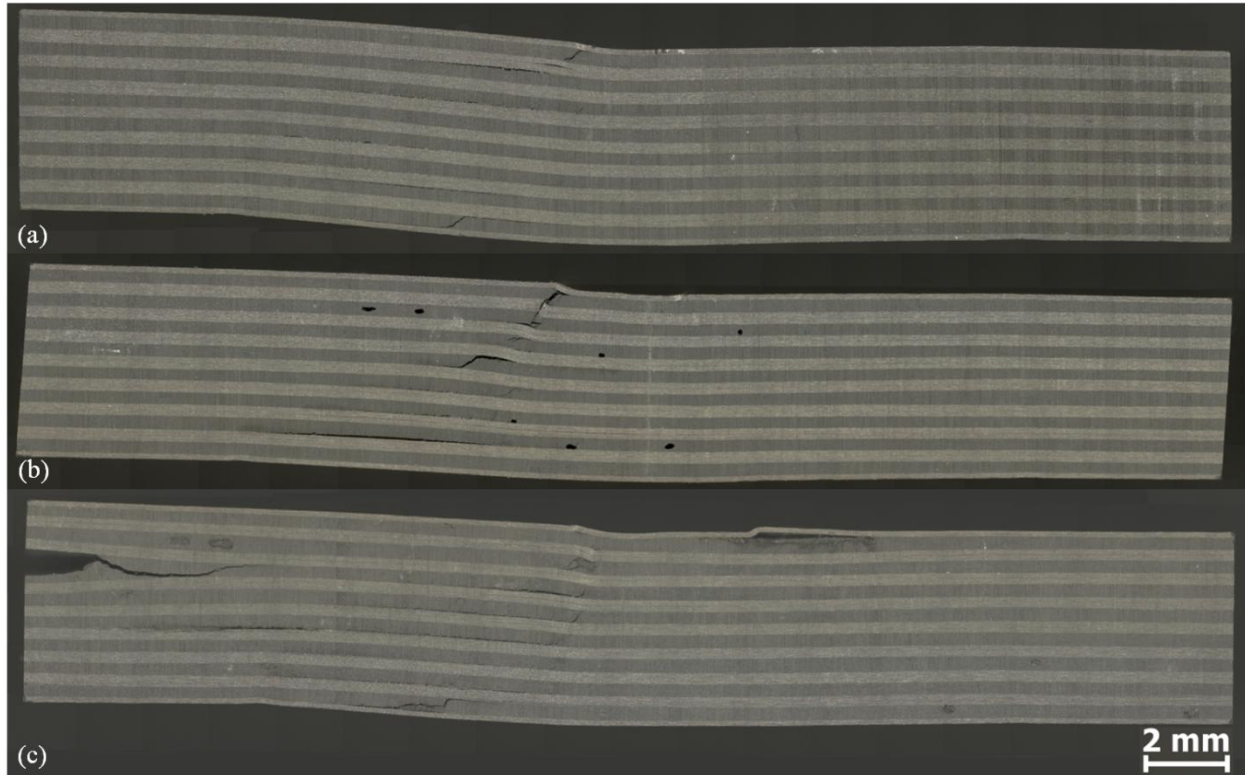


Figure 57. Panel 11 failed H/W SBS specimens from: (a) corner, (b) middle, and (c) center.

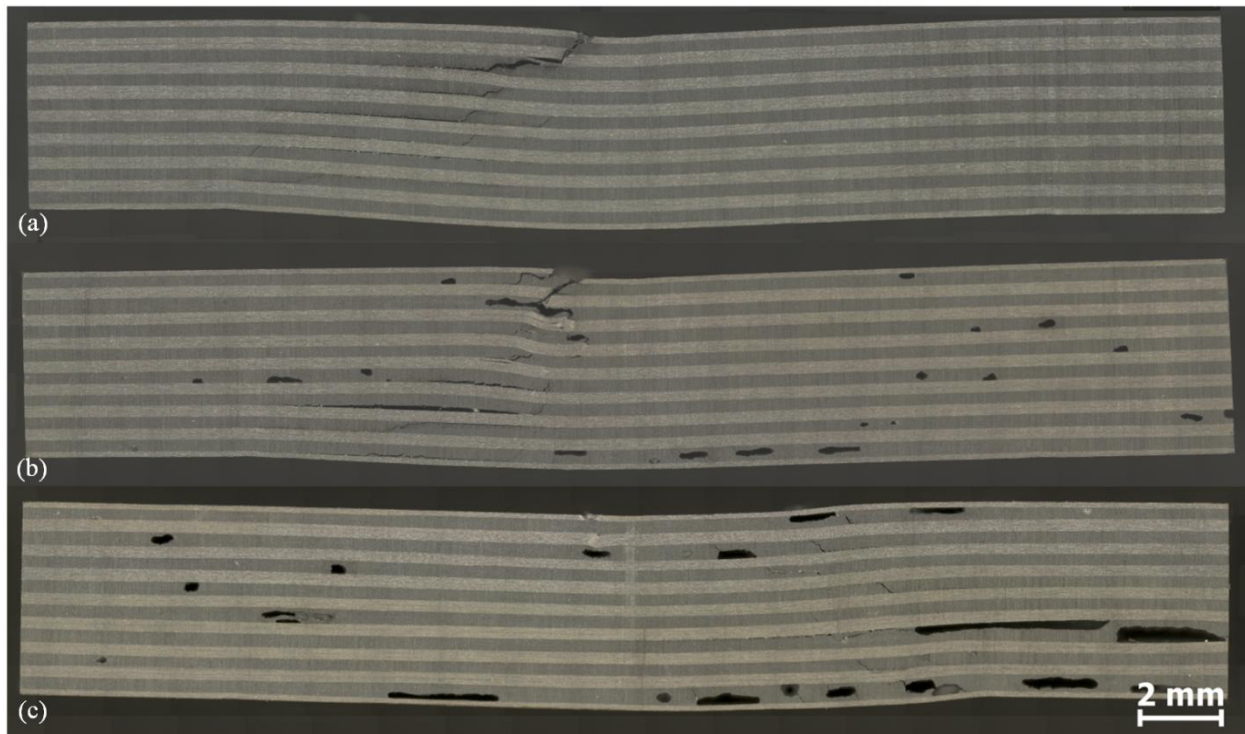


Figure 58. Panel 12 failed H/W SBS specimens from: (a) corner, (b) middle, and (c) center.

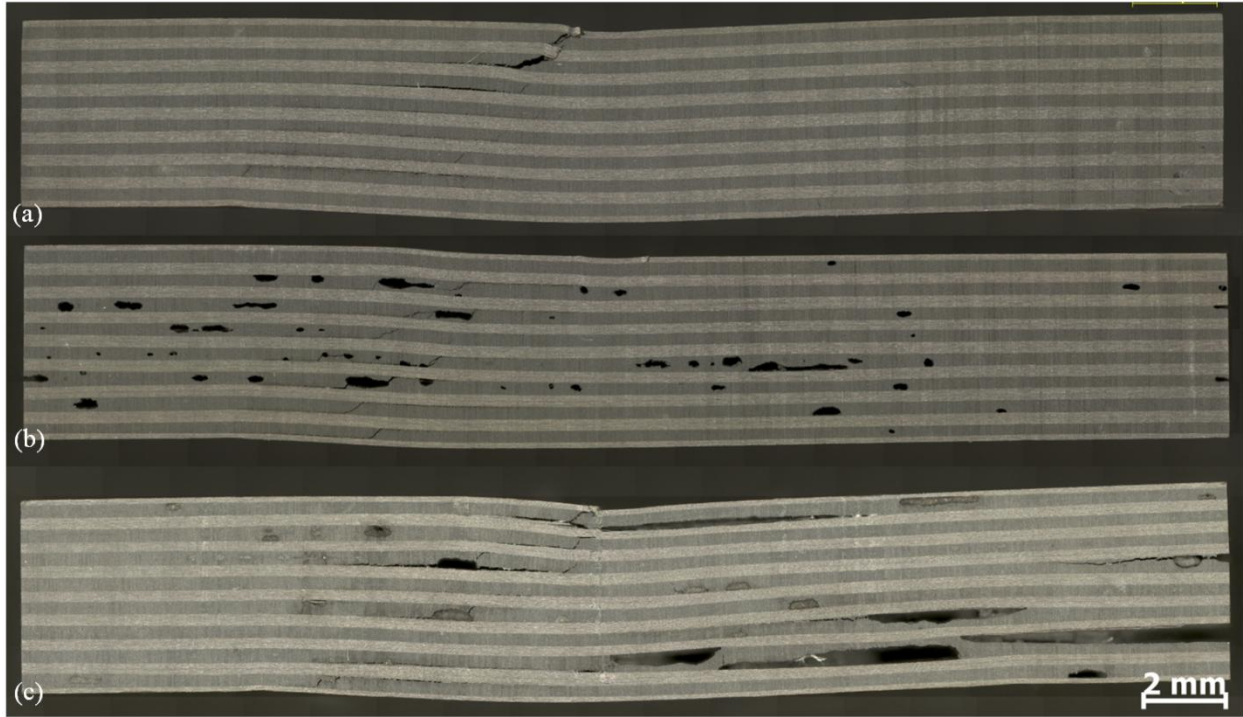


Figure 59. Panel 13 failed H/W SBS specimens from: (a) corner, (b) middle, and (c) center.

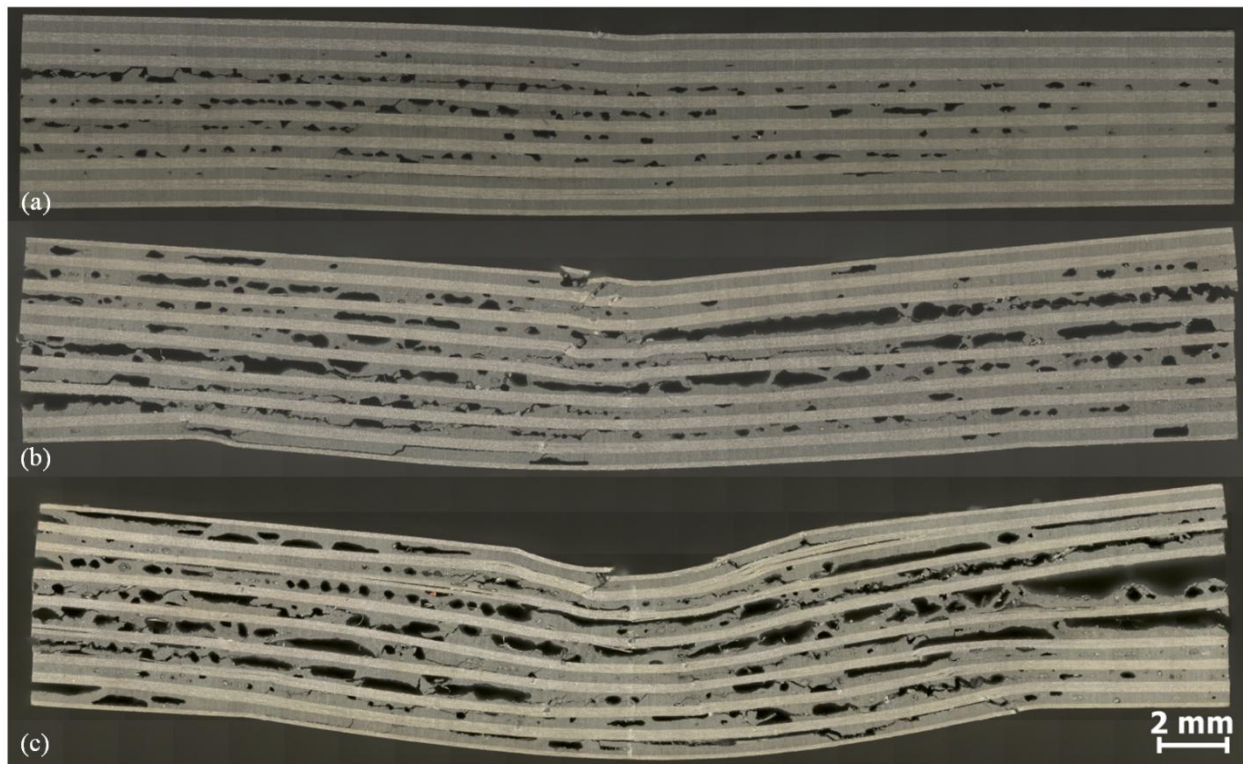


Figure 60. Panel 14 failed H/W SBS specimens from: (a) corner, (b) middle, and (c) center.

The level of void is quite interesting in Figure 60(c), which shows the failed specimen from the center of panel 14. In addition to voids, some debondings can also be seen in this figure. Comparing Figure 60(c) to Figure 60(a), the amount of variation in thickness can also be seen. The increase in the amount of inelastic deformation can be observed for panel 14 by moving from corner to center (increase in void content).

Similar to the RT/D samples, a comparison of samples (a), (b), and (c), especially for panels 12 to 14, revealed the variation in the magnitude of void level as well as the configuration of voids by moving from the corner to the center of the panels. Void content was the highest for the center samples, and the voids transformed from spherical to cylindrical shapes from the corner to the center.

Cracks propagated through the 90° plies across the thickness of the samples. Voids played an important role in crack propagation, and it seems that they facilitated the spread of the cracks. The presence of voids also decreased the ply interface area. These facts are some of the reasons for the lower SBS strength of the laminates with higher void levels.

CHAPTER 5

CONCLUSIONS

5.1 Conclusions

The results from investigation of the effect of cure temperature, cure pressure, and vacuum application time on the thermal properties, porosity and mechanical properties of a commercial carbon fiber prepreg, Cycom 977-2 unidirectional (UD) tape, were presented. The mechanical properties of interest were Room Temperature/dry (RT/D) and Hot/Wet (H/W) short beam shear (SBS) strengths.

The Cyttec-recommended cure cycle for 977-2 UD is 180 minutes hold at 177° C isothermal temperature. The cure pressure for curing 977-2 UD laminates is 586 kPa, and the normal vacuuming procedure is to vent the vacuum once the autoclave pressure reaches 69 kPa.

Fourteen cure cycles were studied which are shown in Table 3. Cure cycles 1 to 5 were designed to study the effect of isothermal cure temperature variation. Cure cycles 6 to 8 were designed to investigate the effect of autoclave pressure variation. Finally, cure cycles 9 to 14 were designed to study the combined effect of autoclave pressure variation as well as maintaining vacuum throughout the cure cycle.

Maintaining the vacuum throughout the cure cycle for panels 9 to 13 resulted in the formation of a cross-shaped high-porosity region in the panel (27Figure 11). The dimension of the cross-shaped defect was increased by decreasing the cure pressure. Panel 14, which was cured with no pressure, had the most widespread defects. The cross-shaped defect observed in the C-scan coincided with observed thickness variations in the panels. The cross-shaped defect was more widespread for panels with higher thickness variation. Panel 14, which was cured with no pressure, had the highest thickness variation.

Panels 1 to 5 had uniform thickness and porosity distribution. As such, the location of SBS and void content test coupons was assigned randomly for these panels. However, this assignment method could not be used for panels 6 to 14 because of thickness variations and non-uniform porosity distribution. The SBS and void content test coupons for these panels were obtained from different porosity levels. Half of the SBS test coupons cut from all the panels were tested at room temperature. The other half were tested at 82° C after being exposed to conditioning at 71° C with 85% humidity for 30 days.

It was found that the porosity and SBS strength of the cured laminates for panels 1 to 4 did not vary significantly over a relatively wide range of cure temperatures (from 160° C to 182° C for RT/D strength and 171° C to 182° C for H/W strength). Moreover, the porosity and SBS strength of the cured laminates for panels 6 and 7 did not vary significantly over a relatively wide range of cure pressures (from 276 kPa to 552 kPa). This suggests that laminates that might otherwise be rejected due to cure temperature or cure pressure variations could still attain acceptable mechanical properties, even if they were cured at temperatures or pressures lower than the process specifications. However, after a certain point, a decreasing trend in the average SBS strength for both H/W and RT/D was observed by reducing the cure temperature as well as the cure pressure.

The correlation between void volume content and cure pressure and also the correlation between void volume content and SBS strength were obtained. The SBS strength decreased exponentially with increasing void content. As such, an exponential model could fit the experimental data closely. The experimental data of SBS strength vs. void volume content were compared with two theoretical models based on voids configuration [20-22]. It was observed that for void volume contents less than 1%, the experimental data agreed well with the theoretical

models. However, as the void volume content increased, the models gradually deviated from the experimental data. Generally, equation (2), for cylindrical voids, was closer to the experimental data than equation (3), for spherical voids. This is consistent with the voids observed in the failed specimens, which appeared to be aligned in the fiber directions.

The failure mechanism and modes for SBS specimens for all panels were analyzed. Investigation of failed SBS specimens indicated a change in both H/W and RT/D SBS failure modes with reduction of cure temperature and cure pressure. However, the change was more dominant in the case of varying the cure temperature.

In the case of the RT/D failed SBS specimens of panels with different cure temperatures (1 to 5), it was found that the failure mode for all cure cycles except cure cycle 5 was compression-interlaminar shear. The failure mode for panel 5 was interlaminar shear. The dominant H/W SBS failure mode for cure cycles 1 to 5 was inelastic deformation. However, for those specimens cured at lower cure temperatures, the inelastic deformation was more pronounced and a slight flexure (compression) could also be observed along with the inelastic deformation.

For the specimens from panels with deviated pressure and/or vacuum-application time (6 to 14), the RT/D failure mode was detected as compression-interlaminar shear. The typical failure mode for panels 6 to 14 in the case of H/W SBS testing was compression-interlaminar shear along with an inelastic deformation. However, the magnitude of elastic deformation increased for specimens with more void content. It should be mentioned that voids played an important role in the propagation of cracks in these panels. Presence of voids assisted the spread of cracks and also reduced the ply interface area. These facts can justify the decrease in the interlaminar shear strength of the samples as the void content increased.

5.2 Recommendation for Further Studies

Considering the major effect of curing condition on the thermal and mechanical properties of laminated composites and based on the conclusions drawn from the current study, the following future works have been proposed:

- Conduct similar studies on different types of prepregs in order to obtain a more comprehensive database of the material response to the variations in autoclave curing condition.
- Investigate the effect of variation in curing parameters on some other mechanical properties, such as compressive strength, open hole compression strength, flexural strength, and tensile strength.
- Study the effect of various vacuum ventilation times during cure on void content, fiber content, density, and ultimately on the mechanical properties of the laminate.
- Investigate the effect of pressure application rate on void content, fiber content, density, and ultimately on the mechanical properties of the laminate.
- Incorporate the presented approach to the out-of-autoclave materials which would be beneficial to the field of composite repair.
- Investigate the effect of curing conditions, especially cure pressure and vacuum, on the properties of sandwich panels.

REFERENCES

LIST OF REFERENCES

- [1] F.C. Campbell, A.R. Mallow, and C.E. Browning, "Porosity in carbon fiber composites an overview of causes," *Journal of Advanced Materials*, Vol. 26, 1995, pp. 18-33.
- [2] P.R. Ciriscioli, G.S. Springer, and W.I. Lee, "An Expert System for Autoclave Curing of Composites," *Journal of Composite Materials*, Vol. 25, No. 12, 1991, pp. 1542-1587.
- [3] J.-M. Tang, W.I. Lee, and G.S. Springer, "Effects of cure pressure on resin flow, voids, and mechanical properties," *Journal of Composite Materials*, Vol. 21, 1987, pp. 421-40.
- [4] F.Y.C. Boey and S.W. Lye, "Void reduction in autoclave processing of thermoset composites: Part 1: High pressure effects on void reduction," *Composites*, Vol. 23, No. 4, 1992, pp. 261-265.
- [5] L. Liu, B.-M. Zhang, D.-F. Wang, and Z.-J. Wu, "Effects of cure cycles on void content and mechanical properties of composite laminates," *Composite Structures*, Vol. 73, No. 3, 2006, pp. 303-309.
- [6] F.Y.C. Boey and S.W. Lye, "Effects of vacuum and pressure in an autoclave curing process for a thermosetting fibre-reinforced composite," *Journal of Materials Processing Technology*, Vol. 23, No. 2, 1990, pp. 121-131.
- [7] C.R. Gernaat, "Correlation Between Rheological and Mechanical Properties in a Low-Temperature Cure Prepreg Composite," Master's Thesis, Department of Mechanical Engineering, Wichita State University, 2008.
- [8] P. Kashani and B. Minaie, "An ex-situ state-based approach using rheological properties to measure and model cure in polymer composites," *Journal of Reinforced Plastics and Composites*, Vol. 30, 2011, pp. 123-133.
- [9] P. Olivier, J.P. Cottu, and B. Ferret, "Effects of cure cycle pressure and voids on some mechanical properties of carbon/epoxy laminates," *Composites*, Vol. 26, 1995, pp. 509-515.
- [10] S.-Y. Lee and G.S. Springer, "Effects of cure on the mechanical properties of composites," *Journal of Composite Materials*, Vol. 22, No. 1, 1988, pp. 15-29.
- [11] Z.-S. Guo, L. Liu, B.-M. Zhang, and S. Du, "Critical void content for thermoset composite laminates," *Journal of Composite Materials*, Vol. 43, 2009, pp. 1775-1790.
- [12] S.R. Alavi, "Thermal, rheological, and mechanical properties of a polymer composite cured at staged cure cycles," Ph.D. Dissertation, Department of Mechanical Engineering, Wichita State University, 2010.

LIST OF REFERENCES (continued)

- [13] K.J. Bowles and S. Frimpong, "Void effects on the interlaminar shear strength of unidirectional graphite-fiber-reinforced composites," *Journal of Composite Materials*, Vol. 26, 1992, pp. 1487-1509.
- [14] M.L. Costa, S.F.M.D. Almeida, and M.C. Rezende, "The influence of porosity on the interlaminar shear strength of carbon/epoxy and carbon/bismaleimide fabric laminates," *Composites Science and Technology*, Vol. 61, No. 14, 2001, pp. 2101-2108.
- [15] M.L. Costa, M.C. Rezende, and S.F.M. De Almeida, "Strength of hygrothermally conditioned polymer composites with voids," *Journal of Composite Materials*, Vol. 39, No. 21, 2005, pp. 1943-1961.
- [16] S.F.M. De Almeida and A.C. De Mas Santacreu, "Environmental effects in composite laminates with voids," *Polymers and Polymer Composites*, Vol. 3, 1995, pp. 193-204.
- [17] H. Jeong, "Effects of voids on the mechanical strength and ultrasonic attenuation of laminated composites," *Journal of Composite Materials*, Vol. 31, 1997, pp. 276-92.
- [18] N.C.W. Judd and W.W. Wright, "Voids and their effects on the mechanical properties of composites-An appraisal," *SAMPE Journal*, Vol. 14, 1978, pp. 10-14.
- [19] A.P. Mouritz, "Ultrasonic and Interlaminar Properties of Highly Porous Composites," *Journal of Composite Materials*, Vol. 34, No. 3, 2000, pp. 218-239.
- [20] C.C. Chamis, "Simplified composite micromechanics equations for hygral thermal and mechanical properties," in *38th Annual Conference Preprint-Reinforced Plastics/Composites Institute, Society of the Plastics Industry, RP/C '83: Composite Solutions to Material Challenges*, Houston, TX, 1983.
- [21] C.C. Chamis, L.M. Handler, and J. Manderscheid, "Composite Nanomechanics: A Mechanistic Properties Prediction," in *NASA/TM—2007-214673*, 2007.
- [22] P.L. Murthy and C.C. Chamis, *Integrated Composite Analyzer (ICAN)-Users and Programmers Manual*. 1998.
- [23] E.C. Botelho, L.C. Pardini, and M.C. Rezende, "Hygrothermal effects on the shear properties of carbon fiber/epoxy composites," *Journal of Materials Science*, Vol. 41, 2006, pp. 7111-18.
- [24] J.J. Imaz, J.L. Rodriguez, A. Rubio, and I. Mondragon, "Hydrothermal environment influence on water diffusion and mechanical behaviour of carbon fibre/epoxy laminates," *Journal of Materials Science Letters*, Vol. 10, No. 11, 1991, pp. 662-665.

LIST OF REFERENCES (continued)

- [25] ASTM International, "Standard Test Method for Short-Beam Strength of Polymer Matrix Composite Materials and Their Laminates," in *ASTM Standard: D 2344/D 2344M – 00*.
- [26] Y. Shindo, R. Wang, and K. Horiguchi, "Analytical and experimental studies of short-beam interlaminar shear strength of G-10CR glass-cloth/epoxy laminates at cryogenic temperatures," *Transactions of the ASME. Journal of Engineering Materials and Technology*, Vol. 123, 2001, pp. 112-18.
- [27] J. Bicerano, *Prediction of Polymer Properties*, 3rd ed., New York, Basel: Marcel Dekker, Inc., 2002.
- [28] Z. Gurdal, A. Omasino, and S.B. Biggers, "Effect of Processing Induced Defects on Laminate Response: Interlaminar Tensile Strength," *SAMPE Journal*, Vol. 27, No. 4, 1991, pp. 3949.
- [29] I.M. Daniel, S.C. Wooh, and I. Komsky, "Quantitative porosity characterization of composite materials by means of ultrasonic attenuation measurements," *Journal of Nondestructive Evaluation*, Vol. 11, No. 1, 1992, pp. 1-8.
- [30] D. Hardt, "Process control of thermosetting composites: context and review," in *Advanced Composites Manufacturing*, ed. T.G. Gutowskis, Wiley, 1997.
- [31] D.E.W. Stone and B. Clarke, "Ultrasonic attenuation as a measure of void content in carbon-fibre reinforced plastics," *Non-Destructive Testing*, Vol. 8, No. 3, 1975, pp. 137-145.
- [32] H. Huang and R. Talreja, "Effects of void geometry on elastic properties of unidirectional fiber reinforced composites," *Composites Science and Technology*, Vol. 65, No. 13, 2005, pp. 1964-1981.
- [33] M.L. Costa, S.F.M.D. Almeida, and M.C. Rezende, "Hygrothermal effects on dynamic mechanical analysis and fracture behavior of polymeric composites," *Materials Research*, Vol. 8, 2005, pp. 335-340.
- [34] B.C. Ray, "Temperature effect during humid ageing on interfaces of glass and carbon fibers reinforced epoxy composites," *Journal of Colloid and Interface Science*, Vol. 298, No. 1, 2006, pp. 111-117.
- [35] R. Selzer and K. Friedrich, "Mechanical properties and failure behaviour of carbon fibre-reinforced polymer composites under the influence of moisture," *Composites Part A: Applied Science and Manufacturing*, Vol. 28, No. 6, 1997, pp. 595-604.

LIST OF REFERENCES (continued)

- [36] E.G. Wolff, "Moisture Effects on Polymer Matrix Composites," *SAMPE Journal (USA)*, Vol. 29, No. 3, 1993, pp. 11-19.
- [37] S.M. Lee, *International Encyclopedia of Composites*, Vol. 1-2, New York: VCH, 1990.
- [38] O. Ishai, "Environmental effects on deformation, strength, and degradation of unidirectional glass-fiber reinforced plastics. II. Experimental study," *Polymer Engineering & Science*, Vol. 15, No. 7, 1975, pp. 491-499.
- [39] L.C. Bank, T.R. Gentry, and A. Barkatt, "Accelerated Test Methods to Determine the Long-Term Behavior of FRP Composite Structures: Environmental Effects," *Journal of Reinforced Plastics and Composites*, Vol. 14, No. 6, 1995, pp. 559-587.
- [40] B.D. Harper, G.H. Staab, and R.S. Chen, "A Note on the Effects of Voids Upon the Hygral and Mechanical Properties of AS4/3502 Graphite/Epoxy," *Journal of Composite Materials*, Vol. 21, No. 3, 1987, pp. 280-289.
- [41] Cytec. *Cycom 977-2 Toughened Epoxy Resin*. <http://www.cytec.com/engineered-materials/products/Datasheets/CYCOM%20977-2.pdf> (accessed November 15, 2009).
- [42] ASTM International, "Standard Test Method for the Assignment of the Glass Transition Temperature by Modulated Temperature Differential Scanning Calorimetry," in *ASTM Standard: E2602 - 09*.
- [43] ASTM International, "Standard Test Methods for Constituent Content of Composite Materials," in *ASTM Standard: D3171 - 09*.
- [44] ASTM International, "Standard Test Methods for Moisture Absorption Properties and Equilibrium Conditioning of Polymeric Matrix Composite Materials," in *ASTM Standard: D5229 / D5229M - 92(2010)*.